Exploring potential human cancer neoantigens as targets for adoptive T cell therapy

DISSERTATION

zur Erlangung des akademischen Grades

Doctor rerum naturalium (Dr. rer. nat.)

eingereicht an der

Lebenswissenschaftlichen Fakultät der Humboldt-Universität zu Berlin

von

Lena Immisch

Präsidentin der Humboldt-Universität zu Berlin

Prof. Dr. Julia von Blumenthal

Dekan der Lebenswissenschaftlichen Fakultät der Humboldt-Universität zu Berlin

Prof. Dr. Dr. Christian Ulrichs

Gutachter:innen:

Prof. Dr. Thomas Sommer

Prof. Dr. Gerald Willimsky

Prof. Dr. Rienk Offringa

Tag der mündlichen Prüfung: 17.10.2022

Berlin, Juli 2022

The present dissertation has been carried out under the supervision of Prof. Dr. Gerald Willimsky in the laboratory of Experimental and Translational Cancer Immunology at the Charité - Universitätsmedizin Berlin, German Cancer Research Center (DKFZ Heidelberg) and Max Delbrück Center (MDC) for Molecular Medicine in the Helmholtz Association in Berlin.

Table of Contents

Summary

Adoptive transfer of T cell receptor (TCR)-engineered T cells against tumour-specific neoantigens is a promising approach in cancer immunotherapy. Ideally, targeted antigens are crucial for cancer cell survival and are generated in sufficient amounts to be recognised by T cells. However, the identification of ideal targets remains challenging and requires intensive characterisation to validate sufficient antigen processing and presentation by the tumour cells using specific TCR-transduced T cells.

This thesis focused on the validation of HLA-A*02:01 binding epitopes carrying the recurrent cancer mutations H3.3K27M, Rac1P29S, Rac2P29L or KrasG12V as targets for adoptive T cell therapy. After peptide immunisation, immune responses in a human transgenic mouse model expressing a diverse human TCR repertoire were elicited and high-affinity TCRs were successfully isolated. Although H3.3K27M-specific T cells showed high functional avidity, no recognition of cells endogenously expressing the H3.3K27M mutation was achieved. Furthermore, a mechanism to target the common melanoma mutation Rac1P29S with a TCR raised against a heterologous mutation with higher peptide-MHC affinity was described. High-affinity TCR-transduced T cells induced cytotoxicity against Rac1P29S expressing melanoma cell lines. Lastly, high-affinity TCRs specific for mutant Kras and Rac2 spliced epitopes generated by proteasome-catalysed peptide splicing were successfully isolated, however, TCR-transduced T cells did not induce an immune response against naturally expressed or overexpressed mutant transgenes. The results indicate that spliced epitopes are probably less abundant than previously estimated and therefore may play a minor role in the generation of targets for adoptive T cell therapy.

These data suggest that target selection using a reverse immunology approach based on binding algorithms and frequency of mutations alone is not sufficient. Thus, additional strategies to improve the selection of suitable targets such as the analysis of the MHC immunopeptidome are required prior to TCR isolation and characterisation.

Zusammenfassung

Der adoptive Transfer von T-Zell-Rezeptor (TZR) modifizierten T-Zellen gegen krebsspezifische Antigene ist ein vielversprechender Ansatz in der Immuntherapie. Geeignete Zielmoleküle für diese Therapie sollten wichtig für das Überleben von Krebszellen sein und zudem in ausreichenden Mengen auf der Zelloberfläche exprimiert werden, um von T-Zellen erkannt zu werden. Die Identifizierung dieser Zielmoleküle ist jedoch eine Herausforderung und erfordert eine intensive Charakterisierung, um eine ausreichende Prozessierung und Präsentation auf den Tumorzellen unter Verwendung spezifischer TZR-transduzierter T-Zellen zu validieren.

Ziel dieser Arbeit war, HLA-A*02:01-spezifische Epitope, welche die häufigen Krebsmutationen H3.3K27M, Rac1P29S, Rac2P29L oder KrasG12V tragen, als Zielmoleküle für adoptive T-Zell-Therapie zu validieren. Dafür wurden erfolgreich Immunantworten in einem humanen transgenen Mausmodell nach Peptidimmunisierung induziert und TZRs mit hoher Affinität isoliert. Im ersten Teil dieser Arbeit wurde festgestellt, dass trotz einer hohen funktionellen Avidität von H3.3K27M-spezifischen T-Zellen keine Erkennung von Tumorzellen, welche die H3.3K27M-Mutation endogen exprimieren, erreicht werden konnte. Zweitens wurde ein Mechanismus beschrieben, um die häufige Melanommutation Rac1P29S mit einem TZR zu erkennen, der gegen eine heterologe Mutation mit höherer Peptid-MHC-Affinität gerichtet ist. Spezifische TZR-transduzierte T-Zellen waren zytotoxisch gegen Rac1P29S-exprimierende Melanomzelllinien. Letztlich wurde beobachtetet, dass TZRs mit hoher Affinität gegen gespleißte Kras und Rac2 Epitope, welche durch Proteasom-katalysiertes Peptidspleißen erzeugt wurden, keine Immunantwort gegen natürlich exprimierte oder überexprimierte mutierte Transgene hervorrufen konnten. Aus diesen Ergebnissen lässt sich schließen, dass gespleißte Epitope wahrscheinlich seltener vorkommen als zuvor angenommen und daher möglicherweise irrelevant für die adoptive T-Zelltherapie sind.

Diese Daten deuten darauf hin, dass die Auswahl von Zielmolekülen für die adoptive T-Zell-Therapie mit Hilfe reverser Immunologie auf der Grundlage von Bindungsalgorithmen und der Häufigkeit von Mutationen allein nicht ausreicht. Daher sind vor der Isolierung und Charakterisierung von TZRs zusätzliche Strategien wie beispielsweise die Analyse des MHC-Immunopeptidoms erforderlich, um die Auswahl geeigneter Zielmoleküle für die T-Zelltherapie zu verbessern.

1. Introduction

1.1 T cell-mediated immunity

The role of the immune system is to protect the host from pathogens by distinguishing between self and non-self. While the innate immune system allows for rapid response against external threats through pattern recognition receptors, the adaptive immune system establishes a long-lasting response by developing immunological memory.

T cells are one of the major cell types of the adaptive immune system. They are categorised into helper T cells and cytotoxic T lymphocytes (CTL). While helper T cells support the immune response of other cell types like B cells by secreting cytokines, CTLs elicit an immune response against intracellular pathogens, including viruses. CTL cytotoxicity is mediated by inducing apoptosis in target cells via the release of perforin and granzymes. While perforin forms pores in the target cell's membrane, granzymes are serine proteases activating apoptosis in the target cell. Additionally, T cells kill via caspase-induced apoptosis by binding of Fas on the target cell to Fas ligand expressed on activated CTL. This mechanism is also involved in regulating lymphocyte numbers after pathogen clearance. Another host defence mechanism of CTLs is the release of cytokines such as interferon gamma (IFNγ). IFNγ can inhibit viral replication and stimulates the immune system by upregulating MHC I expression and activation of macrophages[1,2].

1.1.1 T cell receptor

A hallmark of the T cell-mediated immune response is the high specificity mediated by an unique T cell receptor (TCR) expressed on the surface of each T cell[3,4]. The TCR is a heterodimer consisting of transmembrane polypeptide α and β chains, connected by a disulfide bond in their constant regions. Intracellular signalling through the TCR is mediated by its association with a subunit of the CD3 complex[5]. T cells can recognise a great variety of antigens due to variations in the amino acid sequence in the antigen-binding site of each TCR, the so-called complementarity determining region 3 (CDR3) within the variable region[6]. During gene rearrangement, the sequence of the variable region is assembled by somatic DNA recombination of several gene segments[7]. While the fully rearranged variable region of the α chain contains a variable (V) and a joining (J) gene segment, the β chain contains an additional diversity (D) segment between the V and J segments. V(D)J recombination is mediated by the RAG-1 and RAG-2 enzymes. Lack of RAG enzymes causes severe immunodeficiency, as neither T cells nor B cells can develop without rearranged receptors[8,9]. Additional diversity is

mediated by the enzyme terminal deoxynucleotidyl transferase (TdT), which randomly adds or deletes nucleotides at the junction between V(D)J segments[10]. The high TCR diversity leads to a limited amount of each T cell clone in the naïve repertoire.

1.1.2 Antigen processing and presenting

Antigens are presented by major histocompatibility complexes (MHCs), which are recognised by TCRs uniquely expressed on T cells[11]. There are two classes of MHC molecules: MHC class I and MHC class II molecules. MHC class II molecules are expressed only on professional antigen-presenting (APC) cells to present antigens to $CD4^+$ T helper cells and will not be further discussed here[12]. In contrast, MHC class I molecules are expressed on all nucleated cells and present peptides to $CD8^+$ T cells. The MHC class I molecule consists of two polypeptide chains, an α-chain and a β2-microglobulin (β2m) chain. The α-chain is polymorphic and is crucial for the specific binding of peptides. While the α1 and α2 domains form a peptide-binding cleft, the α3 domain spans the membrane and is noncovalently associated with the smaller, monomorphic β2m-chain[13]. MHC class I molecules usually bind 8-10 amino acid long peptides via the terminal amino and carboxyl groups of both ends of the peptide and the invariant sites of the MHC peptide-binding cleft. Additionally, MHC class I binding peptides have further anchor residues such as a hydrophobic amino acid at the second position and at the carboxyl terminus to further stabilise binding[14,15]. MHC class I molecules bind peptides originating in the cytosol, such as viral proteins and potentially any intracellular antigens. Cytosolic peptides are generated by protein degradation in the proteasome, a multicatalytic protease complex. The proteasome exists in an alternative form called the immunoproteasome, in which certain catalytic subunits are displaced by interferon-inducible subunits. These immunoproteasome subunits prioritise cleavage after hydrophobic amino acids to create peptides with MHC class I binding anchor positions[16,17]. Next, peptides are transported into the endoplasmic reticulum (ER) via the transmembrane proteins TAP1 and TAP2 (transporters associated with antigen processing). TAP proteins originate from the ATP binding cassette (ABC) family and are inducible by interferons[18,19]. Within the lumen of the ER, a second processing step for cytosolic peptides takes place during which the amino terminal is trimmed by an IFNγ upregulated aminopeptidase called endoplasmic reticulum aminopeptidase (ERAP)[20,21]. Next, the 8-10 amino acid long peptides are loaded onto the assembled two MHC class I chains stabilising the MHC class I complex. As a final step, the peptide-MHC complex is exported onto the cell membrane[22].

A strategy of pathogens to hide from a host's immune system is to select for mutations that help escape presentation by MHC molecules. To avoid this, MHC molecules are polygenic and polymorphic to create a high variety of different MHC molecules, contributing to the protection against rapidly evolving pathogens. Polygeny is caused by the presence of three different class I a-chain genes, called human leukocyte antigen (HLA)-A, -B and -C. Additionally, MHC genes are highly polymorphic due to the presence of hundreds of alleles within the human population[23,24]. The distribution of HLA alleles and haplotypes differs between ethnicities and geographic locations. As HLA-A*02:01 is the most frequent HLA-A type in the Western world, it is the most studied HLA type for therapy in these areas to target a broad spectrum of cancer patients[25].

1.1.3 Central and peripheral tolerance of T cells

T cells originate in the bone marrow from multipotent hematopoietic stem cells, but all developmental stages occur in the thymus. Here, T cells switch from a double negative (DN) stage, meaning neither CD4 nor CD8 co-receptors are expressed, to a double positive (DP) stage expressing both co-receptors simultaneously. During this stage, all T cells undergo positive and negative selection to acquire central tolerance. It is crucial that T cells are educated to interact with self-antigens presented by thymic epithelial cells to avoid auto-reactivity[26]. During positive selection, T cells that fail to bind self-MHC/self-antigens will die, accounting for approximately 10-30% of DP cells. After further maturation and expression of high levels of TCRs, T cells that bind self-MHC/self-antigens too strongly undergo apoptosis, known as negative selection[27]. Only about 2% of DP T cells pass the two selections, which then lose one of the co-receptors and become either CD4 or CD8 single-positive T cells[28,29]. Another mechanism to prevent auto-reactivity is peripheral tolerance. When T cells that escape thymic selection react against self-antigens in the periphery in the absence of inflammatory signals they either undergo activation-induced cell death or become anergic[30].

1.2 Cancer immunotherapy

T cells can recognise tumour antigens to eliminate cancer cells. Cancer immunotherapy is a fast-growing field using this tumour recognition by the immune system; it comprises different kinds of therapies, ranging from small molecules to cellular therapies.

1.2.1 Checkpoint inhibition

One way to modify the immune response against cancer cells is the inhibition of checkpoint pathways. Inhibitory receptors expressed by T cells interact with their ligands on the tumor cell

surface or in the tumor microenvironment, which often dampens the immune response[31–33]. Blocking antibodies against the most studied inhibitory receptors CTLA-4 and PD-1 are clinically approved and can improve the survival of cancer patients[34,35]. However, these therapies often induce severe toxicity and only a limited number of patients are responsive to checkpoint inhibition[36,37]. Biomarkers allowing for the prediction on responsiveness are lacking. Tumours with high mutational burden and the presence of neoantigens seem to respond better to checkpoint inhibition, however, further research is required to fully understand the clinical outcomes of this treatment[38,39].

1.2.2 Cancer vaccines

Cancer vaccines stimulate the immune system against antigens and act either as prophylactic or therapeutic vaccines. Prophylactic vaccines using virus-like particles to mount an immune response against virus-associated cancers have shown great success, this includes vaccines against the human papillomavirus (HPV), a cause of cervical cancer[40,41]. In contrast, the efficacy of therapeutic vaccines is still under investigation. Potential antigens to target for therapeutic vaccination include MART-1 in melanoma and a prostate antigen (PA2024)[42,43], however, clinical data have not shown convincing outcomes, possibly due to the patients' tolerance[44].

1.2.3 Adoptive T cell therapy

A challenge using immunotherapies such as checkpoint inhibition and cancer vaccines is the lack of efficient tumour-reactive T cells in patients. An approach to overcome this obstacle is to adoptively transfer tumour-specific T cells into patients. This therapy is successful in treating viral infections such as the Eppstein-Barr virus (EBV) in immunocompromised patients after allogeneic hematopoietic stem-cell transplantation[45–47]. In cancer patients, tumour-infiltrating lymphocytes (TILs) present in the cancer's microenvironment can be expanded *ex vivo* and subsequently transferred back to the patient. Adoptive T cell therapy (ATT) of TILs is successful in a fraction of melanoma patients only[48–50]. A limitation of TIL transfer is that the specificity of the T cells is unknown, although recent data suggest TILs specific for neoantigens drive tumour regression, which explains the success in melanoma, a tumour with high mutational burden[51,52].

A more targeted approach is the transfer of engineered T cells. The idea is to isolate a patient's peripheral blood leukocytes (PBLs), engineer them *ex vivo* to express a TCR specifically targeting a tumour antigen and infuse the cells back into the patient after expansion. The most

common method to stably integrate an exogenous TCR into PBLs is via viral vectors such as lenti- and retroviruses [53,54]. Other non-viral approaches like CRISPR/Cas9 mediated integration into the endogenous TCR locus are currently being explored to improve the signalling of the exogenous TCR[55].

TCRs recognise peptides presented by MHC molecules. A strategy to directly target surface antigens on cancerous cells and therefore avoid MHC matching is to equip T cells with a chimeric antigen receptor (CAR). CARs are modified single-chain antibodies with an intracellular TCR signalling domain. The FDA-approved CD19-CAR T cell therapy is successfully used in the clinic to treat leukaemia of B cell origin[56,57]. However, the number of suitable unique surface antigens on solid tumours targetable with CAR T cells is limited and their success is mainly restricted to haematological cancers.

1.3 Targets for adoptive T cell therapy

An important factor for successful ATT is the selection of a suitable target. An ideal target antigen should be crucial for cancer cell growth and survival to exclude the possibility of therapy escape by downregulation of the target antigen. Ideally, it would also be shared between cancer patients and presented by a common HLA type. To avoid toxicity, it is essential that the selected target is either specifically expressed on cancer cells or expressed only on non-essential patient cells.

1.3.1 Tumour-associated antigens

Tumour-associated antigens (TAAs) are self-antigens which are reactivated or overexpressed in tumours, such as cancer-testis antigens. The expression of cancer-testis antigens is restricted to spermatocytes in testes, an immune-privileged tissue. However, these antigens, such as MAGE proteins or NY-ESO1, are also recurrently expressed on cancer cells and therefore act as good targets as they are not expressed in essential immunocompetent non-cancerous tissues[58,59]. Antitumour effects have been shown in clinical trials targeting NY-ESO1 in melanoma, sarcoma and myeloma[60,61]. Another example of TAAs are embryonic antigens such as carcinoembryonic antigen (CEA), which are also expressed in adult cancers[62,63]. As a third subgroup, antigens which are only expressed in certain stages during cell differentiation such as MART-1 can be targeted by ATT[64,65]. An advantage of TAAs is that they are often shared among cancer patients, however, since these antigens are also present in healthy tissues, on-target off-tumour toxicity was observed in clinical trials[66,67].

1.3.2 Tumour-specific antigens

A more specific approach is ATT using TCRs against tumour-specific antigens (TSAs). The first evidence that the immune system recognises tumour cells was observed in 1943, showing that mice immunised with a methylcholanthrene (MCA)-induced sarcoma were immune against a second inoculation with the same tumour[68]. In 1957, these results were confirmed by additional experiments showing rejection of injected tumour cells after immunisation with small tumour fragments[69]. The mechanism of the rejection was later explained by the recognition of specific cancer mutations by the immune system[70]. Mutations arise after exposure to carcinogens or due to mistakes during cell division, causing missense mutations, frameshift mutations or insertions and deletions in the genome. Normal cells develop into cancer cells if these mutations either activate genes inducing cell growth, so-called oncogenes, or inactivate genes controlling cell division, so-called tumour-suppressor genes[71]. While passenger mutations arise during the uncontrolled growth of cancerous cells, driver mutations are defined as early mutations initiating tumour development[72]. To avoid therapy escape, it is, therefore, crucial to identify driver mutations as targets for immunotherapy[73]. As these mutations can form novel antigens, TSAs are often referred to as neoantigens. *In silico* predictions using algorithms can identify novel antigens for immunotherapy[74]. However, *in vitro* validation of predicted neoepitopes is crucial, as sufficient expression and presentation of antigens are difficult to predict.

1.3.2.1 H3.3K27M mutation in glioma

The brain immune system is tightly regulated, as inflammation in the brain would cause intracranial pressure. In the 1940s, Peter Medawar was the first to postulate that the brain is immunologically privileged. Transplantation experiments showed that grafts implanted into the CNS were not rejected, while skin grafts were rejected[75]. However, this concept of the brain as immune-privileged is obsolete; multiple studies have instead described the brain as immunologically distinct[76].

Glioma is one of the most frequent types of brain cancer originating in glial cells. Diffuse midline glioma (DMG) and diffuse intrinsic pontine glioma (DIPG) are types of brainstem glioma, both occurring primarily in children aged 6-7 years with a median overall survival of only 9-11 months. Due to the tumour's proximity to the brainstem, surgery is often not a therapy option. DMGs and DIPGs are currently treated with radiotherapy and chemotherapy and novel treatments are highly needed [77–79].

Immunotherapy in glioma

Immune checkpoint blockade has so far not shown an improvement in overall survival in glioma patients. Among others, low mutational burden, high intratumoural heterogeneity and immunosuppressive microenvironment are proposed reasons for the failure of checkpoint inhibition in glioma[79–82]. Additionally, dysfunctional T cells are highly abundant in glioma[83].

Cancer vaccines are among the most studied cancer immunotherapies for glioma, primarily glioblastoma. Many phase II and III trials are ongoing or completed with some showing biological activity, however many have failed in the clinics due to a lack of improving overall survival of the patients[84]. In rare cases, an improvement was observed in combinatorial therapies. For example, a clinical trial using a peptide that mimics EGFR variant III (EGFRvIII), a mutant form of EGFR that is heterogeneously expressed on glioma, was terminated early since overall survival was not improved[85]. When combined with an anti-angiogenic therapy, however, a clinical trial showed initial favourable outcomes[86–88].

Due to the distinct properties of brain immunology, it is challenging to isolate TILs from the CNS. One approach to target glioma with adoptive T cell therapy is the use of CMV-specific T cells, because gliomas but not healthy brain tissue often express CMV antigens[89]. Moreover, the presence of CMV antigens in gliomas has been described to increase cellular proliferation and might be a contributing factor to cancer progression[90,91].

Studied targets for CAR T cell therapy treating gliomas are EGFRvIII, HER2 and IL-13Rα2. However, clinical trials have shown significant antigen loss after CAR T cell therapy due to the selective pressure and heterogeneity of the tumours. Additionally, due to antigen expression on normal tissues, on-target off-tumour toxicity can interfere with using CAR T cell therapy against these targets [92–95].

H3.3K27M mutation

A potential target in glioma immunotherapy is a lysine to methionine mutation in the histone 3 gene H3F3A (H3.3K27M). The missense mutation is present in the majority of DMGs, and over 75% of DIPGs express the mutant gene. The mutation leads to reduced histone-3 trimethylation (H3K27me3) pattern and is located in the conserved N-terminus of the histone. Since this locus plays an important role in accessing and regulating chromatin, the mutation has devastating effects leading to aggressive tumour progression[96,97]. Aberrant epigenetic silencing is observed in mutated histones, as methylation is hindered. This is the effect of inhibition of the enzymatic activity of the histone methyltransferase PRC2 (Polycomb repressive complex

2) by the interaction of H3.3K27M peptide with the active site of EZH2 (enhancer of zeste homolog 2)[98].

The affinity between a peptide and the MHC complex is important for the selection of a good target. The peptide-MHC affinity is measured as an IC_{50} value, giving the peptide concentration needed for 50% binding inhibition[99,100]. The H3.3K27M mutation creates an epitope ($H3.3K27M_{26-35}$, RMSAPSTGGV) that was predicted to bind HLA-A*02:01 with higher affinity (285 nM) than the wild type peptide (22651 nM)[101]. The actual affinity of H3.3K27M mutant peptide to HLA-A*02:01 was even higher (151 nM) than wild type peptide (>38687 nM) measured by using a competitive inhibition assay[102].

Table 1: Prediction of binding of peptides to MHC class I molecules (NetMHC 3.4 DTU Health Tech [101]).

	Peptide	**HLA**	**Predicted affinity (nM)**	**Measured affinity (nM)**[102]
H3.3K27M	R**M**SAPSTGGV	HLA-A*02:01	285	151
H3.3 wt	R**K**SAPSTGGV	HLA-A*02:01	22651	>38687

Peptide stimulation of HLA-A*02:01-positive donor peripheral blood mononuclear cell (PBMCs) led to the discovery of a high-affinity TCR against the mutation[102]. Moreover, an ongoing clinical trial studies the epitope for peptide vaccination in HLA-A*02:01 and H3.3K27M positive patients with DMG[103].

Alternatively, H3.3K27M expressing tumours can be targeted with GD2-CAR T cells, as the majority of H3.3K27M positive tumours express the disialoganglioside GD2 at high levels, however, more research is required to exclude on-target off-tumour toxicity as GD2 is also expressed on normal tissues[104].

1.3.2.2 Rac1P29S and Rac2P29L mutations in melanoma

Rac (Ras-related C3 botulinum toxin substrate) proteins are a subfamily of the Rho family of GTPases involved in many cellular processes including cell migration, cytoskeleton reorganization and cell transformation[105]. Due to its role to control a variety of cellular functions, aberrant Rac signalling is often involved in tumourigenesis[106,107].

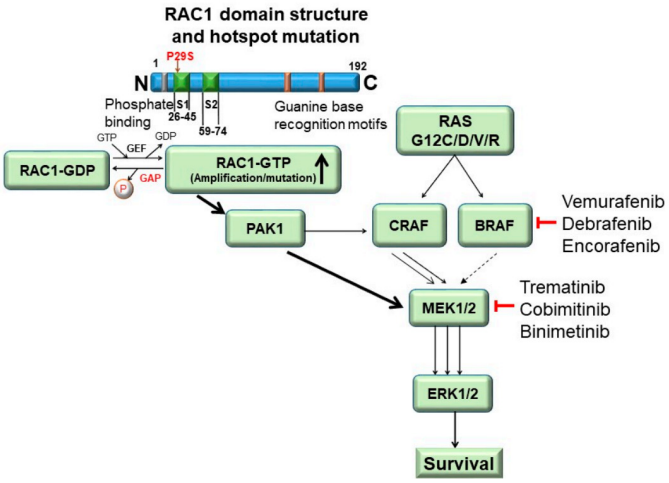

Figure 1: Role of Rac1 in tumourigenesis and drug resistance. Illustration of the downstream pathway of Rac1 after its GEF-mediated activation. Hyperactivation of Rac1 by amplification or mutation leads to Braf inhibitor resistance mediated by Mek and Erk activation by Pak1 (adapted from [108]).

The Rac family comprises Rac1, Rac2 and Rac3; this project mainly focused on Rac1 and Rac2. After Braf and Nras, the Rac1P29S amino acid change caused by a c.85C>T single-nucleotide variant (SNV), is the third most common protein-coding hotspot mutation in melanomas. Up to 9% of sun-exposed melanomas carry this mutation[109,110]. Additionally, the mutation confers resistance to Braf inhibition *in vitro*, suggesting a role of Rac1P29S mutation as a biomarker for Raf inhibitor resistance in melanoma patients[111]. Due to its importance in proliferation, metastasis and drug resistance, Rac1 is a highly important therapeutic target in melanoma. In contrast, Rac2 aberrations are less frequently found in tumourigenesis. However, a P29L (c.86C>T) mutation was also detected in a melanoma patient and a breast cancer sample, confirming an important role of the P29 position in oncogenesis[109,112,113].

Both mutations, Rac1P29S and Rac2P29L, create peptides (F**S**GEYIPTV and F**L**GEYIPTV) predicted to bind HLA-A*02:01 with high affinity, 18.2 nM for F**S**GEYIPTV and 2.3 nM for F**L**GEYIPTV (Table 2)[101]. Peptides binding to MHC class I molecules are defined as strong binders with an IC_{50} value <50 nM and a %Rank <0.5[99,100]. In contrast to the wild type peptide, both mutant epitopes are strong binders, the less frequent Rac2 mutation binds even stronger to the HLA-A*02:01 molecule.

Table 2: Prediction of binding of peptides to MHC class I molecules (NetMHC 4.0 DTU Health Tech [101])

	Peptide	HLA	Affinity (nM)
Rac1P29S	F**S**GEYIPTV	HLA-A*02:01	18.2
Rac2P29L	F**L**GEYIPTV	HLA-A*02:01	2.3
Rac1/2 wt	F**P**GEYIPTV	HLA-A*02:01	573.04

In conclusion, Rac1 is an interesting target candidate for TCR therapy, as it is specifically expressed on cancer cells and is important for the perpetual growth and survival of tumour cells. Additionally, the mutation is found in a large percentage of cancer patients and presented by a frequent HLA-molecule. Therefore, this project aims to explore this mutation (Rac1P29S) together with the less frequent Rac2P29L mutation as targets for adoptive T cells therapy.

1.3.2.3 Spliced epitopes

Some tumour antigens seem promising as targets for ATT, however, are not predicted to bind common HLA molecules with high affinity. Post-translational modifications (PTMs) can expand the repertoire of targetable tumour antigens by creating modified peptides with improved binding to HLA molecules or enhanced T cell recognition. This is an interesting field to expand the search for novel targets for ATT. Most PTMs are enzymatically mediated alterations to specific amino acids such as the deamidation of aspargine to aspartic acid [114]. For instance, T cell recognition of an HLA-A*02:01 binding tyrosinase antigen formed by deamidation has been described in melanoma cells[115].

Another type of PTM is proteasome-catalysed peptide splicing (PCPS) mediated by proteasomal subunits. Here, excised peptide fragments are fused in a reverse proteolysis reaction, leading to the formation of a novel peptide sequence that may have better MHC binding properties or stronger T cell recognition. TIL recognition of spliced peptides of the melanocytic glycoprotein $gp100^{PMEL17}$ and fibroblast growth factor-5 (FGF-5) in cancer patients is described[116,117]. As TILs are not commonly available, algorithms have been developed to predict theoretically spliced epitopes[118,119]. Predicted spliced epitopes can be confirmed by *in vitro* PCPS reaction, which has been suggested to mimic the *in cellulo* situation[120–122]. However, using this reverse immunology approach, it is crucial to confirm the endogenous generation of the predicted spliced epitopes and their recognition by T cells.

Kras is among the most commonly mutated oncogenes in cancers. A glycine to valine mutation at position 12 (G12V) is found in multiple tumours, such as pancreatic, colon and lung cancers. The mutated gene is not predicted to generate a linear high-affinity HLA-A*02:01 binding

epitope, however, using the ProtAG algorithm, a spliced epitope is predicted to bind HLA-A*02:01 with an affinity of 33.4 nM. This spliced epitope is a nonamer fusion of Kras G12V positions 5-8 and 10-14 (KLVV/GAVGV)[101].

Another potential spliced target identified using the ProtAG algorithm is the FLGEYIP/VF Rac2P29L epitope, which is predicted to bind to HLA-A*02:01 with an IC50 of 24.7 nM[101,119]. As described above, the Rac2 mutation is found in human cancers such as melanoma and breast cancer. Broadening the repertoire of potential T cell binding epitopes by including spliced epitopes might expand the applicability of Kras and Rac2 as targets for ATT.

Table 3: Prediction of binding of peptides to MHC class I molecules (NetMHC 4.0, 2020, DTU Health Tech [101,119]).

	Peptide	**HLA**	**Affinity (nM)**
KrasG12V spliced	KLVV/GA**V**GV	HLA-A*02:01	33.4
KrasG12V linear	KLVVVGA**V**G	HLA-A*02:01	9675.66
Rac2P29L spliced	F**L**GEYIP/VF	HLA-A*02:01	24.7

1.3.3 ABabDII mice as a source of human TCRs for T cell therapy

The isolation of antigen-specific TCRs from patients is challenging. Especially high-affinity TCRs against TAA are often not found in patients due to tolerance mechanisms. An alternative source for optimal HLA-A*02:01 restricted TCRs against both TAAs and TSAs is a transgenic mouse model expressing a diverse human TCR repertoire (ABabDII)[123]. The mouse model expresses the entire human TCRαβ gene loci as well as an HLA-A*02:01 human transgene, while the murine counterparts are knocked out. After immunisation, the mice elicit an immune response inducing functional $CD8^+$ T cells against a specific antigen. The therapeutic potentials of the isolated TCRs are shown in a publication by Obenaus et al. describing the isolation and characterisation of MAGE-A1-specific TCRs isolated from the ABabDII mice [124].

2. Aims

Based on the importance of finding suitable targets for cancer immunotherapy, this thesis focused on exploring different strategies to target cancer mutations for ATT. Firstly, a potential neoepitope was studied which is recurrent in glioma, a tumour with limited available treatment options. The second part focused on the heterologous target recognition of a TCR that was isolated after immunisation with a peptide with higher peptide-MHC affinity. Lastly, the potential of post-translationally modified peptides was explored by studying the TCR recognition of two putative proteasomally spliced neoepitopes.

2.1 Characterisation of a histone mutation H3.3K27M as a suitable target for cancer immunotherapy

Due to its recurrence and binding to the common HLA-A*02:01 molecule, the H3.3K27M$_{26-35}$ histone mutant epitope possesses important characteristics of an ideal target for ATT. However, it remains unclear whether the target is also sufficiently processed and presented for T cell recognition. To test this, an H3.3K27M peptide-specific TCR was isolated and used to validate H3.3K27M as a target for ATT. It is crucial to confirm the efficiency of this target, as there are clinical trials ongoing to target this mutation[103].

2.2 Characterisation of Rac1/2-specific T cells against Rac1P29S mutation

In addition to using the recurrent mutated HLA-A*02:01 binding peptide Rac1P29S for TCR isolation in a transgenic mouse model, a heterologous target Rac2P29L was also used for immunisation. The Rac2P29L mutation, which differs from Rac1P29S in only one amino acid, is less common in tumourigenesis; however, it is predicted to bind HLA-A*02:01 with higher affinity. Besides TCR affinity, the binding of the peptide to its MHC molecule is highly important for the TCR interaction with the peptide-MHC complex. High peptide-MHC affinity epitopes are described to mediate tumour eradication and prevent relapse[125]. In this project, the hypothesis was tested, if immunisation with a higher peptide-MHC affinity epitope can lead to the isolation of better TCRs for a more frequent heterologous target. Isolated high-affinity Rac1/2 TCRs were used to validate the recurrent Rac1P29S mutation as a target for ATT.

2.3 Characterisation of two spliced epitopes as targets for adoptive T cell therapy

Proteasome-catalysed peptide splicing can potentially broaden the repertoire of cancer-specific targets by creating MHC binding peptides and/or by enhancing TCR recognition. However, it

remains unclear how abundant spliced peptides are and if they play a role as T cell targets. In this thesis, TCRs against mutations in Kras and Rac2 were tested, whereas for instance for the most common oncogene Kras a suitable linear T cell epitope is not available in HLA-A*02:01. The TCRs were isolated after immunisation of human TCR gene loci transgenic mice with predicted spliced peptides.

3. Materials & Methods

3.1 Peptide immunisation of mice

Mutation-specific T cells were generated in ABabDII mice expressing a diverse human TCR repertoire[123]. Mice were immunised by subcutaneous injection of 100 µg H3.3K27M (R**M**SAPSTGGV), Rac1P29S (F**S**GEYIPTV), Rac2P29L (F**L**GEYIPTV), Rac2P29L spliced (F**L**GEYIPVF) or KrasG12V spliced (KLVVGA**V**GV) peptide in a 1:1 solution of incomplete Freund's adjuvant and PBS containing 50 µg CpG. After priming, the mice received the same immunisation twice as boosts in a three weeks interval. To assess $CD8^+$ T cell responses, peripheral T cells were restimulated *in vitro* with either 10^{-6} M peptide, PBS as a negative control, or 10^6 Dynabeads mouse T activator CD3/CD28 (Gibco) as a positive control. After 2h, Brefeldin A (BD) was added to the cultures and after overnight culturing, specific $CD8^+$ T cells were measured by intracellular IFNγ staining (PE anti-mouse IFNγ XMG1.2, Biolegend).

3.2 Isolation and cloning of TCRs

To isolate specific TCRs, immunised mice were sacrificed; splenocytes and lymphocytes from inguinal lymph nodes were prepared and $CD4^+$ T cells were depleted using microbeads (Miltenyi Biotec). $1x10^6$ splenocytes were cultured in T cell media (TCM, RPMI (Gibco™) containing 10% FCS (Pan Biotech), 1 mM HEPES (Gibco™), 100 IU/ml PenStrep (Gibco™), 50 µM 2-Mercaptoethanol (Gibco™)) supplemented with 100 IU/ml IL-2 (Peprotech) for 10 days in the presence of 10^{-8} M peptide. Four hours prior to the *in vitro* assessment of IFNγ secretion (mouse IFNγ secretion assay, Miltenyi), cells were stimulated with a peptide concentration of 10^{-6} M. To sort IFNγ-secreting $CD8^+$ T cells, cells were stained with anti-mouse CD3-APC (145-2C11, Biolegend) and anti-mouse CD8-PerCP (53-6.7, Biolegend) at 4°C for 30 minutes before the cells were sorted (BD FACS Aria III) into RTL lysis buffer for RNA isolation with RNeasy Micro Kit (QIAGEN). SMARTer™ RacE cDNA Amplification Kit (Clontech Laboratories) was used to synthesise first-strand cDNA synthesis and 5'-RACE PCR. The TCR sequence was specifically amplified using 0.1 µM hTRAC (5'-cggccactttcaggaggaggattcggaac-3') or hTRBC (5'-ccgtagaactggacttgacagcggaagtgg-3') specific primer in a 1-2 µl reverse transcriptase reaction together with 1U Phusion® HotStart II polymerase (Thermo Scientific). The amplicons were analysed on an agarose gel and specific bands were cut out and cloned using a Zero Blunt® TOPO® PCR cloning kit (Life Technologies). A T3 primer (5'-aattaaccctcactaaaggg-3') was used to sequence plasmids from

isolated individual clones (Eurofins Genomics). The dominant TCR-α/β chains were selected and paired as follows:

Table 4: List of TCRs. Name of TCR, details of the alpha and beta chains as well as the CDR3 region are listed

TCR	α chain	β chain	Specificity
27633	TRAV13*01 – CAVRGLTQGGSEKLVF – TRAJ57*01	TRBV27*01 – CASSWGGFPYEQYF – TRBJ2-7*01	H3.3K27M
1H5 [126]	TRAV19*01 – CALSEENDMRF – TRAJ43*01	TRBV27*01 – CASGWGGPYEQYF – TRBJ27*01	H3.3K27M
14/35[127,128]	TRAV20 – CAVQSGTSGSRLTF – TRAJ58	TRBV9 – CASSVVAGFNEQFF – TRBJ2-1	CDK4R24L
A12B20	TRAV12-2*02 – CAAQSARQLTF – TRAJ22*01	TRBV20-1*01(/02) – CSARDLITDTQYF – TRBJ2-3*01	Rac1P29S
5934	TRAV13-1*01– CAASRGGAQKLVF – TRAJ54*01	TRBV3-1*01 – CASSQLAGGPLYNEQFF – TRBJ2-1*01	Rac1P29S
22894	TRAV13-1*03 – CAVGANNLFF – TRAJ39*01	TRBV2*01 – CAASMGNAGNMLTF – TRBJ2-7*01	Rac2P29L
1376[119]	TRAV5*01 – CAESTDSWGKLQF – TRAJ24*02	TRBV4-1*01 – CASSQDLAGYEQYF – TRBJ2-7*01	KrasG12V splice1
20967A2[119]	TRAV20*02 – CAVQAPDSGNTPLVF – TRAJ29*01	TRBV2*01 – CASSDRGAYNEQFF – TRBJ2-1*01	Rac2P29L splice

Corresponding TCR-α/β chains were linked using a P2A element and constant regions of both, the human-derived and mouse-derived TCRs were exchanged with mouse constant regions. The codon-optimised TCR cassettes were synthesised by GeneArt (Thermo Fisher Scientific) and cloned into an MP71 vector as NotI/EcoRI fragments.

3.3 Plasmid constructs and cDNA synthesis

All retroviral packaging plasmid vectors were based on plasmid MP71[129]. Plasmids MP71-A2 encoding HLA-A*02:01, and MP71-CDK4-R24L-i-GFP encoding the full-length cDNA of CDK4 harbouring the R24L mutation and co-expressing EGFP through an IRES element, were a kind gift from M. Leisegang. In order to construct MP71_H3.3K27M-CDS-i-GFP and MP71_H3.3-CDS-i-GFP, expressing H3F3A mutant and wild type full-length cDNA respectively, H3F3A coding sequences were cloned by RT-PCR from cDNA samples synthesised from RNA isolated from SF8628 cells. In brief, RNA was isolated from $5x10^5$ cells using the RNeasy Isolation Plus Mini Kit (QIAGEN). cDNA synthesis was performed with 1 µg of total RNA as template and random hexamers, using the Advantage RT-for-PCR Kit

(Takara Bio) according to manufacturer's protocol. H3F3A coding sequences were amplified by PCR using primers GP001_H3F3A (5'-aaagcggccgcaccatggctcgtacaaagcag-3') and GP002_H3F3A (5'-aaactcgagattcttaagcacgttctccacgta-3') conferring NotI and XhoI restriction sites respectively. The IRES-EGFP element was cloned by PCR using primers GP003_IRES (5'-aaactcgagacgtggcggctagtactcc-3') and GP004_GFP (5'-aaagaattcttgtacagctcgtccatgc-3') conferring XhoI and EcoRI restriction sites respectively. Fragments were digested with the respective restriction enzymes (NEB) and cloned in a two-fragment ligation (DNA ligation mix, Mighty Mix, Takara Bio) into NotI/EcoRI digested MP71. Clones were sequenced and both K27M and wild type clones were selected. To construct MP71-CDK4R24L-P2A-GFP, MP71_H3.3K27M-CDS-P2A-GFP and MP71_H3.3-CDS-P2A-GFP, a P2A-EGFP fragment was PCR amplified from plasmid pcDNA3.1-Hygro(+)-M7PG (kind gift V. Anastasopoulou) using either primer H3.3-P2A_F (5'-acgccgcatacgtggagaacgtgctggcagcggcgccaccaac-3'), or CDK4-P2A_F (5'-acataaggatgaaggtaatccggagggcagcggcgccaccaac-3') combined with GFP-PRE_Rev (5'-aatggcggtaagatgctcgaatttcatttgtacagctcgtccatgc-3'). Produced amplicons bear homologies to the above plasmids and can serve to prime overlap extension PCR (OE-PCR), replacing the IRES-EGFP elements with P2A-EGFP. In brief, the respective OE-PCR amplicon was mixed in a 200 molar excess ratio to 10 ng of either one of MP71-CDK4-R24L-i-GFP, MP71_H3.3K27M-CDS-i-GFP or MP71_H3.3-CDS-i-GFP, in 25 µl PCR reactions and were cycled, using 52°C annealing temperature and a 7-minute extention time at 72°C, for 21 cycles. Reactions were subsequently digested with DpnI and transformed into competent E. coli. H3.3K27M and H3.3 triple-epitope minigenes, encoding three tandem copies of the respective decamer epitope followed by EGFP, separated by the preferred proteasome cleavage site AAY, were synthesised (GeneArt Gene Synthesis, ThermoFischer Scientific) and were cloned into MP71 as NotI/EcoRI fragments (MP71_[triple-H3.3K27M]-GFP and MP71_[triple-H3.3]-GFP). All PCRs described were performed using Q5, High fidelity 2x Master mix (NEB). Unless stated otherwise, all other constructs were synthesised by GeneArt Gene Synthesis, ThermoFischer Scientific and are followed by an AAY sequence and EGFP.

3.4 Cells and cell culture

The cell lines SF8628 (RRID:CVCL IT46, SCC127 Sigma-Aldrich) and A2DR1[130] were cultured in DMEM (Gibco™) supplemented with 10% FCS (Pan Biotech) and 100 IU/ml PenStrep (Gibco™). The human DIPG cell line SF7761 (RRID:CVCL_IT45, SCC126 Sigma-Aldrich) was grown as neurospheres in suspension culture and cultured in ReNcell NSC Maintenance Medium (Cat. No. SCM005), containing 20 ng/mL EGF (Cat. No. GF001), 20

ng/mL FGF-2 (Cat. No. GF003) and 100 IU/ml PenStrep (Gibco™). The retroviral packaging cell lines 293GP-GLV (producing amphotropic retroviral vectors) and Plat-E (producing ecotropic retroviral vectors) were cultured in DMEM supplemented with 10% FCS[131,132]. TAP-deficient T2 cells (RRID:CVCL_2211, ATCC: CRL-1992) and human PBMCs were cultured in T cell media (TCM, RPMI (Gibco™) containing 10% FCS (Pan Biotech), 1 mM HEPES (Gibco™), 100 IU/ml PenStrep (Gibco™), 50 µM 2-Mercaptoethanol (Gibco™)). Mouse T cells were cultured in mouse T cell mesia (mTCM, RPMI (Gibco™) containing 10% FCS (Pan Biotech), 100 IU/ml PenStrep (Gibco™), 50 µM 2-Mercaptoethanol (Gibco™) and Sodium Pyruvate). The cell lines Mel624 (RRID:CVCL_8054), UKRV-Mel-21a (referred to hereafter as Mel21a)[133], Mel20aI (RRID:CVCL_A157), MaMel085 (called here Mel085) (RRID:CVCL_A220), Mel55b (RRID:CVCL_A190), MCF7 (Sigma-Aldrich), HCC1143 (RRID:CVCL_1245), NIH-HHD[134], SW480 (ATCC: CRL-228), SW620 (ATCC: CRL-227) were cultured in RPMI (Gibco™) supplemented with 10% FCS (Pan Biotech) and 100 IU/ml PenStrep (Gibco™). U87MG ATCC (RRID:CVCL_0022) glioblastoma cells were cultured in MEMα (Gibco™) supplemented with 10% FCS (Pan Biotech) and 100 IU/ml PenStrep (Gibco™) [135]. The human cell lines with KrasG12V mutation were obtained from ATTC (AsPC-1 [ATCC: CRL-1682]; Capan-1 [ATCC: HTB-79]; CFPAC-1 [ATCC: CRL-1918]; NCI-H441 [ATCC: HTB-174]; NCI-H727 [ATCC: CRL-5815]; Panc 03.27 [ATCC: CRL-2549]; SW480 [ATCC: CRL-228]; SW620 [ATCC: CRL-227]) or Sigma-Aldrich (Colo668). MC703 cells were kindly provided by M. Leisegang and described in[127].

3.5 Retroviral transduction of TCRs into primary T cells

TCR gene transfer was carried out as described before[129,136]. In brief, for retrovirus generation, 293GP-GLV cells were transfected with MP71 vector carrying the respective TCR cassettes using Lipofectamine 3000 (ThermoFisher Scientific). On the same day, PBMCs from healthy donors were seeded on plates coated with 5 µg/ml anti-CD3 (OKT3, Invitrogen) and 1 µg/ml anti-CD28 antibodies (CD28.2, Invitrogen) in TCM supplemented with 100 IU/ml IL-2 (Peprotech). 48 hours later, the virus supernatant was harvested, filtered and supplemented with 8 µg/ml protamine sulfate (Sigma-Aldrich) and 100 IU/ml IL-2, before spinoculation with the activated T cells at 800g for 90 minutes at 32°C was performed. The next day, a second supernatant was harvested from the same 293GP-GLV cells, transferred to a RetroNectin (Takara Bio) coated plate and centrifuged at 3200g for 90 minutes at 4°C. The PBMCs were harvested, supplemented with 100 IU/ml IL-2 and 8 µg/ml protamine sulfate and spinoculated with the virus-containing plates at 800g for 30 minutes at 32°C. After the second transduction,

T cells were expanded for 10 days, before being transferred to low IL-2 (10 IU/ml). After 48 hours, transduced T cells were harvested, analysed for TCR expression by flow cytometry and frozen for future experiments. To detect the transduction rate of the TCRs transduced into primary T cells, the following antibodies were used in a 1:100 dilution at 4°C for 30 min: anti-human CD3-PerCP (UCHT1, Biolegend), anti-human CD8-APC (HIT8a, Biolegend) and anti-mouse TCR β chain-PE (H57-597, Biolegend).

For mouse transductions, Plat-E cells were transfected with MP71 vector carrying the respective TCR cassettes using Lipofectamine 3000 (ThermoFisher Scientific). On the following day, spleen cells were isolated from TCR1xCD45.1xRag1-/- mice and erythrocytes were lysed by ammonium chloride treatment. $2x10^6$/ml cells were incubated in mTCM supplemented with 1 µg/ml anti-mouse CD3, 0.1 µg/ml antimouse CD28 antibodies (BD Biosciences (BD), Franklin Lakes, NJ, USA) and 10 IU/ml human IL-2 (Proleukin S, Novartis, Basel, Switzerland). On the next day, $1x10^6$ cells were transduced by spinoculation in 24-well non-tissue culture-treated plates pre-coated with 12.5 µg/ml RetroNectin (TaKaRa, Otsu, Japan) and virus particles (3200 x g, 90 min, 4 °C) in 1ml mTCM supplemented with 10 IU/ml IL-2 and $4x10^5$ mouse T-Activator beads (Life Technologies). A second transduction was performed on the following day by spinoculation with 1 ml virus supernatant ($^+$ 10 IU/ml IL-2). T cells were expanded in mTCM ($^+$ 50 ng/ml IL-15 (Miltenyi Biotec, Bergisch Gladbach, Germany)) for 10 days. TCR transduction rate was measured by flow cytometry using the following antibodies in a 1:100 dilution at 4°C for 30 min: anti-mouse CD3-BV421 (UCHT1, Biolegend), anti-mouse CD8-APC (HIT8a, Biolegend) and anti-mouse TCR vβ12-FITC (H57-597, Biolegend).

3.6 Retroviral transduction of tumour cell lines

SF8628-A2, SF7761-A2 and Mel085-A2 cells were generated by transfecting MP71-HLA-A*02:01 into 293GP-GLV cells using Lipofectamine 3000 (ThermoFisher Scientific). 48 hours after transfection, 293GP-GLV virus-containing supernatant was harvested, supplemented with 8 µg/ml protamine sulfate and transferred to the respective glioma cell line. Cells and virus supernatant were spinoculated at 800g for 90 minutes at 32°C. The medium was changed to the respective growth medium 6 hours later. The same transduction protocol was used to overexpress constructs describe in the section plasmid constructs above. To analyse successful transduction, flow cytometry was used to determine the fraction of GFP-positive cells. HLA-A*02:01 transduction was confirmed by flow cytometry using an anti-human HLA-A*02:01-APC (BB7.2, Biolegend) specific antibody and an APC mIgG2b, k isotype control (MPC-11,

Biolegend). MCF7, 624Mel and NIH-HHD cells were retrovirally transduced with the following Kras-specific triple-epitope minigenes separated by AAY and followed by GFP: Kras 35mer G12V$_{1-35}$, Kras linear 10mer G12V$_{5-14}$, Kras spliced 9mer G12V$_{5-8/10-14}$, Kras spliced 9mer wt$_{5-8/10-14}$. NIH-HHD and Mel21a cells were transduced with the following Rac constructs separated by AAY and followed by GFP: Rac2 linear 45mer P29L$_{1-45}$, Rac2 spliced 9mer P29L$_{28-34/36-37}$, Rac2 cDNA. Mel55, Mel085-A2 and Mel20aI cells expressing CDK4R24L-GFP were generated by retroviral transduction using MP71 plasmid expressing the R24L mutant CDK4 full-length cDNA followed by a p2A element and GFP. MC703 cells were transduced with a triple epitope construct of Rac1P29S nonamer separated by AAY cleavage sites tagged with GFP (5'LTR – (P29S)$_3$ – GFP – PRE – 3'LTR) [127].

3.7 Co-culture experiments

All co-culture experiments to detect IFNγ secretion were conducted using $1x10^4$ - $1x10^5$ transduced T cells with $1x10^4$ -$1x10^5$ target cells as indicated for 22-24 hours in a 96 well plate. As a positive control for the T cell activation, 50 ng/ml PMA (Phorbol-12-myristat-13-acetat, (Calbiochem) and 1 µg/ml Ionomycin (Calbiochem) were added to the transduced T cells. T2 cells were loaded with the labelled peptides (JPT Peptide Technologies GmbH) at the indicated concentrations. Secreted IFNγ, TNF and IL-2 amounts in the supernatant were measured by ELISA (BD OptEIA; BD Biosciences).

3.8 Western blot

To determine the endogenous expression and overexpression of the H3.3K27M mutation in the SF8628 and Mel624 cells, $2x10^6$ tumour cells were lysed using a lysis buffer containing 2% SDS and 0.05 M TrisHCl for 10 minutes at 95°C. Subsequently, the protein concentration was measured using the Total Protein Kit, Micro-Lowry (Sigma). 25 µg of protein in LDS sample buffer and DTT was loaded onto a NuPage 4-12% Bis-Tris 1,5 mm gel (Invitrogen) next to a Full Range Rainbow Protein ladder (Sigma-Aldrich) and ran at 200V, 250mA for 42 minutes. The separated proteins were transferred onto a PVCF membrane for 1h at 30V and 250mA. After blocking in 5% milk in TBST, the membrane was incubated in either an H3.3K27M specific antibody (RM192, Rabbit mAb, Abcam) or a beta actin specific antibody (Rabbit mAb, Cell Signaling) diluted 1:1000 in 5% milk shaking at 4°C overnight. The membrane was washed three times for 15 minutes in TBST and stained with a secondary HRP coupled anti-rabbit IgG (Cell Signaling) diluted 1:2000 in 5% milk at room temperature for one hour. After washing, the membrane was soaked in ELC substrates (ThermoFisher) and exposed for 10 minutes on a ChemiDoc XRS$^+$ Gel Imaging System (Biorad).

3.9 Quantitative analysis of cDNA overexpression

cDNA synthesis from all samples was performed as described above. Samples were then diluted 1:5 and 5 µl used as templates in a 20 µl qPCR reaction using SYBR Green PCR Master Mix (Thermo), with 500 nM primer concentration. Following primers were used for real-time PCR. H3.3: F:5'-taaagcacccaggaagcaac-3', R:5'-gtcttcaaaaaggccaacca-3', GAPDH: F:5'-gtgaaggtcggagtcaacg-3', R:5'-tgaggtcaatgaaggggtc-3' Samples were run on the QuantStudio 3 Real-Time PCR system (ThermoFisher) and analysed according to the comparative ΔΔCt method. Samples were sent for sanger sequencing (Eurofins Genomics) to confirm the presence of wild type and mutant H3.3 genes.

3.10 CRISPR/Cas9 knockout of endogenous TCRs

To knock out the endogenous TCR in transduced T cells, the CRISPR/Cas9 system was used with TRAC-gRNA: agagucucucagcugguaca[137] and gRNA2: uggcucaaacacagcgaccu[138] targeting the endogenous human TCR alpha and beta constant regions, respectively. Before RNP complexing, transduced cells were thawed and cultured for one hour in TCM and 10 IU/ml IL-2. Subsequently, cells were washed 2x in TCM and resuspended at $5x10^7$/ml in OptiMEM. 150 pmol of Alt-R tracrRNA (IDT) were annealed to 150 pmol of the respective Alt-R crRNAs (IDT) according to manufacturer's instructions. The resulting TRAC-gRNA and gRNA2 were complexed with 50 pmol Alt-R S.p. HiFi Cas9 Nuclease V3 (IDT) and the RNP complexes were nucleofected into 10^6 T cells in 20 µl OptiMEM, using pulse EO-115 on Lonza 4D-Nucleofector™ Core Unit in Opti-MEM (Gibco™). The cells were cultured for 4 days in TCM containing 10 IU/ml IL-2 and the knockout efficiency of the endogenous TCR was measured by flow cytometry. To analyse the expression of endogenous and transduced TCR, the T cells were first stained with 10 µl of HLA-A*02:01 H3.3K27M Dextramer-PE (Immudex) per 50 µl PBS containing 50% FCS at room temperature for 30 minutes. After washing, the following antibodies were added in a 1:100 dilution at 4°C for 30 minutes in PBS containing 5% FCS: anti-human CD3-PerCP (UCHT1, Biolegend), anti-human CD8-BV421 (HIT8a, Biolegend), anti-human TCR α/β-FITC (BW242/412, Miltenyi Biotec) and anti-mouse TCR β chain-APC (H57-597, Biolegend).

3.11 Cytotoxicity assay

The cytotoxic potential of transduced T cells was analysed using the live cell imaging system IncuCyte Zoom (Essen Bioscience). $3\text{-}5x10^3$ GFP positive target cells were resuspended in TCM without phenol red and seeded into flat-bottom 96 well plates. The following day,

transduced T cells in a 5:1 or 15:1 (effector: target) ratio were added to the respective wells in triplicates. GFP expression in target cells was determined every hour over a time period of 72 hours at 37°C and 5% CO2. For analysis, the average of GFP total area (µm²/image) in the target cells co-cultured with the respective TCR-transduced T cells was calculated and normalised to the average of GFP total area (µm²/image) of the same target cells co-cultured with mock-transduced T cells (% of mock T cells).

3.12 Immunoprecipitation of HLA class I bound peptides

$5x10^6$ U87MG cells overexpressing either full-length cDNAs H3.3K27M or CDK4R24L were injected into NSG mice (performed by EPO, Experimental Pharmacology & Oncology Berlin-Buch). At a size of 1.5-2 cm^3 tumours were isolated and 500 mg tumour pieces snap frozen in liquid nitrogen. Samples were dry cryopulverised immediately using the cryoPREP (Covaris) device. Next, quadruplicate samples of each cell line were lysed using 2xCHAPs buffer containing 400mM TrisCl pH 8.0, 300mM NaCl, 2%CHAPs (Serva) and 2x protease inhibitor (ThermoFisher Scientific) in HPLC grade ultrapure water. To avoid unspecific binding to the beads, the samples were incubated at 4°C for 1 hour with 50 µl/ml ProteinA-Sepharose beads (Merck). Next, samples were stained with 60 µg/ml HLA binding antibody (W6/32, Biolegend) at 4°C for 1 hour. For immune-affinity purification, 100 µl/ml ProteinA-Sepharose beads were added to the precleared and stained samples overnight at 4°C. Samples were eluted with 10% acetic acid. The protocol was kindly provided by Dr. Xiaojing Chen.

3.13 LC-MS/MS analysis of immunoprecipitated peptides

Acidified samples were desalted on stage tips[139]. A mix of heavy synthetic versions of the mutated peptides (CDK4R24L: 25 fmol; H3-3K27M: 5 fmol; source JPT Peptide Technologies) were spiked into each sample and injected into liquid chromatography coupled to mass spectrometry on an orbitrap Exploris 480 mass spectrometer (Thermo Fisher Scientific). A 44 min gradient was applied using an EASY-nLC 1200 system (Thermo Fisher Scientific) with an in-house packed column (C18-AQ 1.9 µm beads; Dr. Maisch Reprosil-Pur 120). MS1 resolution was set to 120’000, a MIPS peptide filter with relaxed restrictions was applied, the minimum intensity threshold was specified to 50’000, dynamic exclusion occurred for 20 s and charge states 1-5+ were allowed as precursors. A mixed mode of data-dependent MS2 scans and PRM was applied with an isolation width of 1.2 Th, an MS2 resolution of 15’000 and a maximum injection time of 100 ms. The cycle time was set to 3 s. For PRM scans, a resolution of 30’000 and a maximum injection time of 150 ms was chosen. The inclusion list contained the mutated H3.3K27M and CDK4R24L peptides in their heavy and light versions at charges

2 and 3 which were identified as most suitable in pre-experiments. For database search, MaxQuant version 2.0.3.0[140] was used. Peptide and site FDRs were specified to 1% while switching protein FDR off. The heavy amino acids of the mutated sequences were set as variable modifications (proline 6 and valine 6) along with oxidised methionine (H3.3K27M peptide) and acetylated protein N-termini. Digestion mode was set to unspecific with a maximum peptide length of 25 amino acids. Match-between runs was switched on. Andromeda search was done against a human Uniprot database (2021) plus the mutated CDK4R24L and H3.3K27M peptide sequences. Downstream analysis was done in R. Quantitation of the peptides of interest was done at MS2 level using the msms.txt table from the MaxQuant output. Fragment ions for the heavy and light versions of both sequences were used for quantitation. For the final quantitation, only charge 2 precursors of the mutated peptides were included for a more robust and consistent quantitation. The LC-MS/MS analysis was performed by Dr. Oliver Popp from the BIH core facility proteomics.

3.14 Tumour challenge and adoptive T cell transfer

12-20 weeks old HHDxRag-/- mice were injected with $1x10^6$ MC703-FSG tumour cells and tumour growth was measured 2-3 times a week. 28 days after tumour injection, mice were treated by adoptive transfer of TCR-engineered HHD T cells by intravenous injection of $1x10^6$ $CD8^+TCR^+$ HHD T cells. Mice were sacrificed and tumours isolated when tumours reached the maximum permitted size.

4. Results

4.1 H3.3K27M mutation is not a suitable target for TCR gene therapy of HLA-A*02:01$^+$ patients with diffuse midline glioma

The recurrent mutation in the histone 3 variant that results in a lysine to methionine amino acid exchange (K27M) creates a potential H3.3K27M$_{26-35}$ decamer peptide epitope (RMSAPSTGGV) which is predicted to bind HLA-A*02:01 at substantial affinity. Here, the potential of this mutation as a target for adoptive T cell therapy was characterised.

4.1.1 A human TCR isolated from TCR transgenic mice recognised H3.3K27M peptide with high functional avidity

To isolate functional TCRs specific for the H3.3K27M mutation, ABabDII mice expressing a diverse human TCR repertoire restricted to HLA-A*02:01 were immunised with the H3.3K27M$_{26-35}$ decamer peptide[123]. Upon peptide restimulation of splenocytes isolated from immunised mice, a reactive CD8$^+$ cell population secreting IFNγ was detected, CD8$^+$IFNγ$^+$ cells were bulk sorted (Figure 2A) and each dominant α and β chain was identified in reactive T cell populations. The human constant regions were replaced by the respective murine ones to reduce mispairing of the endogenous and transduced TCR and the identified TCRαβ pair was synthesised as a bicistronic cassette separated by a picorna virus-derived peptide (P2A) element. The TCR cassette was subsequently cloned into the MP71 vector, followed by retroviral transduction into primary human T cells of healthy donors. The mouse-derived human TCR 27633 was chosen for further analysis and was compared to a published human-derived TCR (henceforth 1H5[102]). Both H3.3K27M-specific TCRs and a well-characterised TCR (TCR 14/35) against the irrelevant target CDK4R24L[127,128] were cloned and transduced into T cells of the same donor. After a 10-day expansion of the PBMCs, 36.4%, 30.6% and 31.4% CD8$^+$ TCR-transduced T cells, respectively, were detected (Figure 2B).

Functional avidity of both TCRs was analysed by co-culture with TAP-deficient T2 cells, exogenously loaded with decreasing concentrations of the H3.3K27M$_{26-35}$ or the wild type H3.3$_{26-35}$ peptide. Both TCRs showed strong IFNγ secretion down to a concentration of 10^{-10} M H3.3K27M$_{26-35}$, suggesting a high functional avidity of both TCRs against the mutant peptide (Figure 1C). Upon binding to the wild type peptide, the human-derived TCR 1H5 induced a robust IFNγ secretion down to 10^{-8} M peptide concentration, while the mouse-derived TCR 27633 did not (Figure 2D).

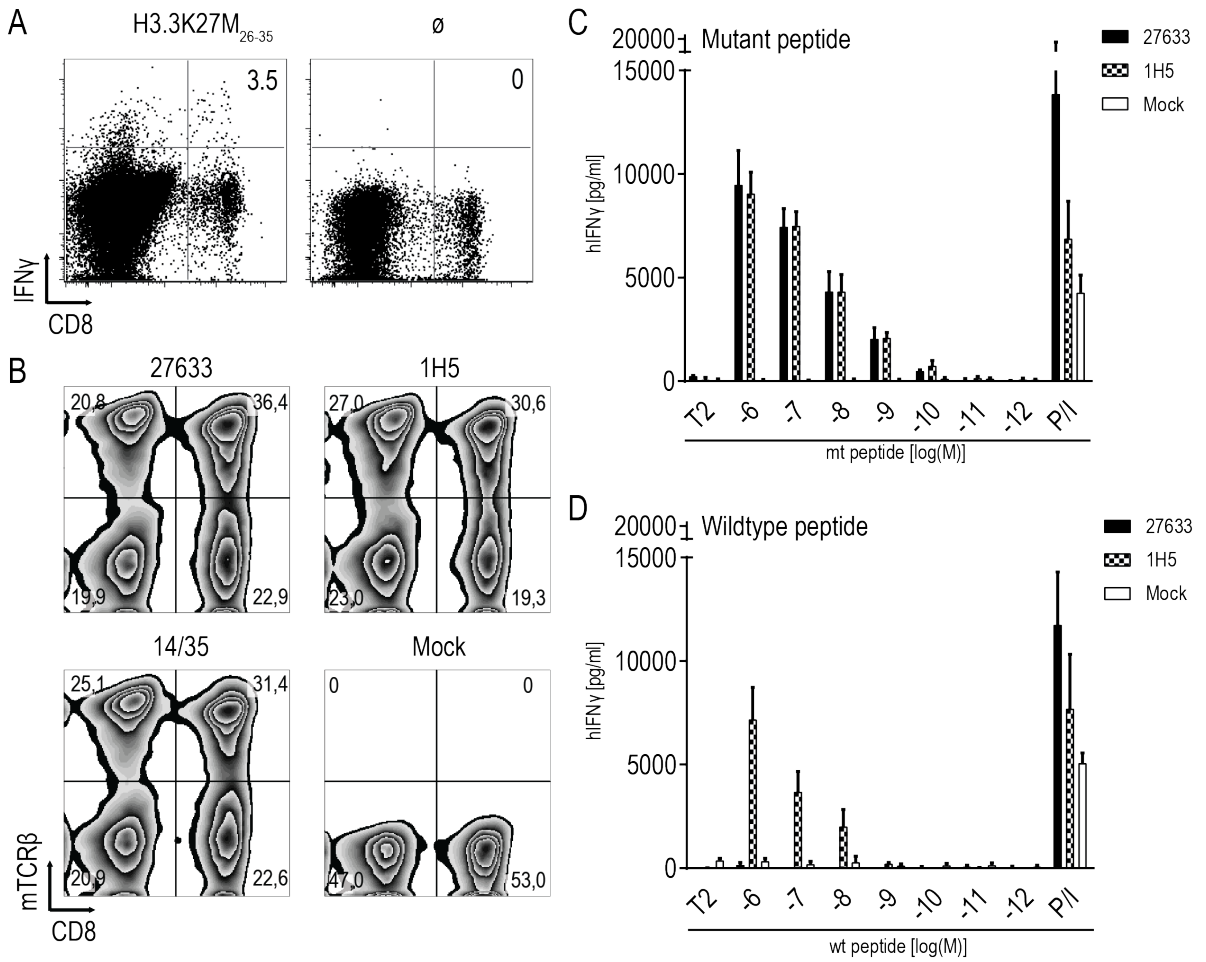

Figure 2. H3.3K27M peptide was recognised by a high avidity human TCR isolated from TCR transgenic mice. (A) Representation of a reactive $CD8^+$ cell population secreting IFNγ upon $H3.3K27M_{26-35}$ peptide (RMSAPSTGGV) restimulation of splenocytes isolated from immunised ABabDII mice, measured by intracellular staining 7 days after the last immunisation. Stimulation without peptide (Ø) was used as a negative control. **(B)** Transgenic TCR expression levels in human PBMCs after retroviral transduction with H3.3K27M-specific TCRs 27633 and 1H5[102], as well as CDK4-specific control TCR14/35[127,128] and untransduced control, were measured by flow cytometry staining for the mouse TCRβ constant region. Percentage of positive transduced $CD8^+$ T cells are shown in the top right quadrant in A and B, cells were gated on $CD3^+$. **(C, D)** Levels of IFNγ secretion of H3.3K27M-specific TCRs 27633- and 1H5-transduced PBMCs, co-cultured with T2 cells loaded with decreasing concentrations of either (C) H3.3K27M mutant or (D) H3.3 wild type peptide. A total of 10^4 $CD8^+$ transduced-TCR^+ cells were co-cultured in a 1:1 E:T ratio with T2 cells. P/I represents maximum IFNγ secretion from PBMCs stimulated with PMA/Ionomycin. The experiment was performed three times with similar results and graphs represent the means of quadruplicate cultures ±SD of one experiment.

4.1.2 Endogenously expressed H3.3K27M mutation was not recognised by specific T cells

To explore whether cells endogenously harbouring the mutation are recognised by the TCR 27633, which is an essential requirement for a potential clinical target, the H3.3K27M^{+} DIPG cell line SF8628 was retrovirally transduced to express HLA-A*02:01 (SF8628-A2) (Figure 3A). Unexpectedly, T cells transduced with either H3.3K27M-specific TCR failed to secrete IFNγ during a 24 hour co-culture with 1x10^{4} tumour SF8628-A2 effector cells (E:T, 1:1) (Figure 3B). To investigate whether this could be due to potential low (heterozygous) expression of the mutant allele in this cell line, either the H3.3K27M mutant or the wild type full-length cDNAs was overexpressed in the SF8628-A2 cells. Expression of the mutation was confirmed by western blot and the level of overexpression of both mutant and wild type cDNA was determined by qPCR (Figure 3C and Figure 3D). However, even an 18-fold overexpression of the H3.3K27M cDNA in SF8628-A2 cells did not induce IFNγ secretion by the TCR-transduced T cells (Figure 3B). In contrast, when a minigene encoding three copies of the H3.3K27M$_{26\text{-}35}$ epitope (triple epitope) leading to artificially high amounts of epitope generation due to AAY separation, a robust IFNγ response was observed, confirming HLA-A*02:01-epitope binding and TCR specificity (Figure 3B). To confirm that SF8628-A2 cells are in general capable of processing and presenting epitopes in an HLA-A*02:01 dependent manner, T cells from the same healthy donor were transduced with TCR 14/35, which specifically recognises the R24L mutation in CDK4[127,128]. As expected, overexpressed full-length CDK4R24L cDNA in the same SF8628-A2 target cells was recognised by the respective TCR, inducing strong IFNγ secretion (Figure 3B). The heterozygous expression of the H3F3A alleles was confirmed by RT-PCR and sanger sequencing (Figure 3E). These results suggest that although both H3.3K27M-specific TCRs are of high functional avidity, they failed to lead to IFNγ production against a glioma cell line, which is functional for antigen processing and presentation.

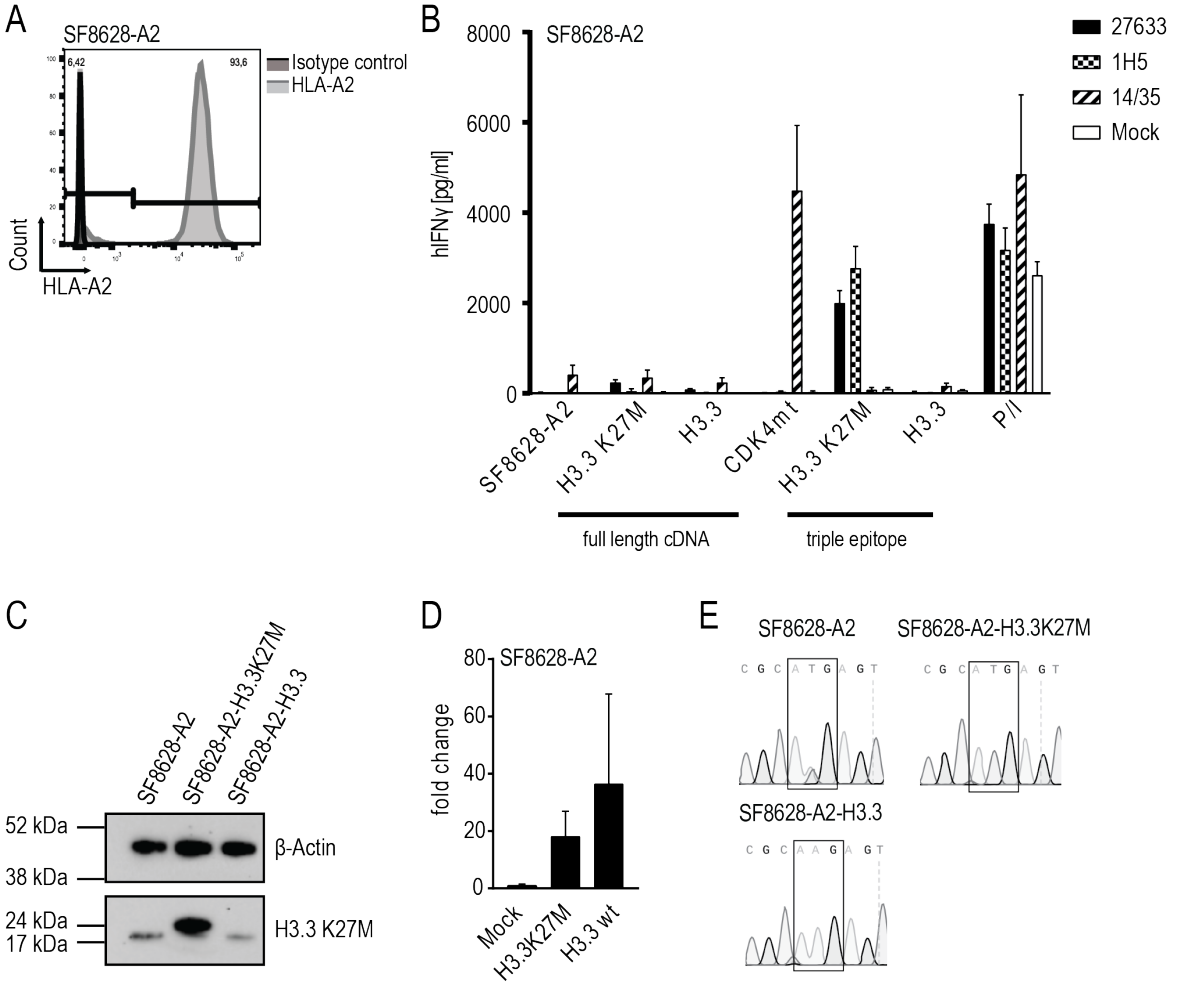

Figure 3. H3.3K27M TCR-transduced T cells failed to recognise a glioma cell line naturally expressing or overexpressing the mutant H3.3 histone. (A) The glioma cell line SF8628 was retrovirally transduced to express HLA-A*02:01. Expression levels were determined by flow cytometry using an HLA-A*02-specific antibody. **(B)** Levels of IFNγ secretion of 27633 and 1H5 TCR-transduced PBMCs, co-cultured with the human SF8628 DIPG cell line. SF8628 cells were retrovirally transduced to express HLA-A*02:01 (SF8628-A2) and additionally contained H3.3K27M full-length cDNA, H3.3 wild type full-length cDNA, CDK4R24L full-length cDNA H3.3K27M RMSAPSTGGV triple epitope, or H3.3 wild type RKSAPSTGGV triple epitope. A total of 10^4 $CD8^+$ transduced cells were co-cultured at a 1:1 E:T ratio. CDK4R24L-specific TCR-transduced T cells (14/35) were used as a positive control to assess processing and presenting capabilities of the cell line. P/I represents maximum IFNγ secretion from PBMCs stimulated with PMA/Ionomycin. The experiment was performed three times with similar results and graphs represent means of triplicate cultures ±SD. **(C)** H3.3K27M protein was detected by western blot. Top panel shows β-actin (45 kDa), lower panel shows H3.3K27M (17 kDa) in parental or transduced SF8628-A2 cells. Size discrepancy between endogenous and overexpressed mutant protein in SF8628-A2 cells is due to 18 amino acids at the C terminal end, encoded by the P2A element in the latter. **(D)** Relative quantitation of all H3.3 transcripts in SF8628-A2 cells. Bars represent fold change of H3.3 expression, normalised to H3.3 expression in the parental cell line. Expression in parental cell line was arbitrarily set to 1. Error bars represent minimum and maximum relative levels of gene expression. **(E)** Presence of endogenous or overexpressed H3.3 wild type or H3.3K27M transcripts in SF8628-A2 cells was verified by RT-PCR and sanger sequencing.

To further support this notion, the well-established, processing and presentation competent HLA-A*02:01$^+$ melanoma cell line Mel624 was used for further experiments. To assess recognition by TCR 27633, Mel624 cells were transduced to overexpress wild type or mutant H3.3 cDNAs (Figure 4A and Figure 4B), and co-cultured with H3.3K27M-specific TCR-transduced T cells. Here too, 27633- and 1H5 TCR-transduced T cells failed to produce detectable amounts of IFNγ (Figure 4C). To exclude that recognition through the transduced TCRs leads to expression of cytokines other than IFNγ, secretion of TNFα and IL-2 was analysed, but neither of the two cytokines was detected (Figure 4C). In contrast, overexpression of the CDK4R24L mutant cDNA in Mel624 cells led to recognition by the 14/35 control TCR and secretion of all three cytokines.

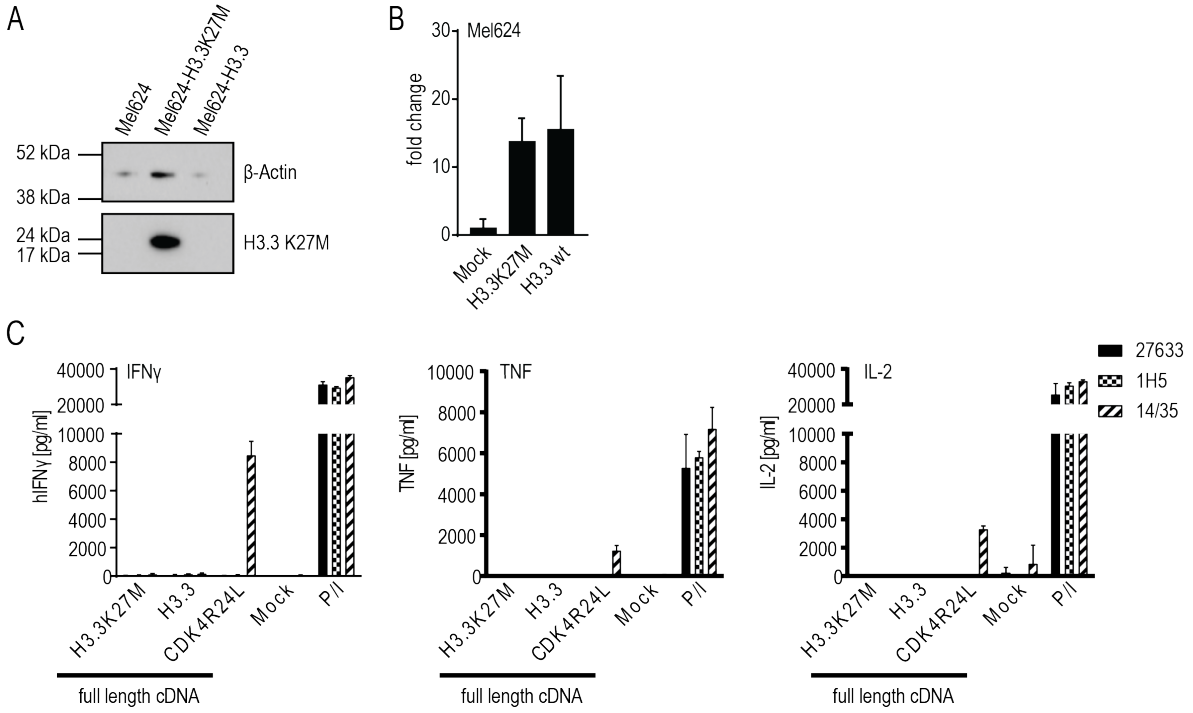

Figure 4. Lack of cytokine secretion against a well-established HLA-A*02:01$^+$ melanoma cell line overexpressing H3.3K27M mutation. (A) H3.3K27M protein was detected by western blot. Top panel shows β-actin (45 kDa), lower panel shows H3.3K27M (17 kDa) in parental or transduced HLA-A*02:01$^+$ Mel624 cells. **(B)** Relative quantitation of all H3.3 transcripts in Mel624 cells. Bars represent fold change of H3.3 expression, normalised to H3.3 expression in the parental cell line. Expression in parental cell line was arbitrarily set to 1. Error bars represent minimum and maximum relative levels of gene expression. **(C)** Levels of IFNγ, TNFα and IL-2 secretion of 27633- and 1H5 TCR-transduced PBMCs, co-cultured with the human Mel624 melanoma cell line retrovirally transduced to express either H3.3K27M, H3.3 or CDK4R24L full-length cDNA. A total of 10^4 CD8$^+$ transduced cells were co-cultured at a 1:1 E:T ratio. A CDK4R24L-specific TCR (14/35) served as a positive control for functional antigen processing and presenting machinery in Mel624 cells. P/I represents maximum IFNγ secretion from PBMCs stimulated with PMA/Ionomycin. Graphs represent means of triplicate cultures ±SD.

Additionally, a second H3.3K27M expressing DIPG cell line (SF7761) was transduced to express HLA-A*02:01 and its recognition by TCR 27633- and 1H5-transduced T cells was analysed (Figure 5A). Corroborating the above results, both TCRs were unable to recognise the endogenously expressed mutant epitope, while the exogenously loaded mutant peptide elicited a robust immune response by both TCRs (Figure 5B). The heterozygous expression of the H3F3A alleles was confirmed by RT-PCR and sanger sequencing (Figure 5C).

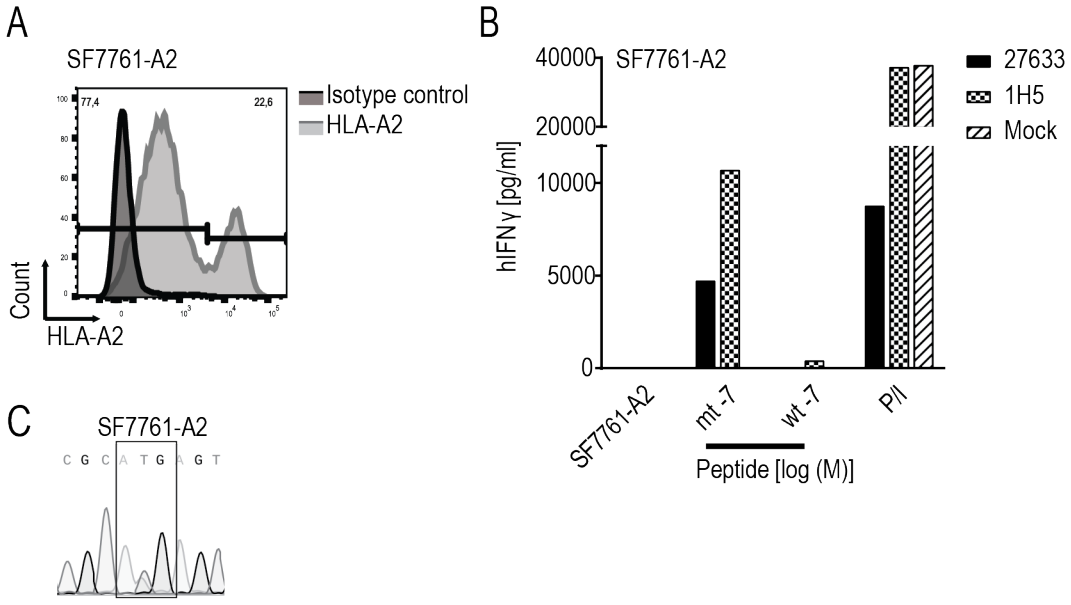

Figure 5. H3.3 overexpression profiles and failure of H3.3K27M TCR-transduced T cells to recognise DIPG cell line SF7761 endogenously expressing mutant H3.3 histone. (A) The glioma cell line SF7761 was retrovirally transduced to express HLA-A*02:01 (SF7761-A2). Expression levels were determined by flow cytometry using an HLA-A*02-specific antibody. **(B)** Levels of IFNγ secretion of 27633 and 1H5 TCR-transduced PBMCs, co-cultured with the human SF7761A2 glioma cell line, harbouring a heterozygous copy of mutant H3.3 histone. A total of 10^4 $CD8^+$ transduced T cells were co-cultured at an E:T ratio of 1:1. The experiment was performed twice and one representative experiment is shown. **(C)** Presence of endogenous or overexpressed H3.3 wild type or H3.3K27M transcripts in SF7761-A2 cells was verified by RT-PCR and sanger sequencing.

To account for possible differences between DMG/DIPG and glioblastoma (GBM) cell lines[141], either H3.3K27M or H3.3 was overexpressed, and as control, CDK4R24L full-length cDNAs in the glioblastoma U87MG cell line used by Chheda et al.[102] (Figure 6A). Again, only CDK4R24L expressing U87MG cells were recognised by the respective 14/35 TCR-transduced PBMCs, whereas neither mutant nor wild type H3.3-expressing U87MG cells induced IFNγ release in 27633 or 1H5 TCR-transduced PBMCs unless the cells were exogenously loaded with peptide (Figure 6B).

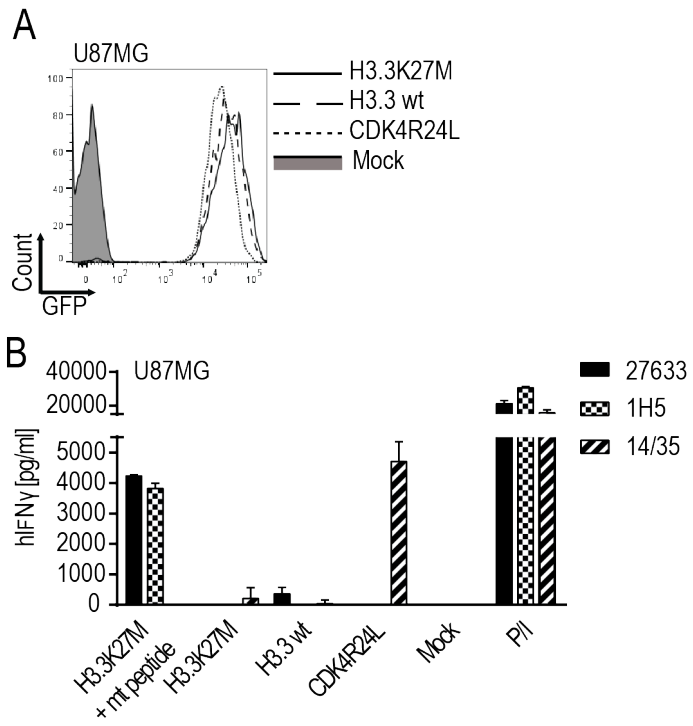

Figure 6. H3.3K27M TCR-transduced T cells failed to recognise U87MG cells overexpressing the mutant H3.3K27M histone. (A) U87MG glioblastoma cell line was retrovirally transduced with GFP tagged H3.3K27M, H3.3 wt or CDK4R24L full-length cDNA, respectively, and sorted for GFP expression. **(B)** Levels of IFNγ secretion of 27633 and 1H5 TCR-transduced PBMCs after co-culture with FACS-sorted U87MG are shown. The CDK4R24L-specific TCR (14/35) served as a positive control for functional antigen processing and presenting machinery in the U87MG cell line as well as IFNγ detection by TCR-transduced T cells.

These results showed that the H3.3K27M TCR-transduced T cells failed to produce cytokines associated with T cell cytotoxicity upon co-culture with cells naturally expressing or overexpressing the H3.3K27M mutation.

To investigate the cytotoxic potential of the H3.3K27M TCR-transduced T cells, a live-cell imaging-based cytotoxicity assay with target cells expressing GFP was used. Upon co-culture of these fluorescent target cells with the respective T cells, the number of target cells surviving was determined relative to the number of control cells over a time period of 72 hours. Consistent with the previous results, no cytotoxic effect of H3.3K27M TCR-transduced T cells was observed, neither when the mutation was expressed naturally, nor when the H3.3K27M cDNA was overexpressed. T cells transduced with either 27633 or 1H5 TCRs failed to lyse HLA-A*02:01 melanoma cell line Mel21a overexpressing full-length H3.3K27M cDNA (Mel21a-H3.3K27M; Figure 7A, top panel). In contrast, the control T cells expressing the CDK4R24L-specific TCR14/35 killed 50% of their target cells, Mel21a-CDK4R24L, within 11 hours (Figure 7A, bottom panel). Additionally, expression of the endogenous H3.3K27M mutation in

the SF8628-CDK4R24L glioma cell line did not lead to lysis by the two H3.3K27M-specific T cells, while co-culture with the control CDK4R24L-specific T cells showed substantial and prompt killing of 50% tumour cells within 9 hours (Figure 7B, top panel). As depicted in Figure 3B (bottom panel), cytotoxicity mediated by the H3.3K27M TCR-transduced T cells was only observed against target cells loaded with the mutant peptide (50% killing within 10 hours), confirming the cytotoxic potential of the H3.3K27M TCR-transduced T cells used in the assay.

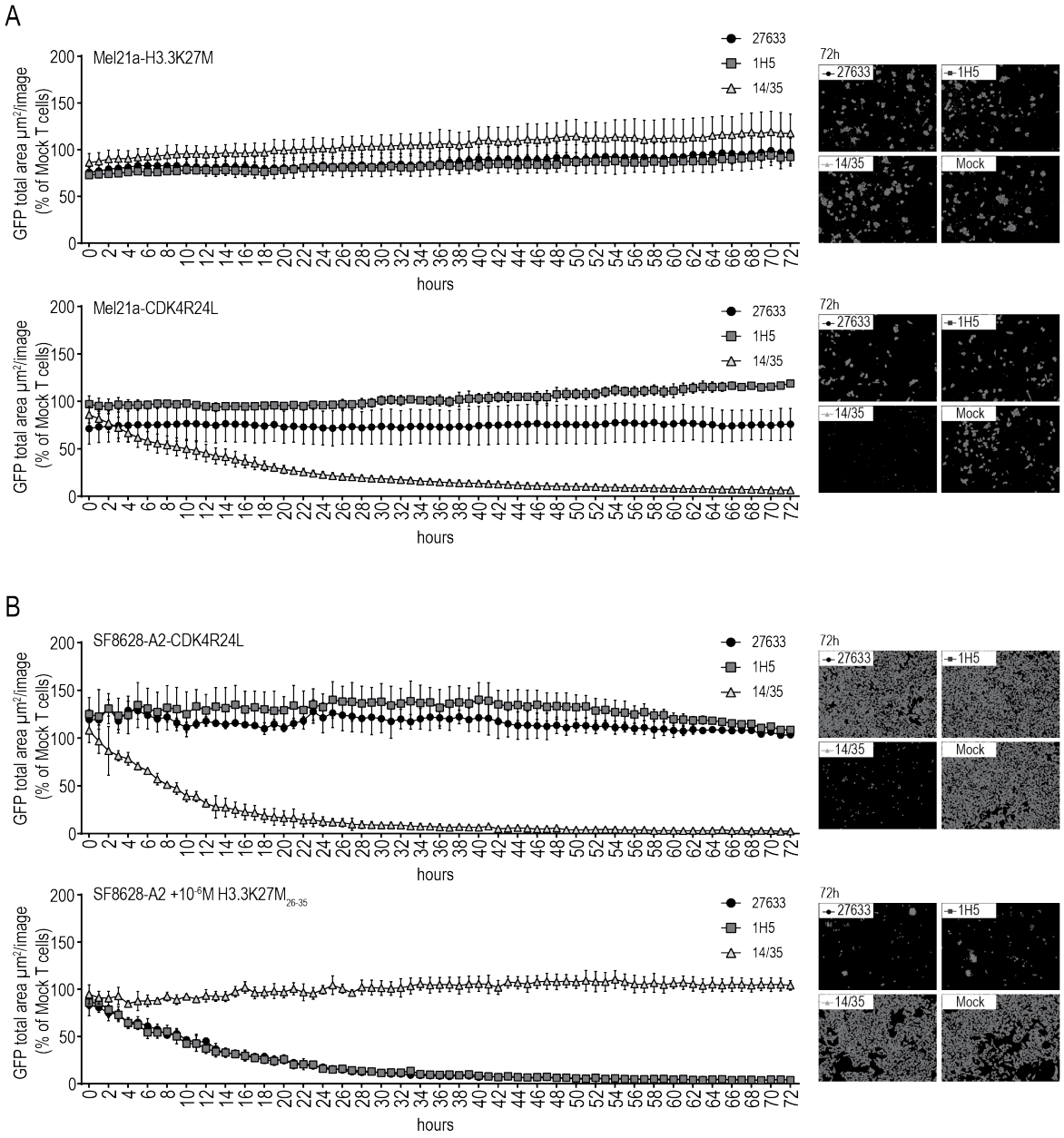

Figure 7. Lack of cytotoxicity against cells naturally expressing or overexpressing mutant H3.3 histone. (A) 15x10^3 transduced CD8$^+$ T cells were co-cultured at a 5:1 E:T ratio with HLA-A*02:01$^+$ Mel21a cells, retrovirally transduced to express either H3.3K27M full-length cDNA (top panel) or CDK4R24 full-length cDNA (bottom panel). Cytotoxicity was observed over 72 hours using the live cell imaging system IncuCyte Zoom (Essen Bioscience). Representative images are shown in the right panels. Values are calculated by normalising the average GFP total area (µm²/image) in the target cells co-cultured with the respective TCR-transduced T cells to the average of that co-cultured with mock transduced T cells. The experiment was performed three times with similar results and graphs represent means of triplicate cultures ±SD. **(B)** 15x10^3 transduced CD8$^+$ T cells were co-cultured at a 5:1 E:T ratio with SF8628-A2 cells, naturally expressing the H3.3K27M mutation and additionally either retrovirally transduced to overexpress CDK4R24L full-length cDNA (top panel) or loaded with 10^{-6} M mutant H3.3K27M peptide (bottom panel). Cytotoxicity was observed over 72 hours using the live cell imaging system IncuCyte Zoom. Representative images are shown in the right panels. Values are calculated as in (A). The experiment was performed three times with similar results and graphs represent means of triplicate cultures ±SD.

These experiments unequivocally showed that the putative mutant H3.3K27M epitope was not recognised by two independently isolated TCRs, regardless of whether the mutant gene was naturally expressed or overexpressed.

4.1.3 CRISPR/Cas9 knockout of endogenous human TCR did not induce the recognition of the H3.3K27M mutation by specific T cells

To exclude that T cell recognition of H3.3K27M was hampered by the presence of the endogenous human TCR chains resulting in mixed dimers, the endogenous TCR in the transduced human T cells was knocked out using the CRISPR/Cas9 system. To confirm the functionality of TRAC/TRBC-specific gRNAs, mock-transduced T cells were targeted with either RNP complex, which led to a knockout efficiency of 73.3% and 29.5%, respectively (Figure 8A). CRISPR targeting with both gRNAs simultaneously in mock-transduced PBMCs led to a marked decrease in the number of hTCRα/β$^+$ cells, from 90.3% to 17.4% (Figure 8B). When 27633 and 1H5 TCR-transduced PBMCs were targeted, the hTCRα/β$^+$mTCR$^+$ double positive populations, representing the population with potential mixed dimers, decreased to 5.8% from 11.6% and to 5.7% from 12.7%, respectively (Figure 8B). CRISPR/Cas9-edited TCR-modified T cells were co-cultured with SF8628-A2 cells, either naturally expressing the H3.3K27M mutation, or overexpressing full-length H3.3K27M cDNA, as well as with H3.3K27M$_{26\text{-}35}$ peptide-loaded T2 cells. As depicted in Figure 8C, no alteration in the capacity of T cells lacking the endogenous human TCR to recognise the expressed mutation was observed. The endogenous, as well as the overexpressed mutation, were still not recognised by the TCR-modified T cells, whereas H3.3K27M$_{26\text{-}35}$ peptide-pulsed T2 cells induced IFNγ secretion by TCR-modified T cells to previously observed levels. Again, 1H5 TCR-modified T cells also recognised wild type H3.3$_{26\text{-}35}$ peptide-pulsed T2 cells, as already shown in Fig 1D. When analysing the binding of H3.3K27M-specific MHC I dextramer, no significant difference in staining intensity was detected for CD8$^+$ T cells expressing H3.3K27M-specific TCRs. Thus, CD8$^+$Dextramer$^+$ T cells modestly decreased upon CRISPR/Cas9 knockout from 23.8% to 19.9% for 27633 TCR and increased from 27.3% to 30% for 1H5 TCR. Additionally, no change in the mean fluorescence intensity (MFI) was observed between both panels. Surprisingly, 22.6% (-Cas9 RNP) and 21.8% (+Cas9 RNP) of CD4$^+$ T cells expressing the human-derived TCR 1H5 were also stained with the dextramer, suggesting that MHC-peptide binding might also be occurring in a CD8 independent manner[142] (Figure 8D). With these CRISPR/Cas9 modifications, potential mispairing between endogenous and transduced human TCR chains was excluded as a mechanism to affect the recognition of the glioma target. This further

strengthens the notion that the H3.3K27M$_{26-35}$ is not a suitable target for TCR gene therapy in HLA-A*02:01^{+} patients with DMG.

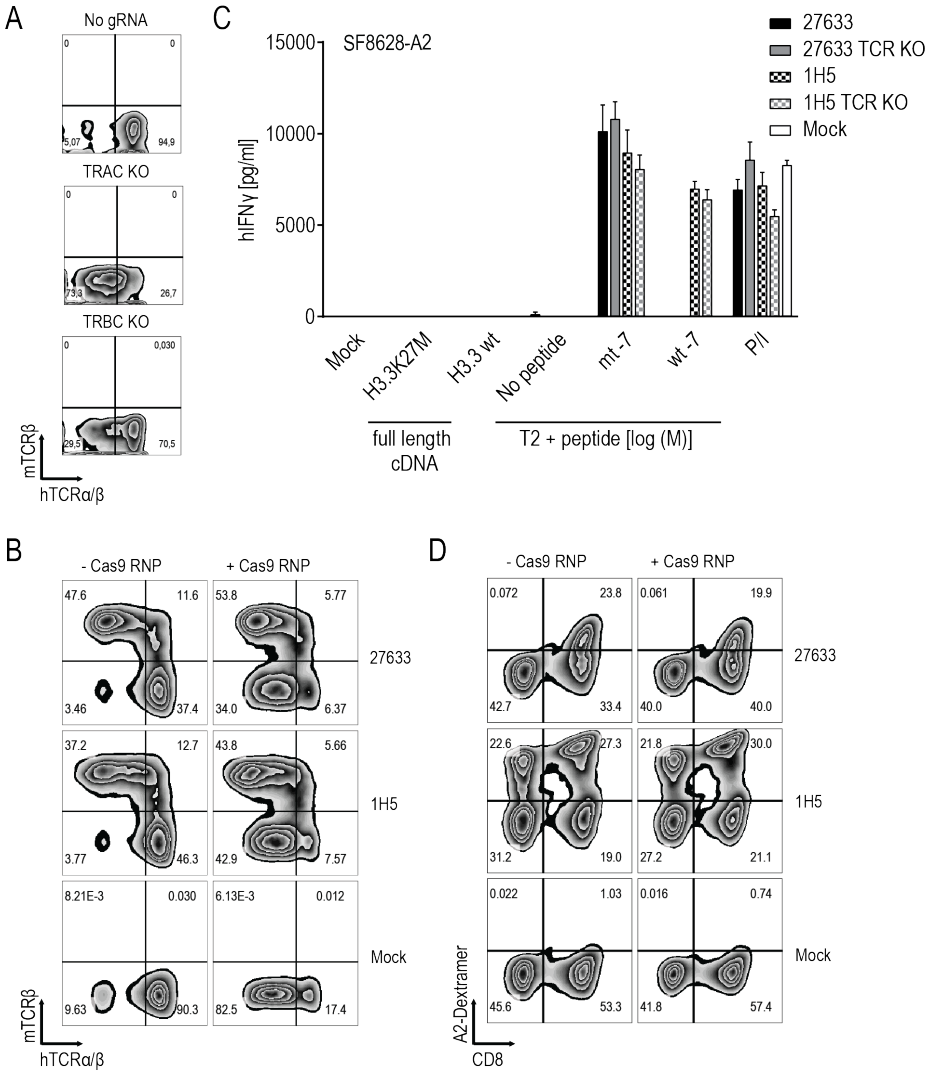

Figure 8. CRISPR/Cas9 knockout of endogenous human TCR did not lead to recognition of the H3.3K27M mutation. (A) Expression of transduced TCR (mTCRβ, y-axis) and endogenous TCR (hTCRα/β, x-axis) after knockout of either endogenous TCR α or β chain with CRISPR/Cas9 in mock-transduced T cells. Cas9 enzyme and gRNAs targeting human TRAC or TRBC loci were complexed and nucleofected into T cells. Endogenous (hTCRα/β) and therapeutic (mTCRβ) TCR expression were assessed by flow cytometry after 4 days in culture on 10 IU/ml IL-2, cells were gated on CD3^{+}. **(B)** 27633-, 1H5- and mock-transduced T cells were nucleofected with sgRNAs and Cas9 protein (right panel) or without Cas9 (left panel) targeting the endogenous human TRAC and TRBC locus together. Endogenous (hTCRα/β) and therapeutic (mTCRβ) TCR expression were assessed by flow cytometry after 4 days in culture on 10 IU/ml IL-2, cells were gated on CD3^{+}. **(C)** Cells described in (B) were co-cultured with SF8628-A2, SF8628-A2-H3.3K27M, SF8628-A2-H3.3 wild type or with peptide-loaded T2 cells (10^{-7} M mutant or wt peptide, respectively). Graphs represent mean IFNγ secretion of triplicate cultures ±SD. **(D)** Staining of the TCRs with H3.3K27M dextramer (y-axis) and CD8 (x-axis) after knockout of human TCR α and β chains with CRISPR/Cas9. FACS staining was performed after 4 days in culture on 10IU/ml IL-2, cells were gated on CD3^{+}**.**

4.1.4 H3.3K27M peptide was not detectable by mass spectrometry in the MHC class I immunopeptidome of cells overexpressing the mutation

Next, it was investigated whether lack of recognition is caused by the absence of the H3.3K27M$_{26-35}$ epitope among the peptides presented on MHC class I molecules, the so-called immunopeptidome. For this, U87MG cells overexpressing the H3.3K27M mutation were collected and class I bound peptides were immunoprecipitated using a pan HLA-specific antibody. To more efficiently collect high amounts of tumour material, the U87MG cells were grown as subcutaneous tumours in NSG mice (Figure 9A). U87MG cells overexpressing CDK4R24L cDNA were used as a positive control since they induce substantial T cell recognition. In addition, the samples were spiked with an H3.3K27M (RmSAp*STGGV) or CDK4R24L (ALDPHSGHFv*) heavy labelled peptide as positive references for the analysis. As shown in Figure 9, the H3.3K27M peptide was not detected by mass spectrometry (samples 1-4), while the CDK4R24L peptide was present with high intensity (samples 5-8, Figure 9B and D). The positive heavy spiked peptides were detected in all samples, respective mass spectrometry spectra of heavy and light CDKR24L and heavy H3.3K27M peptides are depicted in Figure 9C. The absence of the H3.3K27M$_{26-35}$ epitope among eluted MHC class I molecules might explain the failure of H3.3K27M-specific TCR-transduced T cells to recognise the endogenously expressed mutation.

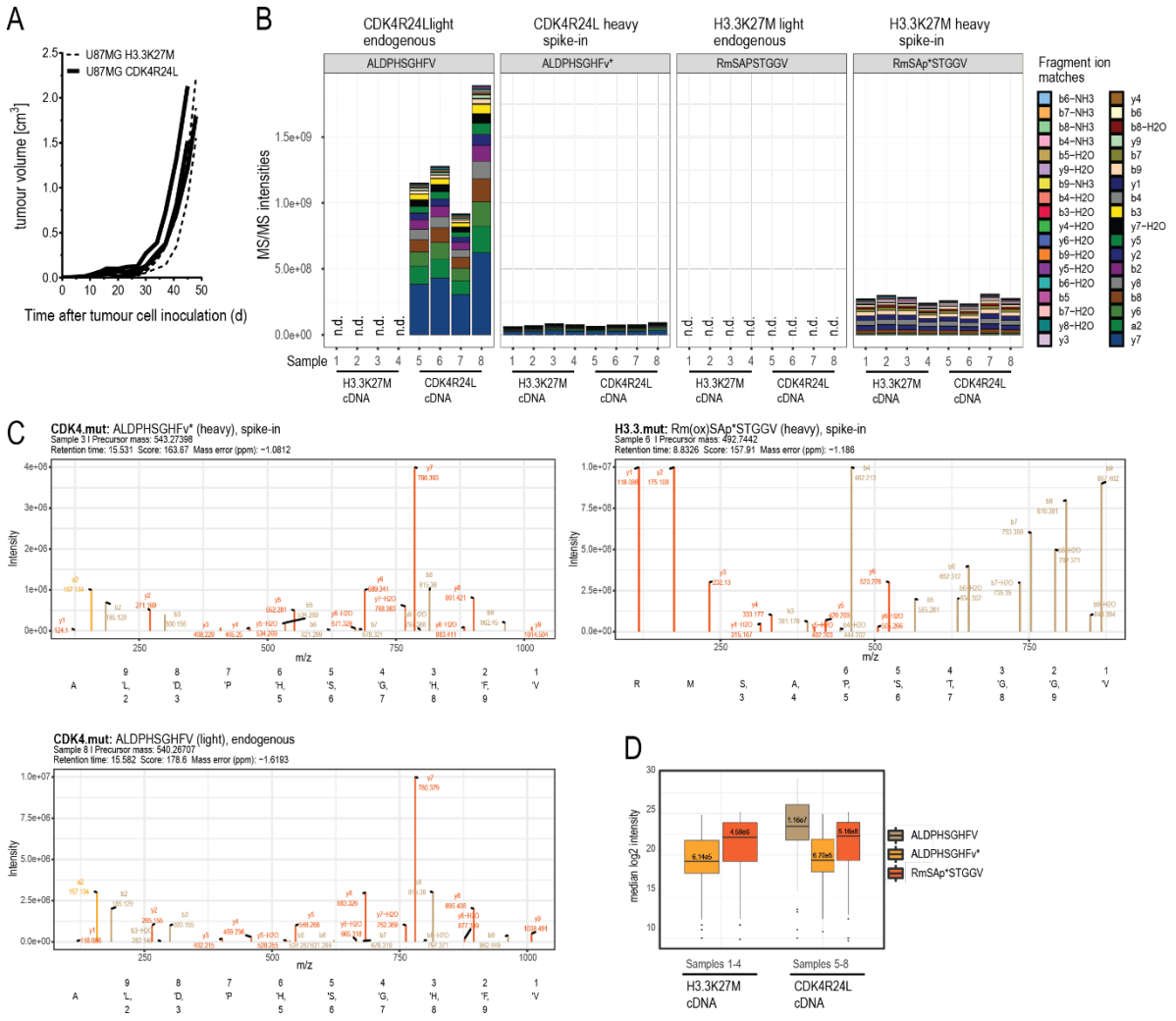

Figure 9. The mutated CDK4 peptide, but not the mutated H3.3 peptide, was detectable in U87MG glioblastoma cells overexpressing the respective cDNAs. (A) 5x10^6 U87MG cells overexpressing either full-length cDNAs H3.3K27M or CDK4R24L were injected into NSG mice. At a size of 1,5-2 cm^3 tumours were isolated, snap frozen and cryo-pulverised for immunoprecipitation of HLA-A*02:01 bound peptides. **(B)** Eluted peptides were analysed using an orbitrap Exploris mass spectrometer (Thermo Fisher Scientific). Samples 1-4 recombinantly express H3.3K27M, samples 5-8 express CDK4R24L (samples are quadruples). Summed MS2 fragment intensities for the endogenous mutated CDK4 and H3.3 peptides and their heavy synthetic counterparts. v* and p* indicate a heavy amino acid with a mass shift of $^+$6 on valine or proline, respectively; m: oxidised methionine; n.d.: not detected. An amount of 25 fmol for CDK4 or 5 fmol for H3-3 of the synthetic heavy labelled peptides were injected along with each sample. Only charge state 2$^+$ was used for the quantitation. Supplementary Figure 3 Samples 1-4 recombinantly express H3.3K27M, samples 5-8 express CDK4R24L. **(C)** Representative annotated MS2 spectra were generated from the MaxQuant output for the mutated CDK4 and H3.3 heavy synthetic peptides (top panel) and their endogenous counterparts (bottom panel). Endogenous mutant H3.3 peptide could not be detected in any of the samples. **(D)** Boxplots show the MS2 intensities by groups. Mass spectrometry experiments were performed in collaboration with Dr. Oliver Popp and Prof. Dr. Philipp Mertins from the BIH core facility proteomics.

4.2 Rac1P29S mutation was recognised by Rac1/2-specific T cells

To study the potential of the recurrent Rac1P29S mutation as a target for ATT, TCRs against Rac1P29S were isolated and characterised. Additionally, TCRs were also raised against Rac2P29L, a mutation that differs in one amino acid but has a higher predicted peptide-MHC affinity than Rac1P29S.

4.2.1 Rac1/2-specific TCRs were successfully isolated after peptide immunisation

The tumour mutations Rac1P29S and Rac2P29L were predicted to create epitopes (F**S**GEYIPTV and F**L**GEYIPTV) that bind HLA-A*02:01 with strong affinity. While the mutation Rac1P29S is more frequent in tumours, its resulting epitope has a weaker peptide-MHC affinity compared to the less common Rac2P29L mutation. Both mutant peptides were used to immunise ABabDII mice, a transgenic mouse model expressing a diverse human TCR repertoire[123]. Peripheral T cells of Rac1 and Rac2 mutant peptide immunised mice showed an immune response upon restimulation, measured by intracellular IFNγ responsiveness (Figure 10A-C). To isolate specific TCRs, splenocytes of responsive mice were cultured in the presence of the respective mutant peptide for 10 days and either peptide HLA-A*02:01 tetramer (pA2 tetramer) positive T cells (Figure 10D) or highly IFNγ positive CD8 T cells (Figure 10E) were sorted.

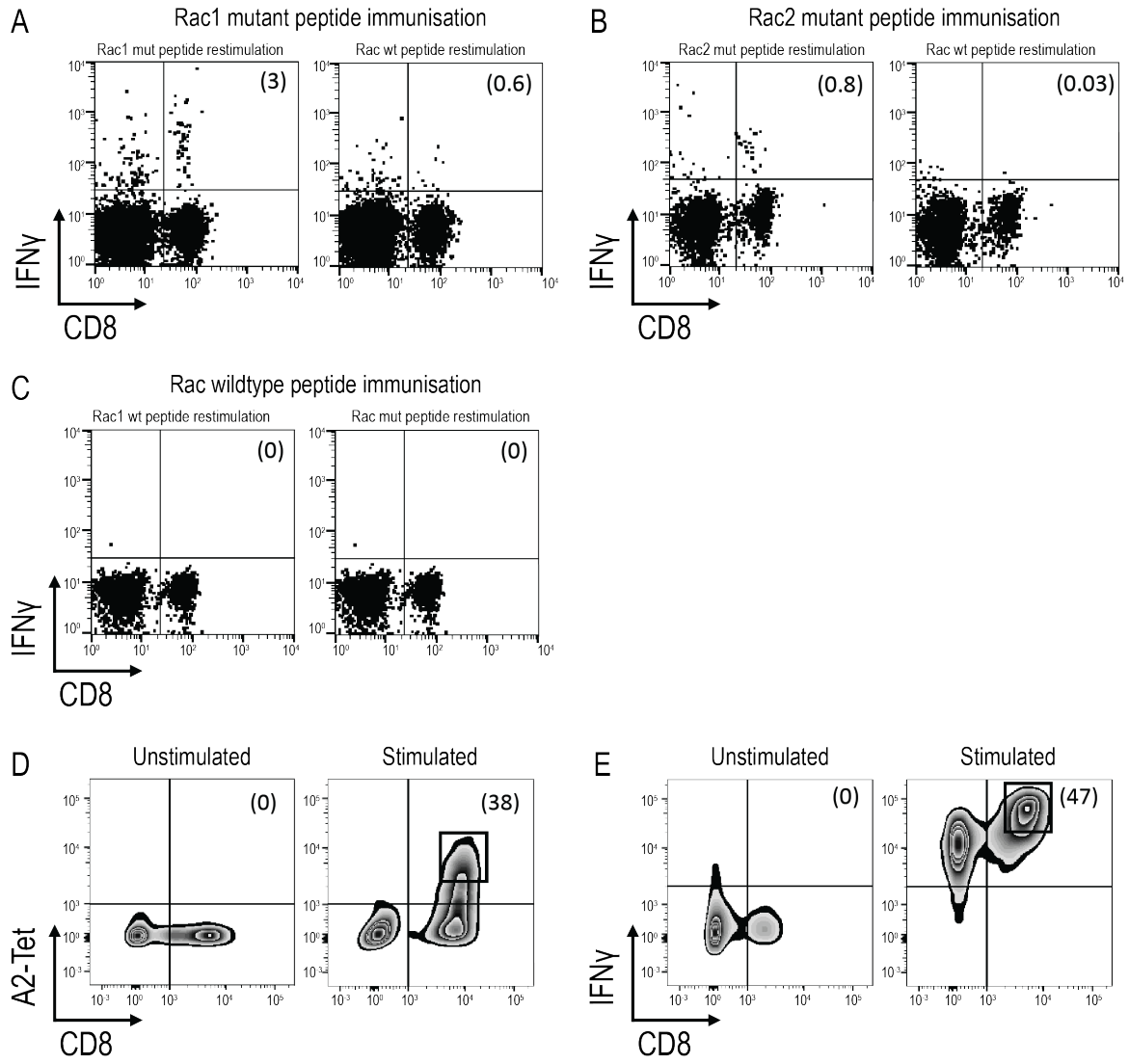

Figure 10. Identification and isolation of mutant Rac1/2-specific CTLs in ABabDII mice. (A-C) Representative example of *ex vivo* intracellular IFNγ staining of peripheral T cells of ABabDII mice immunised with (A) Rac1P29S mutant peptide, (B) Rac2P29L mutant peptide or (C) Rac wild type peptide. Splenocytes were restimulated with the indicated peptide 7 days after the last immunisation of ABabDII mice. **(D)** Representative pA2 tetramer staining of mutant Rac1-specific $CD8^+$ T cells 10 days after spleen cell culture in the presence of 10^{-9} M mutant Rac1 peptide. Cells were gated on lymphocytes and $CD3^+$ T cells. Numbers in brackets represent percent of pA2 $tetramer^+$ $CD8^+$ T cells, unstimulated splenocytes served as a negative control. Sorted cells are depicted in squares. **(E)** Identification of $IFN\gamma^+$ $CD8^+$ T cells using IFNγ-capture assay depicted by representative staining of mutant Rac1-specific $CD8^+$ T cells 10 days after spleen cell culture in the presence of 10^{-8} M mutant Rac1 peptide. Cells were gated on lymphocytes and $CD3^+$ T cells, unstimulated splenocytes served as a negative control. Numbers in brackets represent percent $IFN\gamma^+CD8^+$ T cells. Sorted cells were depicted in squares.

Dominant α and β chains of the responsive mice #22894 (Rac2 mutant immunised), #A12B20 and #5934 (Rac1 mutant immunised) were identified (Figure 11A). After the replacement of

the human constant regions by murine ones to reduce mispairing of the endogenous and transduced TCR, the TCR α and β pairs were synthesised as a bicistronic cassette separated by a P2A element. The TCR cassettes were cloned into the vector MP71 and retrovirally transduced into human T cells of healthy donors. Successful transduction of the three Rac1/2-specific TCRs, as well as a well-characterised CDK4R24L-specific TCR (14/35), was measured by staining for the murine constant β chain in CD8 positive T cells and analysed by flow cytometry (Figure 11B). CD8 and TCR double positive T cells were found at similar percentages ranging from 26.3% to 34.6% of CD3 positive T cells.

A

TCR	Peptide immunisation	Gene name
22894	FLGEYIPTV	Rac2
A12B20	FSGEYIPTV	Rac1
5934	FSGEYIPTV	Rac1

B

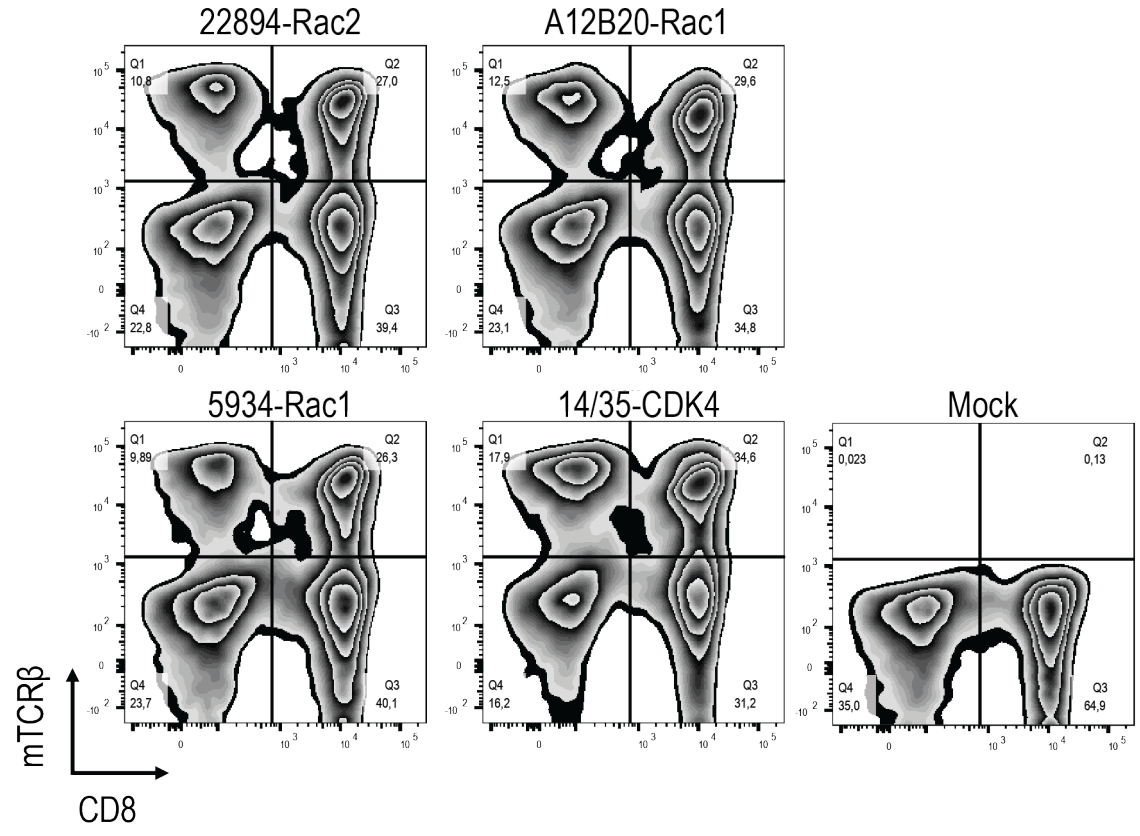

Figure 11. TCRs were successfully transduced into human T cells. (A) Overview of TCRs isolated after peptide immunisation of ABabDII mice. **(B)** TCR transduction rates were determined by staining of the mouse TCRβ constant chain and subsequent analysis by flow cytometry. Mock transduced cells are untransduced with an empty virus, 14/35 TCR-transduced T cells serve as a positive control targeting CDK4R24L mutation. Percentages displayed are based on pregated $CD3^+$ lymphocytes.

4.2.2 High functional avidity of mutant Rac1/2-specific T cells was observed against both mutant peptides

To determine the functional avidity of the isolated TCRs, TAP-deficient T2 cells were loaded with titrated levels of Rac1 mutant (FSG) peptide (Figure 12A), Rac2 mutant (FLG) peptide (Figure 12B) and as a negative control Rac wild type (FPG) peptide (Figure 12C). The two TCRs isolated after Rac1 mutant peptide immunisation showed high affinity to their respective peptide down to a concentration of 10^{-8} M for TCR A12B20-transduced T cells and 10^{-10} M for TCR 5934-transduced T cells. Interestingly, also the TCR 22894, isolated after immunisation with the Rac2 mutant peptide showed high functional avidity towards the Rac1 mutant peptide down to a concentration of 10^{-10} M. When loaded with the Rac2P29L peptide, the mutant Rac1-specific TCRs also recognised the Rac2 mutant peptide. The Rac wild type (FPG) peptide was only recognised when co-cultured with the T cells in the highest peptide concentrations of 10^{-6} M. Since the Rac2P29L mutation is less common in human cancers, the following experiments focused primarily on Rac1P29S mutation as a target for ATT. To determine the binding strength of the TCRs to the Rac1 peptide-MHC (pMHC) complex, the two TCRs 22894 and 5934 that performed best in the affinity assay, were stained with a mutant Rac1-specific pA2 tetramer. As depicted in Figure 12D, the heterologous Rac2-specific TCR 22894-transduced T cells showed a higher MFI of 4889 compared to the Rac1-specific TCR 5934-transduced T cells (MFI 1958).

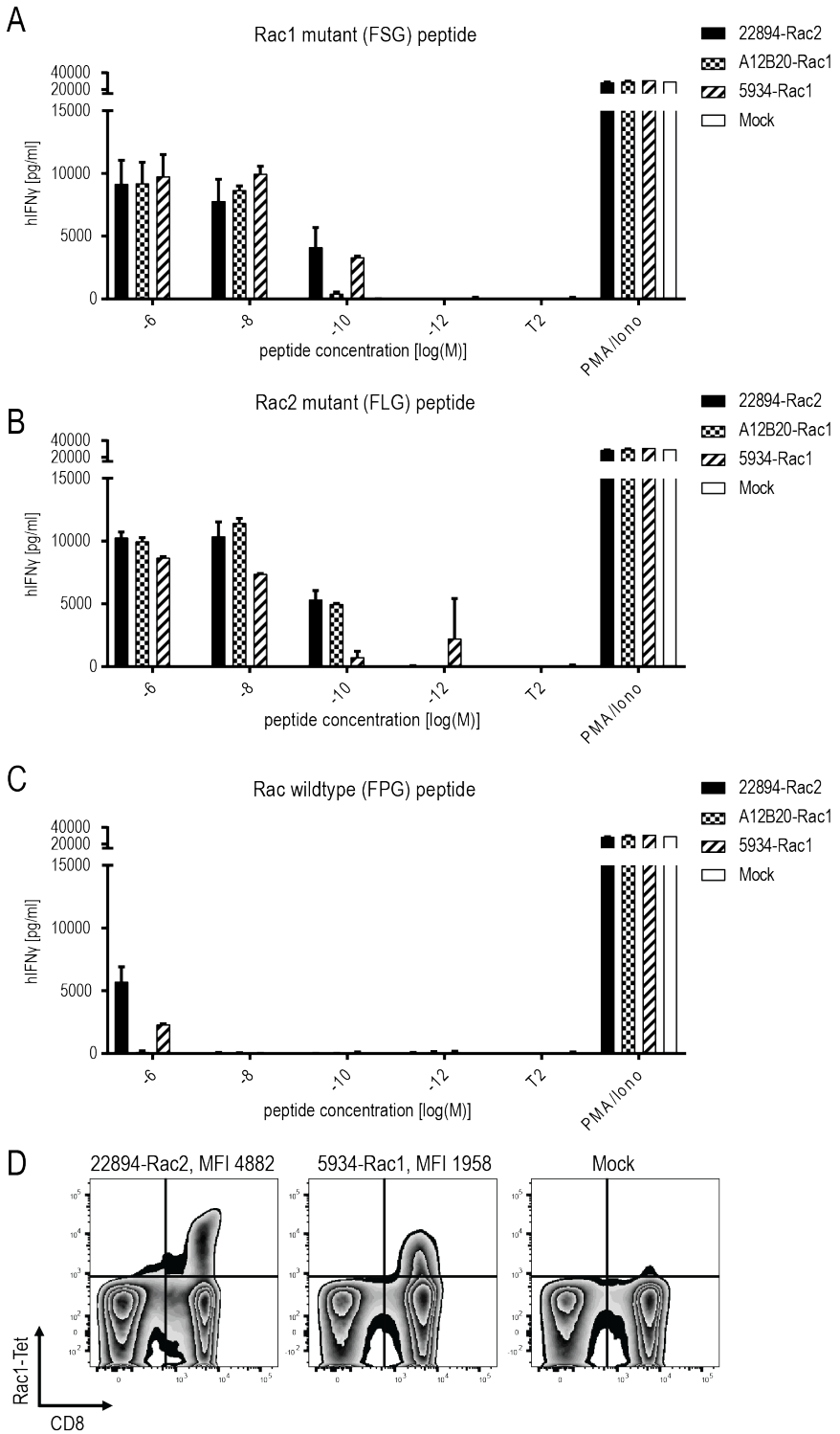

Figure 12. TCR-transduced T cells showed high affinity to Rac1 and Rac2 mutant peptides. (A-C) TCR-transduced T cells were co-cultured with peptide-loaded T cells ($1x10^4$ cells, 1:1 ratio) for 22 hours in triplicates. IFNγ levels were determined in an ELISA assay. PMA and Ionomycin (P/I) stimulation served as a positive control, T2 cells only as a negative control. T2 cells were loaded with indicated concentrations of (A) Rac1 mutant peptide (F**S**GEYIPTV), (B) Rac2 mutant peptide (F**L**GEYIPTV) or (C) Rac wild type peptide (F**P**GEYIPTV). **(D)** Affinity of the TCRs to its peptide-MHC complex was determined using a mutant Rac1-specific pA2 tetramer. Binding to the pA2 tetramer is indicated by mean fluorescence intensity (MFI). The experiment was performed three times with similar results and graphs represent means of triplicate cultures ±SD.

As the Rac2P29L mutation has a higher predicted HLA-A*02:01 binding, it was further investigated if the Rac2-specific 22894 TCR has an advantage over the other two TCRs in recognising mutant Rac1 expressing cell lines.

4.2.3 Melanoma cell lines naturally expressing mutant Rac1 were variably recognised by mutant Rac1/2-specific T cells

When characterising a potential target for ATT, it is crucial to confirm the recognition of tumour cell lines that endogenously express the respective mutation. Therefore, the mutant Rac1/2-specific TCR-transduced T cells were co-cultured with the three melanoma cell lines naturally expressing the Rac1P29S mutation. Despite the high affinity against the peptides loaded on T2 cells, only the Rac1-specific 5934 TCR-transduced T cells secreted IFNγ when co-cultured with Mel55b (Figure 13A), but not with Mel085-A2 (Figure 13B) and Mel20aI (Figure 13C). The other two TCR-transduced T cells (22894-Rac2 and A12B20-Rac1) failed to secrete IFNγ against all cell lines. In line with the previous data, when cells were loaded with mutant Rac1 peptide, a strong immune response was detected. Since Rac1 plays a role in multiple cellular processes including cell migration, cytoskeleton reorganization and cell transformation[105], one of the cell lines (Mel20aI, Figure 13C) was used at a low (20%) and a high (80%) confluency to study if the cell cycle state of the tumour cells is important for recognition. However, none of the two cell conditions was recognised by the three mutant Rac1/2 peptide-specific TCR-transduced T cells. Since Mel085 melanoma cells are HLA-A*02:01 negative, they were retrovirally transduced to express HLA-A*02:01 confirmed by flow cytometry (Figure 13D). The other two cell lines are naturally HLA-A*02:01 positive.

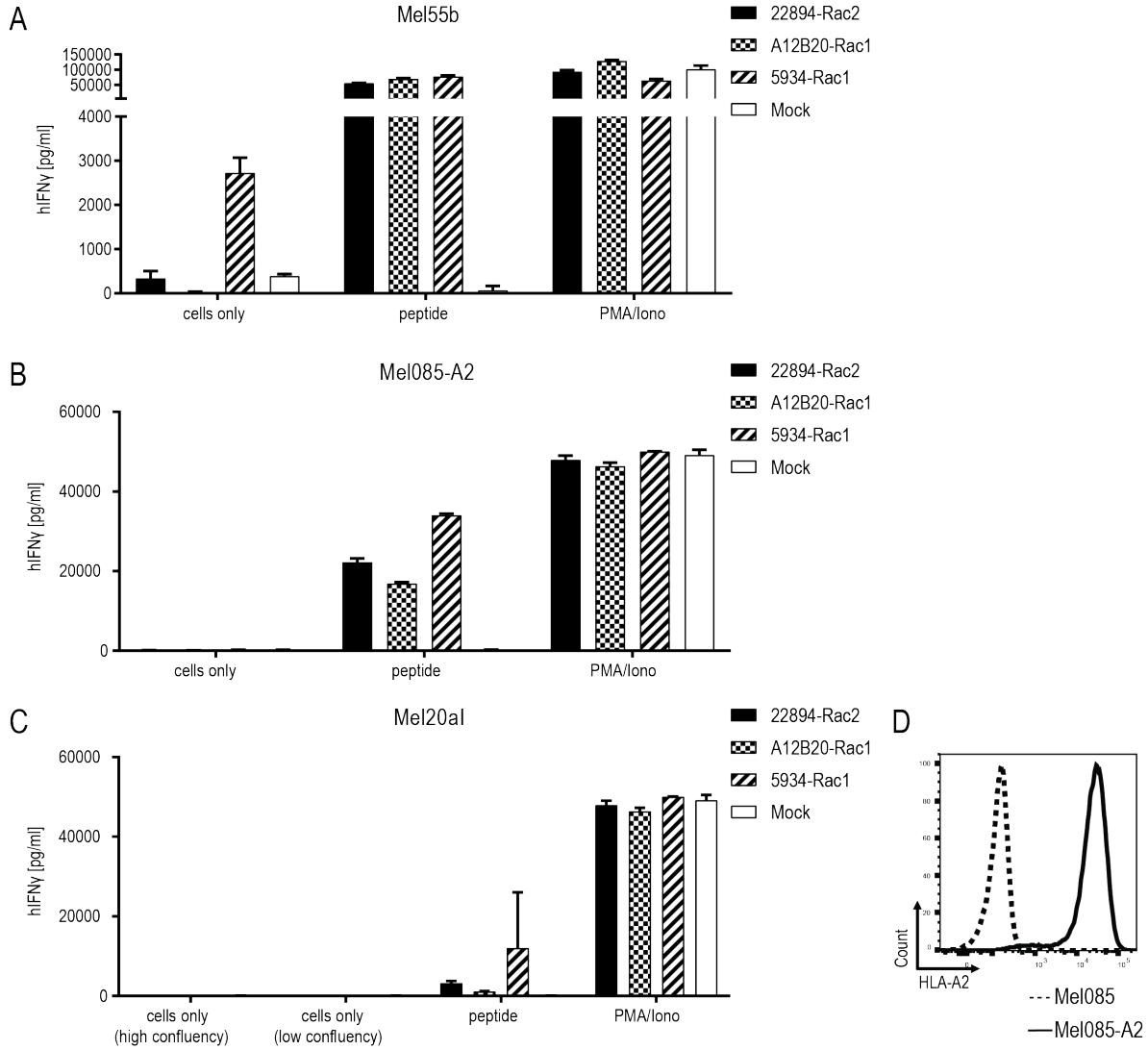

Figure 13. Variable recognition of mutant Rac1 expressing melanoma cell lines. (A-C) TCR-transduced T cells were co-cultured with Rac1 mutant melanoma cell lines (A) Mel55b, (B) Mel085-A2 and (C) Mel20aI ($1x10^5$, 1:1 ratio) for 22 hours in triplicates. IFNγ levels were determined in an ELISA assay. PMA and Ionomycin (P/I) stimulation served as a positive control. Cells were loaded with 10^{-6} M Rac1 mutant FSG peptide as control. Mel20aI cells (C) were seeded at 80% (high) confluency and 20% (low) confluency. **(D)** The HLA-A*02:01 negative cell line Mel085 was retrovirally transduced with HLA-A*02:01 (Mel085-A2). Expression was confirmed by flow cytometry. The experiment was performed three times with similar results and graphs represent means of triplicate cultures ±SD.

In addition to cytokine secretion, we also investigated cytotoxicity mediated by Rac1/2-specific TCR-transduced T cells. To do so, mutant Rac1 expressing tumour cells were co-cultured with TCR-transduced T cells over 72 hours and cytotoxicity was measured by the decrease in GFP expressing target cells determined by live-cell imaging. All tumour cells were GFP positive, as they were retrovirally transduced to express the positive control CDK4R24L coupled to GFP

(Figure 14A). In line with previous data, Rac1-specific 5934 TCR-transduced T cells were able to recognise Mel55 tumour cells (Figure 14B, left panel). The positive control CDK4-specific TCR 14/35-transduced T cells lysed all CDK4R24L overexpressing target cells. In contrast to the previous experiment, not only recognition of Rac1-specific TCR 5934-transduced T cells against Mel55 cells was detected, but also against Mel085-A2 (Figure 14C, left panel) and Mel20aI cells (Figure 14D, left panel). Interestingly, the Mel085-A2 cells were also partially lysed by the Rac2-specific 22894 TCR-transduced T cells, an effect that was not observed in the previous IFNγ secretion assay (Figure 14C, left panel). The greatest killing effect was observed using Mel20aI as target cells, where target to effector cells were seeded in a 1:15 ratio (Figure 14D, left panel). Here, all TCR-transduced T cell groups were able to elicit cytotoxicity against the cells. As a positive control, all three cell lines were recognised by the Rac1/2-specific TCR-transduced T cells when loaded with mutant Rac1 peptide (Figures 14B-D, right panel).

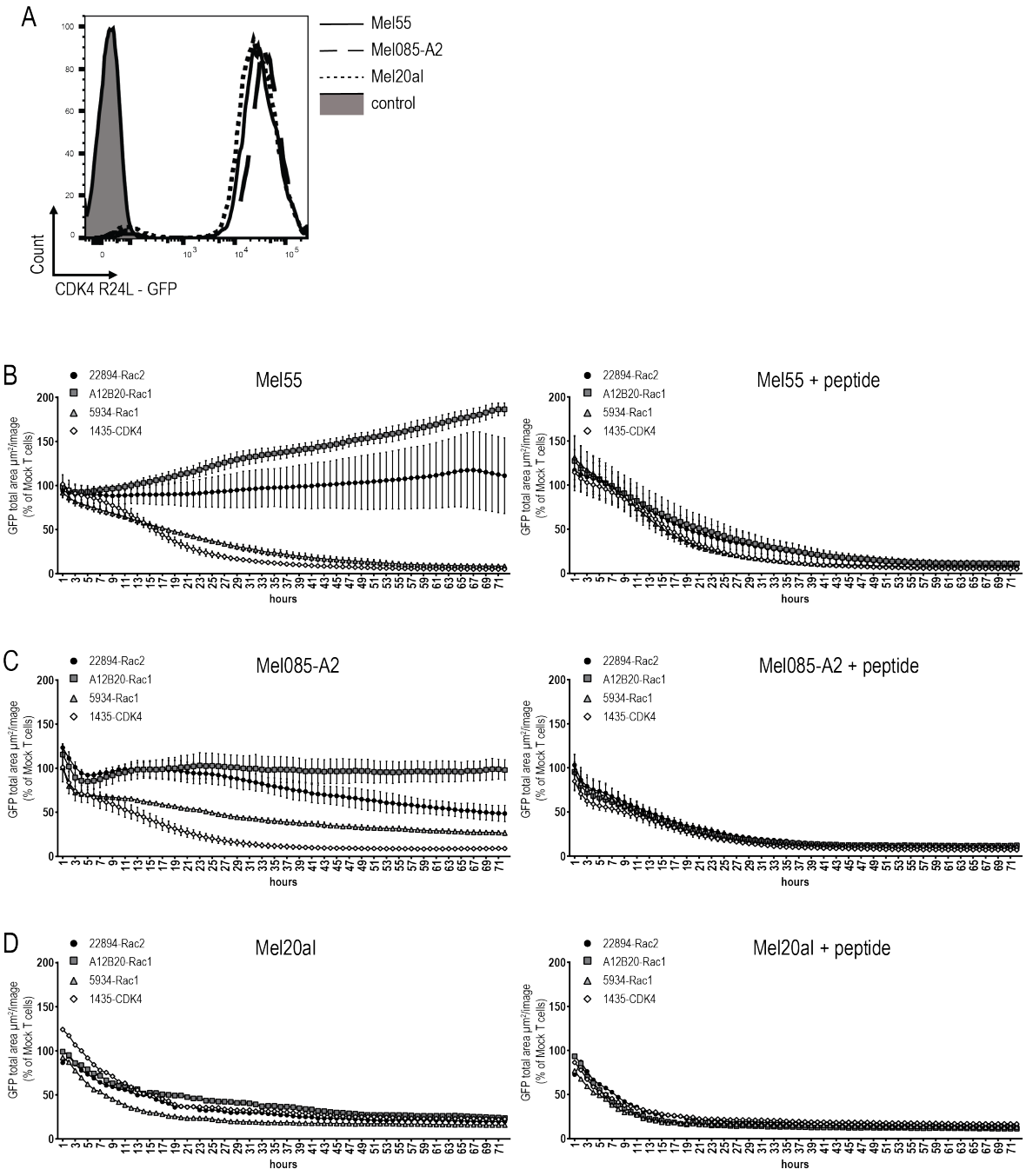

Figure 14. Rac1/2-specific T cells showed cytotoxicity against Rac1P29S expressing melanoma cell lines. (A) GFP intensities of melanoma cell lines after retroviral transduction with CDK4R24L full-length cDNA measured by flow cytometry. Control cells were representative examples of untransduced, GFP negative Mel55 cells. **(B-D)** $15x10^3$ transduced $CD8^+$ T cells were co-cultured as triplicates at a 5:1 E:T ratio with (B) Mel55 cells, (C) Mel085-A2 and as singlets at a 15:1 E:T ratio with (D) Mel20aI cells. Right panels show the same cell line loaded with 10^{-6} Rac1 mutant peptide. Cells were retrovirally transduced to express CDK4R24L full-length cDNA. Cytotoxicity was observed over 72 hours using the live cell imaging system IncuCyte Zoom (Essen Bioscience). Values were calculated by normalising the average GFP total area (µm²/image) in the target cells co-cultured with the respective TCR-transduced T cells to the average of that co-cultured with mock transduced T cells. The experiment was performed three times with similar results and graphs represent means of triplicate cultures ±SD.

In summary, the mutant Rac1/2-specific TCR-transduced T cells were able to lyse most target cells, however, only one of the cell lines induced IFNγ secretion. Whether this is due to different cytolytic pathways or the sensitivity of the assays remains to be determined.

4.2.4 Mutant Rac1 triple epitope was recognised by Rac1/2-specific T cells *in vivo*

The two Rac1/2-specific TCRs that performed best *in vitro*, Rac2P29L-specific TCR 22484 and Rac1P29S-specific TCR 5934, were used to evaluate their ability to reject tumours *in vivo*. The fibrosarcoma cells MC703, which were generated in an HLA-A*02:01-transgenic mouse (HHD, chimeric HLA-A*02:01/H-2D^{b})[127,143], were transduced with the Rac1 triple epitope F**S**GEYIPTV coupled to GFP. Recognition of these cells was confirmed *in vitro* with and without loaded Rac1 mutant peptide (Figure 15A). As shown before, both TCR-transduced T cells recognised the target, recognition by Rac1-specific TCR 5934 was slightly higher compared to the heterologous Rac2-specific TCR 22894. Before the MC703-FSG cells were injected into HHDxRag-/- mice, the expression of FSG-GFP and HLA-A*02:01 was determined by flow cytometry (Figure 15B). Notably, 99% of injected cells were double positive. 28 days post tumour injection, mice were treated with 1x10^{6} TCR-transduced HHD T cells. As a negative control, three mice were also treated with the irrelevant CDK4-specific TCR 14/35. As depicted in Figure 15C, mice treated with Rac1/2-specific 22894 and 5934 TCR-transduced T cells were able to induce regression, while CDK4-specific 14/35 TCR-transduced T cells treated tumours progressively grew after ATT. Interestingly, the heterologous Rac2-specific 22894 TCR-transduced T cells showed greater efficacy in tumour regression compared to the Rac1-specific TCR 5934. Eventually, the tumours relapsed in all groups.

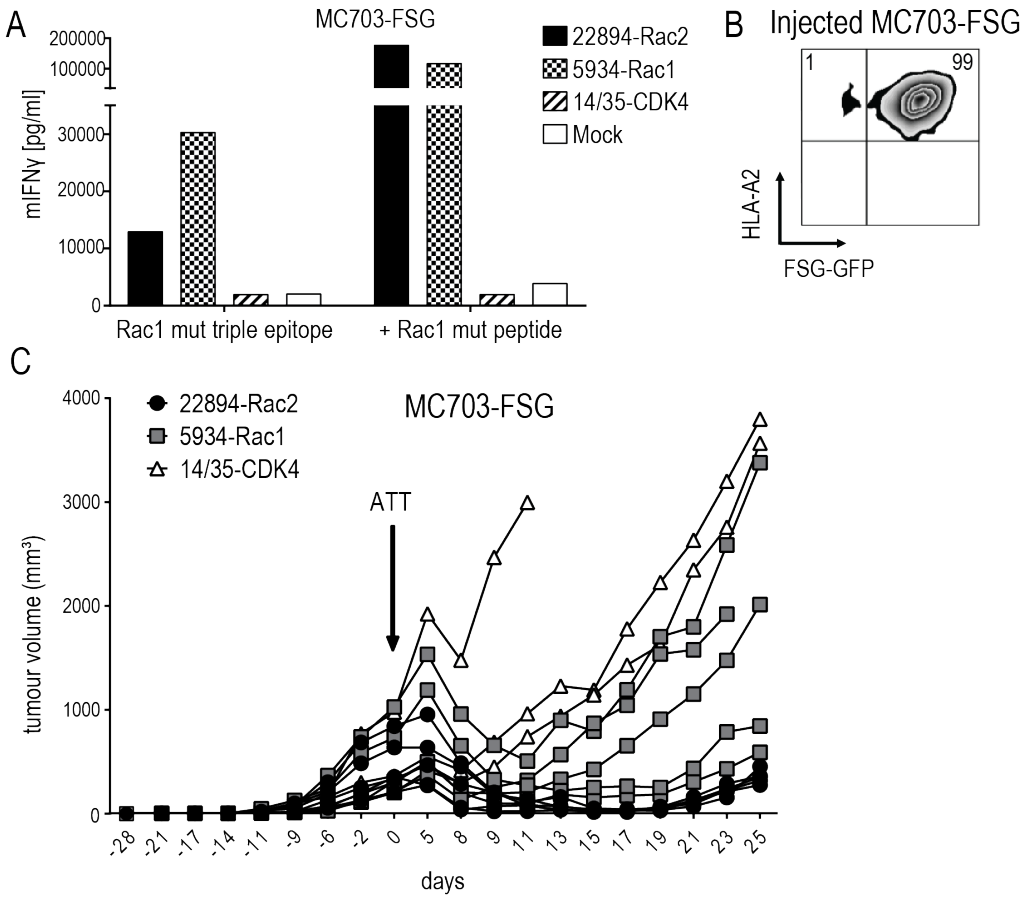

Figure 15. Heterologous Rac2-specific 22894 TCR-transduced T cells elicited tumour regression upon ATT. **(A)** TCR-transduced murine T cells were co-cultured with the mouse tumour cell line MC703[127,143] expressing FSG triple epitope (5'LTR - $(P29S)_3$ - GFP - PRE - 3'LTR) ($1x10^5$, 1:1 ratio) for 24 hours. IFNγ levels were determined in an ELISA assay. Cells were loaded with 10^{-6}M Rac1 mutant FSG peptide as a control. The experiment was performed at least three times, one representative experiment is shown. **(B)** FSG-GFP and HLA-A*02:01 expression of MC703-FSG cells before injection measured by flow cytometry. Number indicates percentage. **(C)** $1x10^6$ MC703-FSG cells were injected into HHDxRag-/- mice. Rac1/2-specific T cells were injected 28 days after tumour injection at a tumour size of up to 1000 mm^3 indicated by the arrow. 5 mice were treated with TCR 22894 and 5934-transduced T cells each, 3 mice with the negative control 14/35 TCR-transduced T cells. The experiment was performed two times.

To investigate potential reasons for tumour relapse after initial regression, the MC703-FSG tumours were reisolated and analysed GFP as well as HLA-A*02:01 expression by flow cytometry (Figure 16A). Mice treated with the more efficient Rac2-specific 22894 TCR-transduced T cells showed almost complete loss of FSG-GFP expression down to 8%, while tumours treated with Rac1-specific 5934 TCR-transduced T cells showed partial loss (38% double positive T cells). Tumours treated with CDK4-specific 14/35 TCR-transduced T cells, which did not have any selective pressure on outgrowing FSG-GFP negative tumours, only showed a reduction in HLA-A*02:01 expression. These data suggest that tumours in the 22894

and 5934 TCR treated groups regressed due to target-specific lysis by T cells but subsequently FSG-GFP negative cells relapsed. As seen in Figure 16B, the injected cells were composed of 1% antigen-negative cells, explaining this outgrowth and the selective pressure induced by target-specific TCR-transduced T cells. To confirm that hypothesis, reisolated tumours were co-cultured with a new batch of TCR-transduced T cells (Figure 16B). In line with previous data, tumours isolated from mice that were treated with Rac2-specific 22894 TCR-transduced T cells were not recognised by Rac1-specific 5934 TCR-transduced T cells, most likely due to outgrowth of antigen-negative variants. Tumours isolated from Rac1-specific 5934 TCR treated mice were partly recognised, while CDK4-specific 14/35 TCR treated tumours induced comparable IFNγ levels to MC703-FSG control cells which were not previously injected into mice. These *in vivo* data suggest that there might be a potential for heterologous ATT by using TCRs that were isolated after immunisation with peptides with stronger predicted peptide-MHC binding.

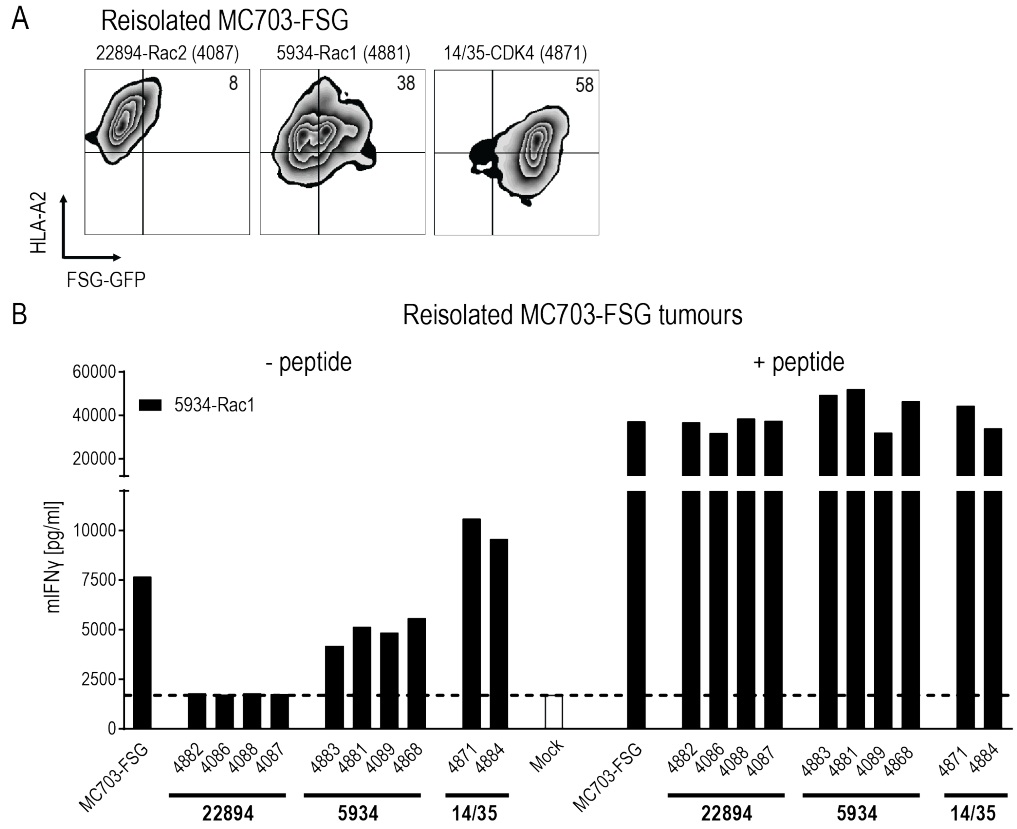

Figure 16. Selection of antigen-negative tumour cells allowed for tumour relapse. (A) Reisolated tumours were analysed for HLA-A*02:01 and FSG-GFP expression by flow cytometry. Numbers in plots indicate percentages. One representative plot per treatment group is depicted, mouse is indicated by numbers in parenthesis. **(B)** Recognition of reisolated tumours was measured in an IFNγ ELISA. Tumours were co-cultured with 5934 TCR-transduced T cells ($1x10^5$, 1:1 ratio) for 24 hours. PMA and Ionomycin (P/I) stimulation served as a positive control. Cells were loaded with 10^{-6} M Rac1 mutant FSG peptide as a control. Mock serves as a negative control with no T cells added. The experiment was performed two times with similar results.

4.3 *In vitro* proteasome processing of spliced epitopes did not predict their presentation *in cellulo*

To explore the potential of novel cancer-specific targets for ATT, TCRs isolated after peptide immunisation with Kras and Rac2 spliced epitopes as a result of proteasome-catalysed peptide splicing (PCPS) were characterised. The analyses of the TCRs have previously been described[119].

4.3.1 KrasG12V splice-specific T cells did not recognise cancer cells naturally expressing or overexpressing mutant Kras

KrasG12V is an interesting target for ATT as it is frequently found in tumours, for example, in 30% of pancreatic ductal adenocarcinoma, in 20% of colon cancers, as well as in non-small cell lung cancers. Unfortunately, there is no suitable HLA-A*02:01 binding epitope predicted harbouring this mutation. However, four spliced epitopes are predicted to bind HLA-A*02:01 with an IC_{50} <100 nM, of which the epitope KLVV/GA**V**GV was chosen for further analysis. This spliced epitope was used to immunise ABabDII mice, a transgenic model expressing a diverse human TCR repertoire[123] and specific TCRs were isolated from splenocytes as described above. The functional avidity of the isolated TCR 1376 was further evaluated by transducing PBMCs from a healthy donor with the 1376 TCR and co-culturing the transduced T cells with TAP-deficient T2 cells loaded with titrated mutant spliced peptide concentrations (Figure 17A). While 1376 TCR-transduced T cells were able to recognise the spliced peptide down to a concentration of 10^{-10} M, the linear KrasG12V peptide was only recognised when loaded in the highest peptide concentrations (Figure 17B).

As this spliced epitope is only predicted *in silico* and not by *in vitro* PCPS reactions, it was even more critical to confirm recognition of KrasG12V mutant cell lines. Therefore, 1376 TCR-transduced T cells were co-cultured with multiple cancer cell lines naturally expressing the KrasG12V mutation (Figure 17C-D). However, both naturally HLA-A*02:01 positive cell lines (Figure 17C), as well as HLA-A*02:01-transduced cell lines (Figure 17D) were not recognised by 1376 TCR-transduced T cells, unless loaded with peptides as positive controls. MCF-7 cells have two copies of Kras wild type and served as a negative control.

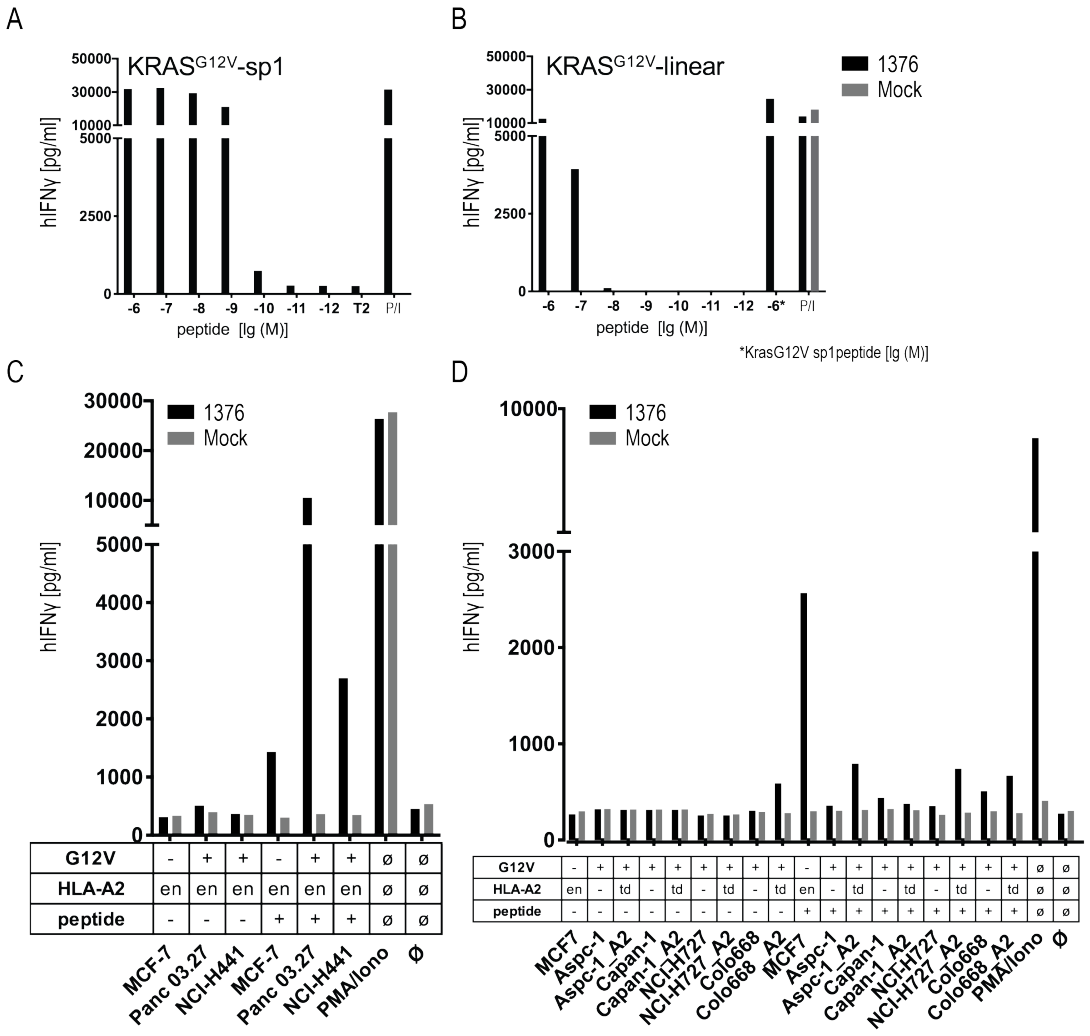

Figure 17. Generation and characterization of TCRs specific for spliced epitope of mutant KrasG12V. (A) TCR gene transfer confers specificity for mutant spliced KrasG12V peptide KLVVGAVGV (sp1). IFNγ production of KrasG12V splice-specific 1376 TCR-transduced T cells upon co-culture with sp1peptide-loaded T2 cells (1376, black bars). As a negative control, T2 cells were not loaded with peptides. PMA and Ionomycin (P/I) stimulation served as a positive control. All target cells were also co-cultured with non-transduced T cells (Ø, grey bars). **(B)** TCR gene transfer conferred cross-reactivity for mutant linear KrasG12V peptide KLVVVGAVGV. IFNγ production of KrasG12V splice-specific 1376 TCR-transduced T cells upon co-culture with KrasG12V linear peptide-loaded T2 cells (1376, black bars). As a negative control, T2 cells were not loaded with peptides. PMA and Ionomycin (P/I) stimulation served as a positive control. All target cells were also co-cultured with non-transduced T cells (Ø, grey bars). Experiments were done at least in duplicate. **(C)** For analysis of natural processing and recognition of KrasG12V epitopes, cell lines naturally expressing HLA-A*02:01 and harbouring the KrasG12V mutation or wild type (+/- peptide) were co-cultured with KrasG12V TCR 1376-redirected T cells. **(D)** HLA-A*02:01 negative cell lines were transiently transduced with an HLA-A*02:01 expressing retroviral construct (td) and co-cultured as in (C). IFNγ production of transduced T cells is shown (1376, black bars). As a positive control, peptide-loaded cells (+) were used, respectively. PMA and Ionomycin (PMA/Iono) stimulation served as a positive control. All target cells were also co-cultured with untransduced T cells (Ø, grey bars); en: endogenous expression of HLA-A*02:01. Representative measurements are shown, and experiments were done at least in duplicate. Figure is adapted from [119].

It was next investigated whether cell lines were recognised when overexpressing the KrasG12V mutation to exclude the possibility that low expression levels were reasons for the failure of 1376 TCR-transduced T cells to recognise the spliced form of the KrasG12V peptide on cancer cells. Therefore, constructs were generated carrying three copies of either a linear G12V mutant 35mer, a linear G12V mutant 10mer epitope (as a negative control), a spliced mutant G12V 9mer epitope (as a positive control) or a spliced wild type 9mer epitope (as an additional negative control) (Figure 18A). The triple epitopes were separated by an AAY sequence that ensures proteasomal cleavage[144]. These constructs were retrovirally transduced into MCF7 (Figure 18B), 624Mel (Figure 18C) or the murine NIH-HHD cells (Figure 18D) and co-cultured with either human or mouse 1376 TCR-transduced T cells. T cells only recognised tumour cells when expressing the positive control spliced G12V 9mer, but failed to elicit an immune response when co-cultured with cells expressing the 35mer, unless loaded with spliced peptide. Overexpression of the 35mer was confirmed by qPCR (Figure 18E). These data suggest that the spliced epitope was not naturally processed and presented in sufficient amounts to be recognised by specific TCRs with high peptide affinity.

A

[MTEYKLVVVGAVGVGKSALTIQLIQNHFVDEYDPT -AAY]3-gfp	35mer (KrasG12V)
M [KLVVVGAVGV -AAY]3-gfp	linear 10mer (KrasG12V)
M [KLVVGAVGV -AAY]3-gfp	spliced 9mer (KrasG12V)
M [KLVVGAGGV-AAY]3-gfp	spliced 9mer (Kras wt)

B

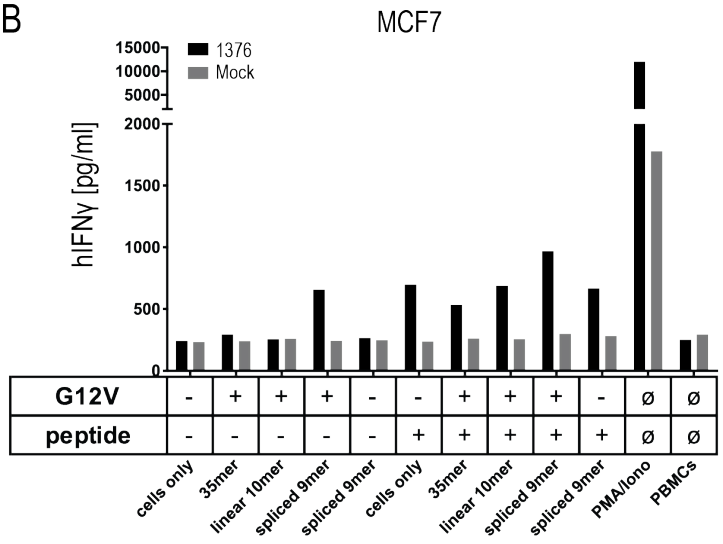

C

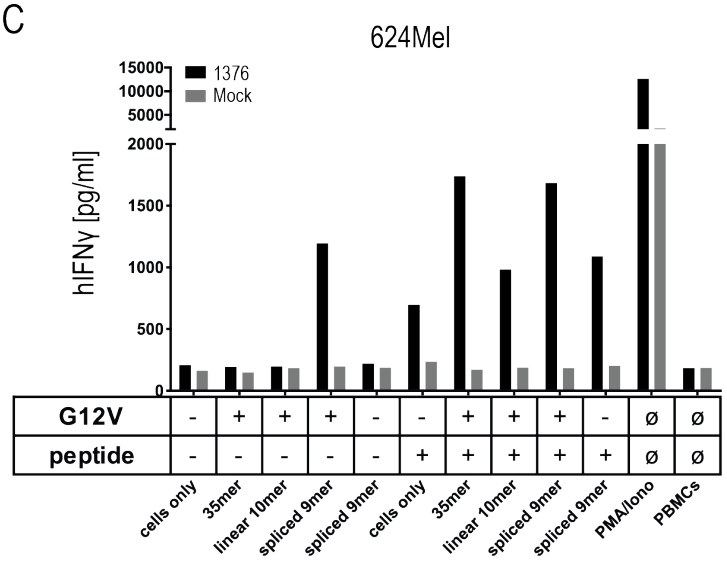

D

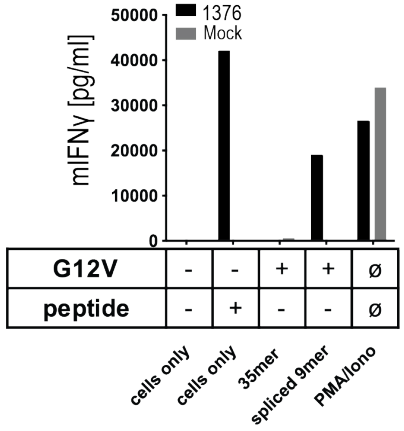

E

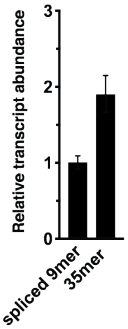

Figure 18. KrasG12V splice-specific TCR did not recognise human and mouse cells expressing KrasG12V cDNA. (A) Schematic representation of KrasG12V and wild type triple epitopes used for recombinant overexpression in MCF7, 624Mel, and NIH-HHD cells. **(B-D)** TCR 1376 was retrovirally transduced into human PBMCs or TCR1xCD45.1xRag1$^{-/-}$ mouse splenocytes, and 10^4 transduced cells were co-cultured 1:1 with (B) MCF, (C) 624Mel and (D) NIH-HHD target cells. Cells were loaded with 10^{-6} M spliced peptide or transduced with either KrasG12V triple minigene 35mer, or KrasG12V triple epitope spliced nonamer. Kras wild type triple epitope spliced nonamer or KrasG12V triple epitope linear decamer. IFNγ production of transduced T cells is shown (1376, black bars). PMA and Ionomycin (PMA/Iono) stimulation served as positive control and all target cells were also co-cultured with non-transduced T cells (Ø, grey bars). Representative measurements are shown, experiments were done at least in duplicate. **(E)** Relative amounts of KrasG12V triple minigene 35mer and KrasG12V triple epitope spliced nonamer were determined by qPCR on transduced NIH-HHD cells. KrasG12V triple epitope spliced nonamer expression is arbitrarily set to 1. Figure is adapted from [119].

4.3.2 Rac2P29L splice-specific T cells failed to recognise overexpressed mutant cDNA

To evaluate a second potential spliced epitope as a target for ATT, a Rac2P29L splice-specific TCR (20967A2) was isolated from ABabDII mice[123] and compared to the above described Rac2P29L linear-specific TCR 22894. Constructs were generated carrying either the whole cDNA of mutant Rac2P29L, three copies of Rac2P29L 45mer or three copies of Rac2P29L spliced 9mer (as a positive control). These constructs were retrovirally transduced in Mel21a (Figure 19A-B) or NIH-HHD (Figure 19C) and co-cultured with TCR-transduced human or murine T cells. However, the splice-specific 20967A2 TCR-transduced T cells failed to elicit an immune response against both the triple epitope 45mer as well as the cDNA, unless loaded with spliced peptide. In contrast, the linear-specific 22894 TCR-transduced T cells recognised both the 45mer and the cDNA. In line with the KrasG12V data, also the mutant RacP29L splice-specific TCR-transduced T cells were able to recognise the spliced epitope, suggesting that also here the spliced epitope is not generated by the tumour cells in sufficient amounts. Overexpression was confirmed by qPCR (Figure 19E).

A

MQAIKCVVVGDGAVGKTCLLISYTTNAFLGEYIPTV[…]ACSLL-IRES-gfp — cDNA (Rac2P29L)
[MQAIKCVVVGDGAVGKTCLLISYTTNAFLGEYIPTVFDNYSANV -AAY]3-gfp — 45mer (Rac2P29L)
M [FLGEYIPVF -AAY]3-gfp — spliced 9mer (Rac2P29L)

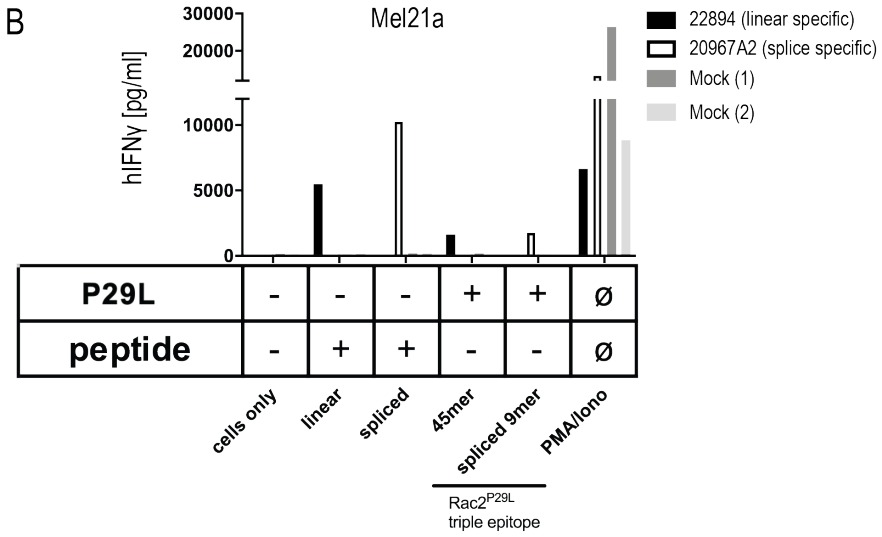

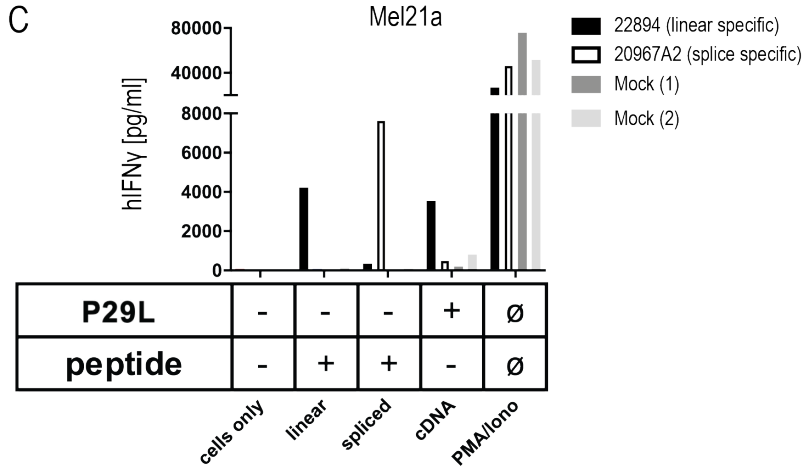

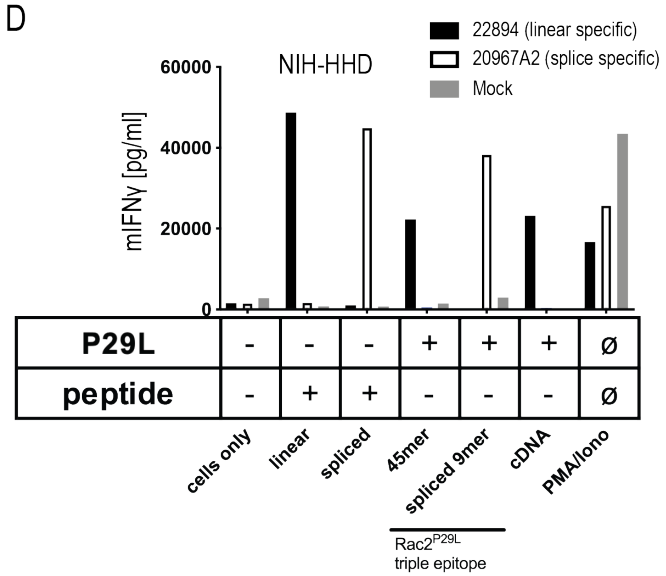

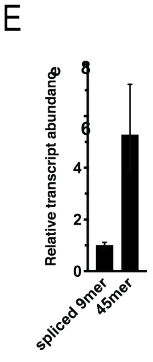

Figure 19. Rac2P29L splice-specific T cells did not recognise cells expressing mutant Rac2P29L cDNA. (A) Schematic representation of Rac2P29L cDNA and triple epitopes used for recombinant overexpression in Mel21a and NIH-HHD cells. **(B, C)** TCRs were retrovirally transduced into human PBMCs and 10^4 transduced cells were co-cultured 1:1 with Mel21a target cells. Human target cells were loaded with 10^{-6} M spliced or non-spliced Rac2 peptide, or transduced with either Rac2 triple epitope 45mer (B), Rac2P29L triple epitope nonamer (B), or Rac2P29L cDNA (C). IFNγ production of transduced T cells is shown (22894, black bars and 20967A2, white bars). PMA and Ionomycin (PMA/Iono) stimulation served as positive control and all target cells were also co-cultured with non-transduced T cells (Ø, grey bars). Representative measurements are shown, experiments were done at least in duplicate. **(D)** TCRs were retrovirally transduced into TCR1xCD45.1xRag1$^{-/-}$ mouse splenocytes, and 10^4 transduced cells were co-cultured 1:1 with NIH-HHD target cells. Murine target cells were loaded with 10^{-6} M spliced or non-spliced Rac2 peptide, or transduced with either Rac2 triple epitope 45mer, Rac2P29L triple epitope nonamer, or Rac2P29L cDNA. Upon co-culture with recombinant TCR$^+$ T cells, IFNγ release was measured (22894, black bars and 20967A2, white bars). PMA and Ionomycin (PMA/Iono) stimulation served as a positive control, and all target cells were also co-cultured with non-transduced T cells (Ø, grey bars). Representative measurements are shown, and experiments were done at least in duplicate. **(E)** Relative amounts of Rac2P29L triple epitope 45mer and Rac2P29L triple epitope nonamer were determined by qPCR on transduced NIH-HHD cells. Rac2P29L triple epitope nonamer expression is arbitrarily set to 1. Figure is adapted from [119].

In summary, these data showed that high avidity TCRs can be generated against spliced epitopes, however, it remains questionable whether and how often tumour cells generate sufficient amounts of spliced epitopes for T cell recognition.

5. Discussion

Target identification and validation are crucial factors for successful adoptive T cell therapy. Ideal targets must be important for cancer cell survival, such as driver mutations, to minimise therapy escape. Additionally, the target should be processed and presented on MHC complexes in sufficient amounts. This thesis focused on the validation of three tumour targets by measuring T cell responses mediated by high-affinity TCRs.

Firstly, an HLA-A*02:01 restricted high-affinity TCR against the common glioma mutation H3.3K27M was isolated. However, despite high peptide reactivity, H3.3K27M TCR-transduced T cells failed to secrete cytokines and to elicit cytotoxicity against cells naturally expressing or overexpressing H3.3K27M mutation.

Secondly, TCRs against potential neoepitopes bearing the melanoma mutations Rac1P29S and Rac2P29L were isolated and characterised. Here, it was investigated whether TCRs isolated after immunisation with a peptide that is predicted to have stronger binding to the MHC complex can be used for heterologous treatment against a more frequent mutation with weaker predicted peptide-MHC binding. Indeed, in this proof-of-principle study the heterologous TCR 22894-transduced T cells performed better *in vivo* in inducing regression of Rac1P29S mutant tumours compared to TCR 5934-transduced T cells, a TCR obtained after immunisation with the cognate mutation (Rac1P29S). Cytotoxicity against Rac1P29S expressing melanoma cell lines was observed after co-culture with Rac1/2-specific T cells.

Thirdly, evidence was provided that generation of spliced epitopes cannot be sufficiently predicted by algorithms and *in vitro* proteasome processing. It was found that two potential spliced neoepitopes generated by proteasome-catalysed peptide splicing (PCPS) were not recognised by high-affinity TCRs, thereby suggesting that this post-translational modification mechanism does not lead to enough antigen presentation for successful T cell therapy at least for the targets analysed here.

Together, these projects suggest that even high-affinity TCRs against in principle ideal targets can fail if the epitopes are not sufficiently generated, meaning processed and presented on MHC complexes. Thus, it will be discussed here how important improved strategies to identify T cell epitopes as targets for TCR therapy are prior to isolation and characterization of TCRs. In general, it is challenging to select suitable immunogenic neoepitopes for ATT, because identification is primarily based on epitope predictions. Limitations in correctly predicting

neoepitopes include variability between algorithms and platforms as well as failure to predict proteasomal processing and post-proteasomal modifications. It has been shown that half of predicted high-affinity binding epitopes are immunogenic, out of which only 15% are processed. Among these MHC binding, immunogenic and processed epitopes, only 11% were ultimately recognised by T cells[145,146]. Therefore, a reverse immunology approach, in which TCRs are cloned based on predicted peptides, might not be a feasible pipeline, unless thoroughly validated by, for example, immunopeptidome analysis as discussed below.

5.1 Isolation of potential neoantigen-specific TCRs with high functional avidity from a transgenic mouse model

In this thesis, the potential of three TSAs as targets for adoptive T cell therapy was investigated. TSAs are often referred to as neoantigens, meaning novel antigens that were absent before a somatic mutation happened and are therefore an exquisite target for T cell therapy. In contrast, TAAs are derived from proteins that are also found in non-cancerous cells but show aberrant expression in tumours[147]. An advantage of TSA-specific TCRs is that they can be isolated from humans, while T cells against TAAs are subjected to central tolerance. Moreover, the lower risk of on-target off-tumour cytotoxicity remains a major advantage of TCRs against TSAs rather than against TAAs[148,149].

To isolate specific TCRs, ABabDII mice were immunised with synthetic peptides constituting of *in silico* predicted HLA-A*02:01 binding epitopes. These humanised mice are deficient of endogenous mouse class I molecules as well as the murine TCR alpha and beta chains, while they carry the human TCR alpha and beta gene loci by germline transmission of human TRA and TRB yeast artificial chromosomes (YACs)[123,150]. Additionally, the ABabDII mice express the modified human HLA-A*02:01 (HHD) molecule, which is a chimeric construct consisting of the human β2m and HLA-A*02:01 α1 and α2 domains[143]. To ensure mouse CD8 binding, the α3, transmembrane and cytoplasmic regions are of mouse origin. Other mouse models, in which only the MHC complexes are humanised and the TCR loci remain of mouse origin, bear the risk of isolating immunogenic TCRs[66,151,152]. Hence, the ABabDII mouse model used here is superior for TCR isolation and was previously shown to successfully generate TCRs with clinical potential[124,153].

After immunisation of the ABabDII mice with the H3.3K27M peptide, a specific TCR (27633) was identified, which recognised its cognate target with high affinity. In contrast to the mouse-derived TCR, the published TCR (1H5[102]) obtained from mutant peptide-stimulated HLA-

A*02:01-positive donor PBMCs also recognised the wild type peptide at peptide concentrations down to 10^{-8} M, which is a substantial disadvantage of this TCR. Therefore, TCR 27633 would be the better candidate for further studies. Likewise, further TCRs were successfully isolated after immunisations with peptides derived from Rac1P29S, linear and spliced versions of Rac2P29L as well as spliced KrasG12V. TCR-transduced T cells consistently showed high cytokine secretion against the cognate mutant epitopes. Since all TCRs showed high functional avidity, they were further used to validate if these recurrent mutations could be used as targets for ATT.

5.2 Importance of high peptide-MHC affinity

In addition to high TCR affinity, the interaction between the TCR and the peptide-MHC complex also depends on the binding strength of the peptide to the MHC molecule. Engels et al. provided evidence that only high-affinity peptides act as rejection epitopes leading to relapse-free tumour regression[125].

In this project, high peptide-MHC affinity was especially important to consider for the isolation of a TCR against the common KrasG12V mutation. Unfortunately, no linear KrasG12V epitope with high binding affinity to HLA-A*02:01 was predicted. However, the spliced version KLVV/GA**V**GV has a strong predicted binding affinity of 33.4 nM, while the linear version binds HLA-A*02:01 only with a low predicted affinity of 9675.66 nM.

Notably, high peptide-MHC and TCR affinity alone are not sufficient to predict a good T cell target. Other factors like antigen processing, presenting, posttranslational modifications or expression levels might still interfere with successfully targeting a high-affinity antigen.

5.3 Beneficial cross-reactivity against a heterologous target

An interesting observation was made while characterising three high-affinity TCRs isolated from the ABabDII mouse model against the two mutant epitopes Rac1P29S (F**S**GEYIPTV) and Rac2P29L (F**L**GEYIPTV). All TCRs were cross-reactive against both mutant peptides with high affinity suggesting the mutant position does not interfere with TCR binding. This instance was also recapitulated by respective alanine scan analysis (data not shown). Additionally, the Rac2-specific 22894 TCR showed stronger binding to the Rac1-specific pA2 tetramer. The two epitopes differ in one amino acid, while the Rac1 mutant epitope has a proline to serine exchange at position 2 of the epitope, the Rac2 mutant epitope consists of a leucine at position 2. Position 2 is an important anchor position in HLA-A*02:01 restricted epitopes, often

consisting of the hydrophobic amino acid leucine in strong binding epitopes[14]. As a result, the Rac2P29L mutation has a higher predicted peptide-MHC binding affinity of 2.3 nM, while Rac1P29S is predicted to bind HLA-A*02:01 with an affinity of 18.2 nM. Therefore, the epitope Rac2P29L is a better target candidate in terms of strong binding to HLA-A*02:01 and might have led to the isolation of a better TCR with the potential to induce tumour regression more efficiently. However, the Rac2P29L mutation is only rarely described in tumours. In contrast, the Rac1P29S mutation is the third most common protein-coding hotspot mutation in melanoma and therefore a more interesting target for ATT. Thus, the finding that the Rac2-specific TCR 22894 isolated after Rac2P29L peptide immunisation also recognises the Rac1P29S peptide might be an alternative strategy to isolate high-affinity TCRs against a heterologous target.

5.3.1 Rac2-specific T cells induced regression of tumours expressing the Rac1P29S as a triple epitope *in vivo*

To further investigate that hypothesis, the Rac2-specific TCR 22894 was compared to the Rac1-specific TCR 5934 for ATT in a syngeneic mouse model. The other Rac1-specific A12B20 TCR was excluded from the *in vivo* experiment, since it performed worse *in vitro* compared to the other two Rac1/2-specific TCRs. The aim was to study tumour rejection against the Rac1P29S mutation *in vivo*. For this, MC703 cells, a fibrosarcoma cell line derived from a transgenic mouse expressing a chimeric HLA-A2 and H-2D^b molecule (HHD), were injected into HHDxRag-/- mice lacking B and T cells[9,127,143]. This mouse model allowed us to study *in vivo* tumour rejection using human MHC complexes, TCRs and antigens, while cellular components like tumour cells and T cells are of mouse origin[127].

Interestingly, the Rac2-specific 22894 TCR-transduced T cells induced more potent regression of the tumour cells expressing the Rac1P29S mutation as triple epitopes than Rac1-specific 5934 TCR-transduced T cells. The 22894 TCR was isolated after Rac2P29L mutant peptide immunisation and showed similar reactivity as Rac1-specific TCR 5934 against the mutant Rac1 peptide. Since the Rac2P29L mutation has a higher predicted peptide-MHC affinity as described above, this might be the reason for the advantage of the Rac2-specific 22894 TCR over the Rac1-specific 5934 TCR. Despite initial tumour regression, the tumours relapsed. The reason for the relapse is an outgrowth from the 1% antigen-negative tumour cells that were present as impurity in the inoculated tumour cells. Complete rejection might be achieved in future experiments by using a pure antigen-positive starting tumour population for tumour injection.

Notably, the *in vivo* experiments were performed using MC703 cells that were transduced to overexpress the Rac1P29S mutation as triple epitopes and not with the full-length DNA[144]. This means the mutation was already present as a 9mer in three copies and processing was ensured by an AAY cleavage site. Thus, with this experiment, only the performance of the TCR-transduced T cells against the mutant epitope was evaluated, but proof that the epitope is generated naturally in sufficient amounts needs to be further investigated.

Despite the relapse, these results showed for the first time that a TCR isolated against a target with a stronger peptide-MHC binding can induce improved tumour regression of tumours expressing a heterologous target *in vivo*. There are multiple driver mutations described, in which certain amino acids are frequently mutated to other amino acids, for example, KrasG12V, G12D, and G12C. Hence, this approach might also be used to obtain high-affinity TCRs against other heterologous mutant epitopes.

5.4 Importance of sufficient natural generation of potential targets

High-affinity TCRs were isolated against antigens which are recurrent in tumours, important for cancer cell survival and presented by the common HLA-A*A2:01 molecule. Therefore, it seemed promising to detect substantial recognition of tumours expressing these supposedly ideal target mutations. However, even T cells expressing a high-affinity TCR can fail to recognise a target if it is not processed and presented in sufficient amounts, as described by Popović et al.[134]. Insufficient generation can be explained by too low levels of processed epitope or destructive proteasomal cleavage sites within the epitope.

Notably, this project focused on the development of TCR-based immunotherapies for HLA-A*02:01$^+$ patients only. These results do not exclude the possibility that other epitopes harbouring for instance the H3.3K27M mutation are sufficiently presented by other class I or class II MHC molecules and therefore good targets for ATT.

5.4.1 H3.3K27M is unlikely a suitable target for TCR gene therapy in HLA-A*02:01$^+$ patients with DMG

Although TCRs generated against the H3.3K27M mutation showed high affinity to their cognate peptide *in vitro*, TCR-transduced T cells did not recognise the endogenously expressed mutation, which is a prerequisite for TCRs to possess a clinical potential. The published TCR 1H5[102] was tested side by side with a high-affinity mouse-derived H3.3K27M peptide-specific TCR in co-culture experiments measuring IFNγ, TNFα and IL2 secretion as well as cytotoxicity. However, reactivity even to overexpressed H3.3K27M was not observed by any

of the TCRs; therefore, the applicability of this adoptive T cell targeting approach in HLA-A*02:01$^+$ DMG patients is questionable. Additionally, the overexpression of mutant H3.3 protein was confirmed by western blot. Since protein detection in a western blot is less sensitive than epitope recognition by T cells, it is unexpected that H3.3K27M-specific T cells would not recognise a cell line overexpressing the protein, unless epitope processing or presentation did not work as expected.

Overall, these findings are in contrast to those reported by Chheda et al., where 1H5 TCR-modified T cells were shown to mediate cytotoxicity upon co-culture with DIPG cells naturally expressing the H3.3K27M mutation[102]. The discrepancies between these findings and previously published ones were not resolved, even when the same cell line (U87MG) was used for presentation. Using the U87MG cell line, it was ruled out that factors in the processing machinery or within the antigen itself account for the discrepancies. Reeves et al. present a study showing how different activity of ERAP polymorphisms explain differences in the presented peptide repertoire and varying T cell responses among individuals[154]. Here, it cannot be excluded that proteasomal cleavage within the epitope causes the lack of epitope generation[134]. Alternatively, the presence or absence of methionine oxidation in the H3.3K27M/HLA-A*02:01 epitope could alter the T cell response[155]. It was shown that oxidative modifications as a result of oxidative stress observed in situations like inflammation and cancer might alter the T cell response severely. However, since recognition of the H3.3K27M expressed as a triple epitope was observed, a limited TCR specificity against oxidised methionine only is unlikely. In conclusion, the absence of T cell response can be explained by the insufficient generation of the epitope and hence H3.3K27M is unlikely a suitable target for TCR gene therapy in HLA-A*02:01$^+$ patients with DMG.

In contrast, in a study using a decamer mutant peptide vaccine in DMG patients, the authors claim to detect H3.3K27M-specific vaccine responses[103]. However, it is unlikely that the CD8$^+$ T cells in this clinical trial were effective against cancer cells because it was shown here that the epitope is not presented in sufficient amounts to be recognised by T cells. In line with these findings, the H3.3K27M epitope vaccination treatment strategy (PNOC007, NCT02960230) did not improve the overall outcome in H3.3K27M$^+$ patients with DMG[103]. This pilot trial assessed the safety, immunoreactivity and efficacy of the H3.3K27M synthetic peptide as a therapeutic vaccine. They showed that overall survival at 12 months (OS12) was 40% in DIPG patients and 39% in nonpontine DMG. However, a recent analysis from the International and European DIPG registries reported a similar OS12 of 42.3% in untreated patients[156], suggesting

the vaccine did not improve overall survival. Importantly, the trial only showed expansion of peptide-specific $CD8^+$ T cells, however, no evidence for effectiveness in patients and/or presentation of the epitope in sufficient amounts was provided. Higher overall survival among patients with $CD8^+$ T cell expansion might simply be a result of better general immunological fitness among these patients. Additionally, a second trial (NCT04749641, Guangdong TCRCure Biopharma Technology Co., Ltd) testing histone H3.3-K27M neoantigen vaccine therapy in HLA-A*02:01^+ patients is actively recruiting, which likely will provide similar ineffective outcomes. Thus, clinical studies like these might raise false hope in at least HLA-A*02:01^+ patients and resources might be better used to focus on other mutations or different class I or class II HLA molecule-restricted epitopes.

5.4.2 Rac1P29S expressing melanoma cells were variably recognised by Rac1/2-specific T cells

Despite the high IFNγ release by the Rac1/2-specific TCR-transduced T cells against peptide-loaded cells and *in vivo* regression of tumour cells expressing the mutation as a triple epitope, cytokine release was observed against only one of three melanoma cell lines naturally expressing the Rac1P29S mutation. In contrast, the TCR-transduced T cells performed substantially better in a live-cell imaging-based toxicity assay. Due to the importance of IFNγ secretion for tumour regression[157], further investigations are required to conclude whether the recurrent melanoma mutation Rac1P29S is a suitable target for adoptive T cell therapy.

Nevertheless, the Rac1-specific 5934 TCR-transduced T cells showed high cytolytic activity and detectable IFNγ secretion against naturally expressing melanoma cells, which is a prerequisite to validating this TCR for clinical use. Next steps could include toxicity assays such as further alanine scans and scanning approaches using a combinatorial peptide library to identify epitopes with the same recognition pattern to exclude off-target toxicity of this TCR[158,159]. Additionally, MHC alloreactivity of the TCRs can be excluded by performing co-culture experiments with a panel of EBV–transformed lymphoblastoid B cell lines (LCLs) to detect reactivity against other MHCs.

While the Rac1-specific 5934 TCR-transduced T cells performed better in the cytotoxicity assay, the Rac2-specific 22894 TCR-transduced T cells induced more potent regression of the Rac1 triple epitope expressing tumour cells *in vivo*. Discrepancies between *in vitro* and *in vivo* T cell responses are frequently described. For instance, Leisegang et al. published a study where a TCR mounted similar immune responses against two mutant CDK4 isoforms (R24L and

R24C), however, tumour rejection *in vivo* differed dramatically between the two targets[127]. Therefore, *in vivo* validation of targets and TCRs in mouse models remains inevitable. For the project described in this thesis, *in vivo* studies using the full-length DNA of mutant Rac1 would enlighten the potency of the Rac1/2-specific TCRs to reject tumours expressing the Rac1P29S mutation endogenously.

5.4.3 None of the two potential spliced neoepitopes was recognised by specific T cells

Predicting spliced epitopes remains challenging due to the complexity of protein sequences and missing data on cleavage strength to determine the efficiency of spliced epitope generation[160–162]. As a result, many predicted spliced epitopes turn out to be false positives, as described in this project. Therefore, predicted epitopes must be thoroughly validated by for instance mass spectrometry analysis of the immunopeptidome and more importantly T cell assays *in vitro* and *in vivo*[163–165]. Using these prediction and validation approaches, several spliced epitopes such as melanocytic glycoprotein gp100^{PMEL17} and fibroblast growth factor-5 (FGF-5) in cancer patients are described[116,117]. However, an important topic of debate remains the question of how abundant these spliced epitopes are. Initially, spliced epitopes were reported to contribute to up to 30% of the HLA ligandome[166], however, more recent studies provided solid evidence that the frequency of spliced epitopes within the HLA ligandome is more likely around 2-6% or even less[167,168].

The putative spliced neoepitopes KrasG12V (KLVV/GAVGV) and Rac2P29L (FLGEYIP/VF) were previously predicted to bind HLA-A*02:01 with high affinity using the ProtAG algorithm[119]. Using these spliced epitopes for peptide immunisations in ABabDII mice, high-affinity TCRs were successfully isolated, however, TCR-transduced T cells repeatedly failed to detect cell lines naturally expressing or overexpressing one of the two mutations. The Rac2P29L spliced epitope was previously detected by *in vitro* PCPS generation[119] and therefore seemed an interesting candidate for T cell validation. However, no immune response was observed when endogenous processing and presenting of the epitope were required. One possible explanation for the failure to verify the *in vitro* PCPS reaction could be the higher substrate and proteasome concentration used for *in vitro* PCPS reaction compared to the physiological *in vivo* situation[119].

These results raise the general concern whether spliced epitopes are sufficiently generated and presented to elicit a T cell immune response *in vivo*. These data suggest that the epitopes are not sufficiently generated, as the TCRs were highly specific and showed high functional avidity

against the mutant spliced epitopes but failed to detect natural expression as well as overexpression of a 35mer, a 45mer and the full-length cDNA. As described before, the abundance of spliced epitopes among the immunopeptidome is much lower than previously estimated and therefore might not play a major role in the generation of targets for T cell therapy. Therefore, a previously highlighted pipeline for the identification of immune-relevant spliced neoantigens is not sufficient to detect suitable targets and further validation steps to identify good targets are required[169].

Nevertheless, these data do not exclude the possibility that other post-translational modifications such as enzymatically mediated alterations create well-expressed epitopes and therefore expand the repertoire of targetable cancer antigens by T cells. Moreover, $CD8^+$ T cell response against HIV-derived spliced epitope was confirmed[170], however, to which extent spliced epitopes contribute to targetable T cell epitopes remains elusive.

5.5 T cell modifications to enhance T cell functions

Next, it was investigated whether the efficiency of TCR-transduced T cells against insufficiently expressed targets can be enhanced by modifying the T cells themselves. One successful example of how tumour rejection of CAR-expressing T cells was enhanced is described by Eyquem et al.[171]. Here, the CAR was integrated into the TRAC locus by targeted CRISPR/Cas9 delivery instead of random viral integration. This not only improved T cell potency but also delayed effector T cell differentiation and exhaustion. This approach was also described to preserve near-physiological T cell function after orthotopic replacement of the endogenous TCR receptor with five exogenous TCRs targeting epitopes[172].

Another strategy to enhance adoptive T cell therapy was described by Oda et al., where a Fas/Fas ligand-mediated death signal was converted to a 4-1BB costimulatory pro-survival signal on mouse and human T cells[173]. Using a Fas-4-1BB fusion protein they improved multiple T cell functions such as cytokine production and T cell expansion *in vitro* as well as enhanced T cell survival in a pancreatic cancer model *in vivo*.

Alternatively, the efficiency of ATT can be enhanced by modifying proteins that negatively influence T cell cytolytic activities. An interesting candidate is the estrogen receptor-binding fragment-associated antigen 9 (EBAG9), which is a negative regulator of the Ca^{2+}-dependent regulated secretion of effector molecules[174]. It was shown that lack of EBAG9 increased the cytolytic activity of T cells by inducing the release of secretory lysosomes and therefore an EBAG9 knockout might enhance ATT.

5.5.1 The endogenous TCR did not interfere with effector functions of the transduced TCR

In this thesis, one strategy to modify T cells to enhance T cell functions including cytotoxicity and cytokine secretion was investigated using the H3.3K27M-specific TCRs. To perform T cell *in vitro* assays, T cells from healthy donors were engineered to express an exogenous mutation-specific TCR. However, these T cells already express their original TCR and therefore, mispairing of the endogenous and exogenous TCR might interfere with TCR expression. To reduce the risk of mispairing, the exogenous TCR was engineered to express a murine constant region enhancing the chances that the two transduced alpha and beta chains pair with each other instead of the endogenous chains forming mixed dimers[175]. However, this does not fully exclude the possibility that mispaired TCRs hamper the immune response of TCR-transduced T cells *in vitro*. The Chheda et al. study used siRNAs to additionally knock down the endogenous TCR to ensure excellent expression of the transgene TCR genes[102,176,177]. Since opposing results to their data were observed, the possibility that mispairing interfered with T cell recognition of the H3.3K27M mutation in these results was investigated. Therefore, the CRISPR/Cas9 system was used to knock out the endogenous alpha and beta chains, respectively, in the H3.3K27M TCR-transduced T cells. Even though the proportion of $hTCR\alpha/\beta^{+}mTCR^{+}$ double positive cells in the therapeutic TCR-transduced PBMCs was quite low, probably due to stronger expression and preferential pairing of transduced TCR chains, the successful knockout was also reflected in the $hTCR\alpha/\beta^{+}mTCR^{-}$ populations. Despite these high knockout efficiencies and the reduced frequency of mixed dimers, neither T cell activity against the H3.3K27M mutation was restored nor pA2 tetramer binding was improved and hence the possibility that mispairing interfered with target recognition can be excluded.

5.6 Strategies to improve the selection of suitable target epitopes prior to TCR isolation and characterisation

In this thesis, the targets were selected using a reverse immunology approach based on mutation recurrence in tumours and predicted binding strength to HLA-A*02:01. However, in line with these results, many targets failed to be recognised by high-affinity TCRs due to insufficient generation by tumour cells or lack of immunogenicity. Thus, novel and improved strategies need to be identified to select suitable epitopes before TCRs are isolated and characterised.

5.6.1 MHC class I immunopeptidome analysis

As described in this thesis, the analysis of the MHC class I immunopeptidome can confirm if a target epitope is generated and presented on MHC molecules. To do so, MHC class I bound

peptides were immunoprecipitated using MHC class I specific antibodies bound to sepharose beads. The eluted peptides were then analysed by mass spectrometry. Either a discovery run can be performed, where all class I bound peptides are analysed, or the presence or absence of specific peptides of interest can be analysed by a targeted search[178]. The latter approach was performed in this project as part of the analysis to ask if H3.3K27M is a suitable target for T cell therapy. In line with the results obtained from the T cell assays, the R**M**SAPSTGGV peptide was not detected among the MHC class I eluted peptides of mutant H3.3 overexpressing U87MG cells. As a positive control, a heavy labelled variant of the peptide (R**M**SAPSTGGv*) that was spiked into the sample was successfully detected. In contrast, the overexpressed positive control CDK4R24L peptide was highly abundant in the respective samples. These results suggest that the lack of T cell response towards the H3.3K27M peptide was due to the absence of presented epitopes on the tumour cells. These data are contradicting the mass spectrometry analysis in the Chheda et al. publication[102], where they claim to detect H3.3K27M peptides among the eluted epitopes. However, the authors did not show reproducibility of the data and the results are only depicted as singlets. Therefore, the detected signal might only be background. In this project, evidence was provided that the respective signal is missing in four replicates while the positive control mutant CDK4 was clearly detectable.

A limiting factor using immunopeptidome analysis for target discovery is the requirement for high cell numbers to elute sufficient amounts of peptide for the mass spectrometry analysis. Using a more sensitive mass spectrometer might reduce the high number of required tumour cells. Alternatively, the tumour cells were here grown in NSG mice to gain larger cell numbers in a shorter time, as recently described by Rijensky et al. for PDX models[179]. This increases the efficiency of tumour cell collection in terms of time and workload. Similar experiments to investigate whether the Rac2 spliced as well as the Kras spliced epitope is present among the class I immunopeptidome would also enlighten if this is the mechanism behind insufficient target recognition by T cells expressing high-affinity TCRs.

In conclusion, integrating mass spectrometry analysis of the MHC immunopeptidome as a novel routine method during the epitope discovery pipeline can improve the finding of suitable targets dramatically, especially when performed prior to TCR isolation and characterisation.

5.6.2 Full-length DNA immunisation

Another strategy to find suitable epitopes is to initially immunise the ABabDII transgenic mice with a vector carrying the full-length antigens instead of using the predicted peptide only. For

instance, high T cell response with a low amount of DNA was achieved by gene gun-based nucleic acid injection, a method based on high-pressure injection of plasmid-coated gold beads into the skin[180]. Full-length DNA vaccinations have the advantage that the epitope has to be processed and presented *in vivo*, and only if that is happening in sufficient amounts, reactive T cells can be isolated. Therefore, one could avoid cases as described here, where T cells were isolated without the need for natural expression of the antigen. However, it remains elusive in which way differences in the processing and presenting machinery between mice and humans may modify the presented antigens and if the human epitope generation can be correctly mimicked in the ABabDII mouse model[181].

5.6.3 Systematic discovery of T cell epitopes

Alternatively, high-throughput *in vitro* screenings can facilitate the selection of suitable epitopes. An interesting approach to identifying antigens recognised by T cells is "T-scan" described by Kula et al.[182]. Here, T cell recognition of human antigens that are endogenously generated and presented by MHC complexes was detected using a reporter system based on granzyme B activity. Thereof, epitopes of reactive reporter cells could be identified and used for further TCR generation without the need for predictive algorithms. Previously described similar high-throughput approaches using for example yeast-bound MHC molecules that covalently bind random peptides also successfully identified T cell epitopes, however, without the need for endogenous processing prior to antigen presentation[183]. Thus, the ability of the T-scan approach to detect only physiologically generated epitopes makes it an interesting new tool that might replace reverse immunology approaches based on predicted epitopes.

In conclusion, high-affinity TCRs against the recurrent cancer-specific mutations H3.3K27M, Rac1P29S, Rac2P29L and KrasG12V for adoptive T cell therapy were isolated and tested, however, these data suggest that selecting antigens using a reverse immunology approach based on prediction algorithms is not sufficient. Additional methods such as the described analysis of the MHC class I immunopeptidome prior to isolation and characterisation of TCRs will likely improve the selection of endogenously processed and presented neoantigens. A method to more efficiently collect high numbers of tumour cells to facilitate the analysis of MHC class I bound peptides was described and applied here. Additionally, it was shown that immunisation against a stronger peptide-MHC binding heterologous target can lead to the isolation of TCRs that can better induce regression of epitope-expressing tumours *in vivo*.

6. References

1. Weninger, W., Manjunath, N. & Von Andrian, U. H. Migration and differentiation of CD8+ T cells. *Immunological Reviews* **186**, 221–233 (2002).

2. Russell, J. H. & Ley, T. J. Lymphocyte-mediated cytotoxicity. *Annual Review of Immunology* **20**, 323–370 (2002).

3. Koga, Y. *et al.* A human T cell-specific cDNA clone (YT16) encodes a protein with extensive homology to a family of protein-tyrosine kinases. *European Journal of Immunology* **16**, 1643–1646 (1986).

4. Hedrick, S. M., Cohen, D. I., Nielsen, E. A. & Davis, M. M. Isolation of cDNA clones encoding T cell-specific membrane-associated proteins. *Nature* **308**, 149–153 (1984).

5. Call, M. E., Pyrdol, J., Wiedmann, M. & Wucherpfennig, K. W. The organizing principle in the formation of the T cell receptor-CD3 complex. *Cell* **111**, 967–979 (2002).

6. Davis, M. M. & Bjorkman, P. J. T-cell antigen receptor genes and T-cell recognition. *Nature* **334**, 395–402 (1988).

7. Samelson, L. E. *et al.* Expression of genes of the T-cell antigen receptor complex in precursor thymocytes. *Nature* **315**, 765–768 (1985).

8. Shinkai, Y. *et al.* RAG-2-deficient mice lack mature lymphocytes owing to inability to initiate V(D)J rearrangement. *Cell* **68**, 855–867 (1992).

9. Mombaerts, P. *et al.* RAG-1-deficient mice have no mature B and T lymphocytes. *Cell* **68**, 869–877 (1992).

10. Komori, T., Okada, A., Stewart, V. & Alt, F. W. Lack of N Regions in Antigen Receptor Variable Region Genes of TdT-Deficient Lymphocytes. *Science* **261**, 1171–1175 (1993).

11. Beck, S. *et al.* Complete sequence and gene map of a human major histocompatibility complex. *Nature* **401**, 921–923 (1999).

12. Villadangos, J. A. Presentation of antigens by MHC class II molecules: getting the most out of them. *Molecular Immunology* **38**, 329–346 (2001).

13. Bjorkman, P. J. *et al.* Structure of the human class I histocompatibility antigen, HLA-A2. *Nature* **329**, 506–512 (1987).

14. Falk, K., Rotzschke, O., Stevanovic, S., Jung, G. & Rammenseet, H.-G. Allele-specific motifs revealed by sequencing of self-peptides eluted from MHC molecules. *Nature* **351**, 290–296 (1991).

15. Bouvier, M., Wiley, D. C., Bouvier, M. & Wiley, D. C. Importance of Peptide Amino and Carboxyl Termini to the Stability of MHC Class I Molecules. *Proceedings of the National Academy of Sciences of the USA* **346**, 2745 (1990).

16. Tanaka, K. Role of proteasomes modified by interferon-γ in antigen processing. *Journal of Leukocyte Biology* **56**, 571–575 (1994).

17. Sijts, E. J. A. M. & Kloetzel, P. M. The role of the proteasome in the generation of MHC class I ligands and immune responses. *Cellular and Molecular Life Sciences* **68**, 1491–1502 (2011).

18. Neefjes, J., M Jongsma, M. L., Paul, P. & Bakke, O. Towards a systems understanding of MHC class I and MHC class II antigen presentation. *Nature Reviews Immunology* (2011).

19. Pamer, E. & Cresswell, P. Mechanisms of MHC class I--restricted antigen processing. *Annual Review of Immunology* **16**, 323–358 (1998).

20. Hammer, G. E., Gonzalez, F., Champsaur, M., Cado, D. & Shastri, N. The aminopeptidase ERAAP shapes the peptide repertoire displayed by major histocompatibility complex class I molecules. *Nature Immunology* **7**, 7–9 (2006).

21. Serwold, T., Gonzalez, F., Kim, J., Jacob, R. & Shastri, N. Competing interests statement ERAAP customizes peptides for MHC class I molecules in the endoplasmic reticulum. *Nature* **419**, 480–483 (2002).

22. Bouvier, M. Accessory proteins and the assembly of human class I MHC molecules: A molecular and structural perspective. *Molecular Immunology* **39**, 697–706 (2003).

23. Robinson, J. *et al.* The IPD and IMGT/HLA database: allele variant databases. *Nucleic Acids Research* **43**, 423–431 (2015).

24. Apanius, V., Penn, D., Slev, P. R., Ruff, L. R. & Potts, W. K. The nature of selection on the major histocompatibility complex. *Critical Reviews in Immunology* **17**, 179–224 (1997).

25. Schmidt, A. H. *et al.* Estimation of high-resolution HLA-A, -B, -C, -DRB1 allele and haplotype frequencies based on 8862 German stem cell donors and implications for strategic donor registry planning. *Human Immunology* **70**, 895–902 (2009).

26. Gotter, J., Brors, B., Hergenhahn, M. & Kyewski, B. Medullary Epithelial Cells of the Human Thymus Express a Highly Diverse Selection of Tissue-specific Genes Colocalized in Chromosomal Clusters. *The Journal of Experimental Medicine* **199**, 155–166 (2004).

27. Surh, C. D. & Sprent, J. T-cell apoptosis detected in situ during positive and negative selection in the thymus. *Nature* **372**, 100–103 (1994).

28. Klein, L., Kyewski, B., Allen, P. M. & Hogquist, K. A. Positive and negative selection of the T cell repertoire: what thymocytes see (and don't see). *Nature Reviews Immunology* **14**, 377–391 (2014).

29. Starr, T. K., Jameson, S. C. & Hogquist, K. A. Positive and Negative Selection of T Cells. *Annual Review of Immunology* **21**, 139–176 (2003).

30. Mueller, D. L. Mechanisms maintaining peripheral tolerance. *Nature Immunology* **11**, 21–27 (2009).

31. Leach, D. R., Krummel, M. F. & Allison, J. P. Enhancement of Antitumor Immunity by CTLA-4 Blockade. *Science* **271**, 1734–1736 (1996).

32. Brown, J. A. *et al.* Blockade of programmed death-1 ligands on dendritic cells enhances T cell activation and cytokine production. *Journal of Immunology* **170**, 1257–1266 (2003).

33. Bennett, F. *et al.* Program death-1 engagement upon TCR activation has distinct effects on costimulation and cytokine-driven proliferation: attenuation of ICOS, IL-4, and IL-21, but not CD28, IL-7, and IL-15 responses. *Journal of Immunology* **170**, 711–718 (2003).

34. Phan, G. Q. *et al.* Cancer regression and autoimmunity induced by cytotoxic T lymphocyte-associated antigen 4 blockade in patients with metastatic melanoma. *Proceedings of the National Academy of Sciences of the USA* **100**, 8372–8377 (2003).

35. Larkin, J. *et al.* Combined Nivolumab and Ipilimumab or Monotherapy in Untreated Melanoma. *New England Journal of Medicine* **373**, 23–34 (2015).

36. Beck, K. E. *et al.* Enterocolitis in patients with cancer after antibody blockade of cytotoxic T-lymphocyte-associated antigen 4. *Journal of Clinical Oncology* **24**, 2283–2289 (2006).

37. Schachter, J. *et al.* Pembrolizumab versus ipilimumab for advanced melanoma: final overall survival results of a multicentre, randomised, open-label phase 3 study. *Lancet* **390**, 1853–1862 (2017).

38. Snyder, A. *et al.* Genetic Basis for Clinical Response to CTLA-4 Blockade in Melanoma. *New England Journal of Medicine* **371**, 2189–99 (2014).

39. Rizvi, N. A. *et al.* Mutational landscape determines sensitivity to PD-1 blockade in non-small cell lung cancer. *Science* **348**, 124–128 (2015).

40. Frazer, I. H. Prevention of cervical cancer through papillomavirus vaccination. *Nature Reviews Immunology* **4**, 46–55 (2004).

41. Kirnbauer, R., Booy, F., Cheng, N., Lowy, D. R. & Schiller, J. T. Papillomavirus L1 major capsid protein self-assembles into virus-like particles that are highly immunogenic. *Proceedings of the National Academy of Sciences of the USA* **89**, 12180 (1992).

42. Tarhini, A. A. *et al.* Safety and immunogenicity of vaccination with MART-1, gp100, and tyrosinase in adjuvant with PF-3512676 and GM-CSF in metastatic melanoma. *Journal of Immunotherapy* **35**, 359–366 (2012).

43. Kawalec, P., Paszulewicz, A., Holko, P. & Pilc, A. Sipuleucel-T immunotherapy for castration-resistant prostate cancer. A systematic review and meta-analysis. *Archives of Medical Science* **8**, 767 (2012).

44. Rosenberg, S. A., Yang, J. C. & Restifo, N. P. Cancer immunotherapy: moving beyond current vaccines. *Nature Medicine* **10**, 909–915 (2004).

45. Heslop, H. E. *et al.* Long–term restoration of immunity against Epstein–Barr virus infection by adoptive transfer of gene–modified virus–specific T lymphocytes. *Nature Medicine* **2**, 551–555 (1996).

46. Tzannou, I. *et al.* Off-the-Shelf Virus-Specific T Cells to Treat BK Virus, Human Herpesvirus 6, Cytomegalovirus, Epstein-Barr Virus, and Adenovirus Infections After Allogeneic Hematopoietic Stem-Cell Transplantation. *Journal of Clinical Oncology* **35**, 3547–3557 (2017).

47. Riddell, S. R. *et al.* Restoration of Viral Immunity in Immunodeficient Humans by the Adoptive Transfer of T Cell Clones. *Science* **257**, 238–241 (1992).

48. Dudley, M. E., Wunderlich, J. R., Shelton, T. E., Even, J. & Rosenberg, S. A. Generation of Tumor-Infiltrating Lymphocyte Cultures for Use in Adoptive Transfer Therapy for Melanoma Patients. *Journal of Immunotherapy* **26**, 332–342 (2003).

49. Rosenberg, S. A. *et al.* Clinical Durable Complete Responses in Heavily Pretreated Patients with Metastatic Melanoma Using T-Cell Transfer Immunotherapy. *Clinical Cancer Research* **17**, 4550–4557 (2011).

50. Tran, E., Robbins, P. F. & Rosenberg, S. A. "Final common pathway" of human cancer immunotherapy: targeting random somatic mutations. *Nature Immunology* **18**, 255–262 (2017).

51. van Rooij, N. *et al.* Tumor exome analysis reveals neoantigen-specific T-cell reactivity in an ipilimumab-responsive melanoma. *Journal of Clinical Oncology* **31**, (2013).

52. Lu, Y.-C. *et al.* Mining exomic sequencing data to identify mutated antigens recognized by adoptively transferred tumor-reactive T cells. *Nature Medicine* 1–17 (2013).

53. Schambach, A. & Baum, C. Clinical Application of Lentiviral Vectors – Concepts and Practice. *Current Gene Therapy* **8**, 474–482 (2008).

54. Baum, C., Schambach, A., Bohne, J. & Galla, M. Retrovirus Vectors: Toward the Plentivirus? *Molecular Therapy* **13**, 1050–1063 (2006).

55. Roth, T. L. *et al.* Reprogramming human T cell function and specificity with non-viral genome targeting. *Nature* **559**, 405–409 (2018).

56. Maude, S. L. *et al.* Chimeric Antigen Receptor T Cells for Sustained Remissions in Leukemia. *New England Journal of Medicine* **371**, 1507–1517 (2014).

57. Chavez, J. C., Bachmeier, C. & Kharfan-Dabaja, M. A. CAR T-cell therapy for B-cell lymphomas: clinical trial results of available products. *Therapeutic Advances in Hematology* **10**, 145–157 (2019).

58. Chen, Y. T. *et al.* A testicular antigen aberrantly expressed in human cancers detected by autologous antibody screening. *Proceedings of the National Academy of Sciences of the USA* **94**, 1914–1918 (1997).

59. van der Bruggen, P. *et al.* A Gene Encoding an Antigen Recognized by Cytolytic T Lymphocytes on a Human Melanoma. *Science* **245**, 1643–1647 (1991).

60. Robbins, P. F. *et al.* A pilot trial using lymphocytes genetically engineered with an NY-ESO-1-reactive T-cell receptor: Long-term follow-up and correlates with response. *Clinical Cancer Research* **21**, 1019–1027 (2015).

61. Rapoport, A. P. *et al.* NY-ESO-1-specific TCR-engineered T cells mediate sustained antigen-specific antitumor effects in myeloma. *Nature Medicine* **21**, 914–921 (2015).

62. Hammarström, S. The carcinoembryonic antigen (CEA) family: structures, suggested functions and expression in normal and malignant tissues. *Seminars in Cancer Biology* **9**, 67–81 (1999).

63. Bos, R. *et al.* Balancing between antitumor efficacy and autoimmune pathology in T-cell-mediated targeting of carcinoembryonic antigen. *Cancer Research* **68**, 8446–8455 (2008).

64. Kawakami, Y. *et al.* Cloning of the gene coding for a shared human melanoma antigen recognized by autologous T cells infiltrating into tumor. *Proceedings of the National Academy of Sciences of the USA* **91**, 3515–3519 (1994).

65. Morgan, R. A. *et al.* Cancer regression in patients after transfer of genetically engineered lymphocytes. *Science* **314**, 126–129 (2006).

66. Johnson, L. A. *et al.* Gene therapy with human and mouse T-cell receptors mediates cancer regression and targets normal tissues expressing cognate antigen. *Blood* **114**, 535–546 (2009).

67. Parkhurst, M. R. *et al.* T cells targeting carcinoembryonic antigen can mediate regression of metastatic colorectal cancer but induce severe transient colitis. *Molecular Therapy* **19**, 620–626 (2011).

68. Gross, L. Intradermal Immunization of C3H Mice against a Sarcoma That Originated in an Animal of the Same Line. *Cancer Research* **3**, 326–333 (1943).

69. Prehn, R. T. & Main, J. M. Immunity to Methylcholanthrene-Induced Sarcomas. *JNCI: Journal of the National Cancer Institute* **18**, 769–778 (1957).

70. Monach, P. A., Meredith, S. C., T.Siegel, C. & Schreiber, H. A unique tumor antigen produced by a single amino acid substitution. *Immunity* **2**, 45–59 (1995).

71. Land, H., Parada, L. F. & Weinberg, R. A. Cellular Oncogenes and Multistep Carcinogenesis. *Science* **222**, 771–778 (1983).

72. Greenman, C. *et al.* Patterns of somatic mutation in human cancer genomes. *Nature* **446**, 153–158 (2007).

73. Schietinger, A., Philip, M. & Schreiber, H. Specificity in cancer immunotherapy. *Seminars in Immunology* **20**, 276–285 (2008).

74. Fotakis, G., Trajanoski, Z. & Rieder, D. Computational cancer neoantigen prediction: current status and recent advances. *Immuno-Oncology and Technology* **12**, 100052 (2021).

75. Medawar, P. B. Immunity to Homologous Grafted Skin. III. The Fate of Skin Homographs Transplanted to the Brain, to Subcutaneous Tissue, and to the Anterior Chamber of the Eye. *British Journal of Experimental Pathology* **29**, 58 (1948).

76. Kipnis, J. Multifaceted interactions between adaptive immunity and the central nervous system. *Science* **353**, 766–771 (2016).

77. Louis, D. N. *et al.* The 2007 WHO Classification of Tumours of the Central Nervous System. *Acta Neuropathologica* **114**, 97–109 (2007).

78. Hoffman, L. M. *et al.* Clinical, radiologic, pathologic, and molecular characteristics of long-term survivors of Diffuse Intrinsic Pontine Glioma (DIPG): A collaborative report from the International and European Society for Pediatric Oncology DIPG registries. *Journal of Clinical Oncology* **36**, 1963–1972 (2018).

79. Price, G., Bouras, A., Hambardzumyan, D. & Hadjipanayis, C. G. Current knowledge on the immune microenvironment and emerging immunotherapies in diffuse midline glioma. *EBioMedicine* **69**, (2021).

80. Dix, A. R., Brooks, W. H., Roszman, T. L. & Morford, L. A. Immune defects observed in patients with primary malignant brain tumors. *Journal of Neuroimmunology* **100**, 216–232 (1999).

81. Brooks, W. H., Netsky, M. G., Normansell, D. E. & Horwitz, D. A. Depressed cell-mediated immunity in patients with primary intracranial tumors. Characterization of a humoral immunosuppressive factor. *The Journal of Experimental Medicine* **136**, 1631–1647 (1972).

82. Hodges, T. R. *et al.* Mutational burden, immune checkpoint expression, and mismatch repair in glioma: implications for immune checkpoint immunotherapy. *Neuro-Oncology* **19**, 1047–1057 (2017).

83. Woroniecka, K. I., Rhodin, K. E., Chongsathidkiet, P., Keith, K. A. & Fecci, P. E. T-cell Dysfunction in Glioblastoma: Applying a New Framework. *Clinical Cancer Research* **24**, 3792–3802 (2018).

84. Lim, M., Xia, Y., Bettegowda, C. & Weller, M. Current state of immunotherapy for glioblastoma. *Nature Reviews Clinical Oncology* **15**, 422–442 (2018).

85. Weller, M. *et al.* Rindopepimut with temozolomide for patients with newly diagnosed, EGFRvIII-expressing glioblastoma (ACT IV): a randomised, double-blind, international phase 3 trial. *The Lancet Oncology* **18**, 1373–1385 (2017).

86. Reardon, D. A. *et al.* ReACT: Overall survival from a randomized phase II study of rindopepimut (CDX-110) plus bevacizumab in relapsed glioblastoma. *Journal of Clinical Oncology* **33**, 2009–2009 (2015).

87. Fukumura, D., Kloepper, J., Amoozgar, Z., Duda, D. G. & Jain, R. K. Enhancing cancer immunotherapy using antiangiogenics: opportunities and challenges. *Nature Reviews Clinical Oncology* **15**, 325–340 (2018).

88. Khan, K. A. & Kerbel, R. S. Improving immunotherapy outcomes with anti-angiogenic treatments and vice versa. *Nature Reviews Clinical Oncology* **15**, 310–324 (2018).

89. Schuessler, A. *et al.* Autologous t-cell therapy for cytomegalovirus as a consolidative treatment for recurrent glioblastoma. *Cancer Research* **74**, 3466–3476 (2014).

90. Dziurzynski, K. *et al.* Consensus on the role of human cytomegalovirus in glioblastoma. *Neuro-Oncology* **14**, 246–256 (2012).

91. Cinatl, J., Scholz, M., Kotchetkov, R., Vogel, J. U. & Doerr, H. W. Molecular mechanisms of the modulatory effects of HCMV infection in tumor cell biology. *Trends in Molecular Medicine* **10**, 19–23 (2004).

92. Brown, C. E. *et al.* Bioactivity and safety of IL13Rα2-redirected chimeric antigen receptor CD8+ T cells in patients with recurrent glioblastoma. *Clinical Cancer Research* **21**, 4062–4072 (2015).

93. Brown, C. E. *et al.* Regression of Glioblastoma after Chimeric Antigen Receptor T-Cell Therapy. *New England Journal of Medicine* **375**, 2561–2569 (2016).

94. Ahmed, N. *et al.* HER2-Specific Chimeric Antigen Receptor-Modified Virus-Specific T Cells for Progressive Glioblastoma: A Phase 1 Dose-Escalation Trial. *JAMA Oncology* **3**, 1094–1101 (2017).

95. O'Rourke, D. M. *et al.* A single dose of peripherally infused EGFRvIII-directed CAR T cells mediates antigen loss and induces adaptive resistance in patients with recurrent glioblastoma. *Science Translational Medicine* **9**, 1–15 (2017).

96. Sturm, D. *et al.* Hotspot mutations in H3F3A and IDH1 define distinct epigenetic and biological subgroups of glioblastoma. *Cancer Cell* **22**, 425–437 (2012).

97. Schwartzentruber, J. *et al.* Driver mutations in histone H3.3 and chromatin remodelling genes in paediatric glioblastoma. *Nature* **482**, 226–231 (2012).

98. Lewis, P. W. *et al.* Inhibition of PRC2 activity by a gain-of-function H3 mutation found in pediatric glioblastoma. *Science* **340**, 857–861 (2013).

99. Zhao, W. & Id, S. Systematically benchmarking peptide-MHC binding predictors: From synthetic to naturally processed epitopes. *PLoS Computational Biology* **14**, 1–28 (2018).

100. Sette, A. *et al.* Peptide binding to the most frequent HLA-A class I alleles measured by quantitative molecular binding assays. *Molecular Immunology* **31**, 813–822 (1994).

101. Jurtz, V. *et al.* NetMHCpan-4.0: Improved Peptide–MHC Class I Interaction Predictions Integrating Eluted Ligand and Peptide Binding Affinity Data. *The Journal of Immunology* **199**, 3360–3368 (2017).

102. Chheda, Z. S. *et al.* Novel and shared neoantigen derived from histone 3 variant H3.3K27M mutation for glioma T cell therapy. *The Journal of Experimental Medicine* **215**, 141–157 (2018).

103. Mueller, S. *et al.* Mass cytometry detects H3.3K27M-specific vaccine responses in diffuse midline glioma. *Journal of Clinical Investigation* **130**, 6325–6337 (2020).

104. Mount, C. W. *et al.* Potent antitumor efficacy of anti-GD2 CAR T cells in H3-K27M+ diffuse midline gliomas letter. *Nature Medicine* **24**, 572–579 (2018).

105. Didsburys, J., Weber, R. F., Bokochqt, G. M., Evans, T. & Snyderman, R. Rac, a Novel ras-related Family of Proteins That Are Botulinum Toxin Substrates. *The Journal of Biological Chemistry* **264**, 1637–16382 (1989).

106. Mack, N. A., Whalley, H. J., Castillo-Lluva, S. & Malliri, A. The diverse roles of Rac signaling in tumorigenesis. *Cell Cycle* **10**, 1571–1581 (2011).

107. Porter, A. P., Papaioannou, A. & Malliri, A. Deregulation of Rho GTPases in cancer. *Small GTPases* **7**, 123–138 (2016).

108. De, P., Aske, J. C. & Dey, N. RAC1 Takes the Lead in Solid Tumors. *Cells* **8**, 382 (2019).

109. Hodis, E. *et al.* A landscape of driver mutations in melanoma. *Cell* **150**, 251–263 (2012).

110. Krauthammer, M. *et al.* Exome sequencing identifies recurrent somatic RAC1 mutations in melanoma. *Nature Genetics* **44**, 1006–1014 (2012).

111. Watson, I. R. *et al.* The RAC1 P29S hotspot mutation in melanoma confers resistance to pharmacological inhibition of RAF. *Cancer Research* **74**, 4845–4852 (2014).

112. Sjöblom, T. *et al.* The consensus coding sequences of human breast and colorectal cancers. *Science* **314**, 268–274 (2006).

113. Kawazu, M. *et al.* Transforming mutations of RAC guanosine triphosphatases in human cancers. *Proceedings of the National Academy of Sciences of the USA* **110**, 3029–3034 (2013).

114. Engelhard, V. H., Altrich-Vanlith, M., Ostankovitch, M. & Zarling, A. L. Post-translational modifications of naturally processed MHC-binding epitopes. *Current Opinion in Immunology* **18**, 92–97 (2006).

115. Skipper, J. C. A. *et al.* An HLA-A2-restricted tyrosinase antigen on melanoma cells results from posttranslational modification and suggests a novel pathway for processing of membrane proteins. *The Journal of Experimental Medicine* **183**, 527–534 (1996).

116. Vigneron, N. *et al.* An Antigenic Peptide Produced by Peptide Splicing in the Proteasome. *Science* **304**, 587–590 (2004).

117. Hanada, K. I., Yewdell, J. W. & Yang, J. C. Immune recognition of a human renal cancer antigen through post-translational protein splicing. *Nature* **427**, 252–256 (2004).

118. Liepe, J. *et al.* The 20S Proteasome Splicing Activity Discovered by SpliceMet. *PLOS Computational Biology* **6**, 123–131 (2010).

119. Willimsky, G. *et al.* In vitro proteasome processing of neo-splicetopes does not predict their presentation in vivo. *Elife* **10**, 1–20 (2021).

120. Ebstein, F. *et al.* Proteasomes generate spliced epitopes by two different mechanisms and as efficiently as non-spliced epitopes. *Scientific Reports* **6**, 1–12 (2016).

121. Warren, E. H. *et al.* An antigen produced by splicing of noncontiguous peptides in the reverse order. *Science* **313**, 1444–1447 (2006).

122. Platteel, A. C. M. *et al.* Multi-level Strategy for Identifying Proteasome-Catalyzed Spliced Epitopes Targeted by CD8 + T Cells during Bacterial Infection. *Cell Reports* **20**, 1242–1253 (2017).

123. Li, L. P. *et al.* Transgenic mice with a diverse human T cell antigen receptor repertoire. *Nature Medicine* **16**, 1029–1034 (2010).

124. Obenaus, M. *et al.* Identification of human T-cell receptors with optimal affinity to cancer antigens using antigen-negative humanized mice. *Nature Biotechnology* **33**, 402–407 (2015).

125. Engels, B. *et al.* Relapse or eradication of cancer is predicted by peptide-MHC affinity. *Cancer Cell* **23**, 516 (2013).

126. Okada, H. & Hou, Y. Patent: H3.3 ctl peptides and uses thereof (WO2016179326A1). (2016).

127. Leisegang, M., Kammertoens, T., Uckert, W. & Blankenstein, T. Targeting human melanoma neoantigens by T cell receptor gene therapy. *Journal of Clinical Investigation* **126**, 854–858 (2016).

128. Wölfel, T. *et al.* A p16INK4a-insensitive CDK4 mutant targeted by cytolytic T lymphocytes in a human melanoma. *Science* **269**, 1281–1284 (1995).

129. Engels, B. *et al.* Retroviral Vectors for High-Level Transgene Expression in T Lymphocytes. *Human Gene Therapy* **14**, 1155–1168 (2003).

130. Ochs, K. *et al.* K27M-mutant histone-3 as a novel target for glioma immunotherapy. *OncoImmunology* **6**, (2017).

131. Ghani, K. *et al.* Efficient human hematopoietic cell transduction using RD114- and GALV-pseudotyped retroviral vectors produced in suspension and serum-free media. *Human Gene Therapy* **20**, 966–974 (2009).

132. Morita, S., Kojima, T. & Kitamura, T. Plat-E: an efficient and stable system for transient packaging of retroviruses. *Gene Therapy* **7**, 1063–1066 (2000).

133. Sun, Y. *et al.* Expression of the Proteasome Activator PA28 Rescues the Presentation of a Cytotoxic T Lymphocyte Epitope on Melanoma Cells 1. *Cancer Research* **62**, 2875–2882 (2002).

134. Popovic, J. *et al.* The only proposed T-cell epitope derived from the TEL-AML1 translocation is not naturally processed. *Blood* **118**, 946–954 (2011).

135. Allen, M., Bjerke, M., Edlund, H., Nelander, S. & Westermark, B. Origin of the U87MG glioma cell line: Good news and bad news. *Science Translational Medicine* **8**, (2016).

136. Uckert, W. *et al.* Efficient Gene Transfer into Primary Human CD8 1 T Lymphocytes by MuLV-10A1 Retrovirus Pseudotype. *Human Gene Therapy* **11**, 1005–1014 (2000).

137. Ren, J. *et al.* A versatile system for rapid multiplex genome-edited CAR T cell generation. *Oncotarget* **8**, 17002–17011 (2017).

138. Legut, M., Dolton, G., Mian, A. A., Ottmann, O. G. & Sewell, A. K. CRISPR-mediated TCR replacement generates superior anticancer transgenic T cells. *Blood* **131**, 311–322 (2018).

139. Rappsilber, J., Mann, M. & Ishihama, Y. Protocol for micro-purification, enrichment, pre-fractionation and storage of peptides for proteomics using StageTips. *Nature Protocols* **2**, 1896–1906 (2007).

140. Cox, J. & Mann, M. MaxQuant enables high peptide identification rates, individualized p.p.b.-range mass accuracies and proteome-wide protein quantification. *Nature Biotechnology* **26**, 1367–1372 (2008).

141. Capper, D. *et al.* DNA methylation-based classification of central nervous system tumours. *Nature* **555**, 469–474 (2018).

142. Choi, E. M.-L. *et al.* High avidity antigen-specific CTL identified by CD8-independent tetramer staining. *Journal of Immunology* **171**, 5116–5123 (2003).

143. Pascolo, S. *et al.* HLA-A2.1-restricted education and cytolytic activity of CD8(+) T lymphocytes from beta2 microglobulin (beta2m) HLA-A2.1 monochain transgenic H-2Db beta2m double knockout mice. *The Journal of Experimental Medicine* **185**, 2043–2051 (1997).

144. Spiotto, M. T. *et al.* Increasing Tumor Antigen Expression Overcomes "Ignorance" to Solid Tumors via Crosspresentation by Bone Marrow-Derived Stromal Cells. *Immunity* **17**, 737–747 (2002).

145. Assarsson, E. *et al.* A quantitative analysis of the variables affecting the repertoire of T cell specificities recognized after vaccinia virus infection. *Journal of Immunology* **178**, 7890–7901 (2007).

146. Blankenstein, T., Leisegang, M., Uckert, W. & Schreiber, H. Targeting cancer-specific mutations by T cell receptor gene therapy. *Current Opinion Immunology* **33**, 112–119 (2015).

147. Schreiber, H. Cancer Immunology. in *Fundamental Immunology* vol. 7 1200–1234 (2012).

148. Schreiber, H. & Rowley, D. A. Cancer: Quo vadis, specificity? *Science* **319**, 164–165 (2008).

149. Anders, K. & Blankenstein, T. Molecular pathways: Comparing the effects of drugs and T cells to effectively target oncogenes. *Clinical Cancer Research* **19**, 320–326 (2013).

150. Li, L. & Blankenstein, T. Generation of transgenic mice with megabase-sized human yeast artificial chromosomes by yeast spheroplast–embryonic stem cell fusion. *Nature Protocols* **8**, 1567–1582 (2013).

151. Parkhurst, M. R. *et al.* Characterization of Genetically Modified T-Cell Receptors that Recognize the CEA:691-699 Peptide in the Context of HLA-A2.1 on Human Colorectal Cancer Cells. *Clinical Cancer Research* **15**, 169 (2009).

152. Davis, J. L. *et al.* Cancer Therapy: Clinical Development of Human Anti-Murine T-Cell Receptor Antibodies in Both Responding and Nonresponding Patients Enrolled in TCR Gene Therapy Trials. *Clinical Cancer Research* **16**, (2010).

153. Poncette, L., Chen, X., Lorenz, F. K. M. & Blankenstein, T. Effective NY-ESO-1-specific MHC II-restricted T cell receptors from antigen-negative hosts enhance tumor regression. *Journal of Clinical Investigation* **129**, (2019).

154. Reeves, E. *et al.* HPV Epitope Processing Differences Correlate with ERAP1 Allotype and Extent of CD8þ T-cell Tumor Infiltration in OPSCC. *Cancer Immunology Research* **7**, 1202–1213 (2019).

155. Weiskopf, D. *et al.* Oxidative stress can alter the antigenicity of immunodominant peptides. *Journal of Leukocyte Biology* **87**, 165–172 (2010).

156. Carceller, F. Long-term survivors of diffuse intrinsic pontine glioma (DIPG): myth or reality. *Translational Cancer Research* **8**, 343–345 (2019).

157. Barth, R. J., Mull, J. J., Spiess, P. J. & Rosenberg, S. A. Interferon y and Tumor Necrosis Factor Have a Role in Tumor Regressions Mediated by Murine CD8+ Tumor-infiltrating Lymphocytes. *The Journal of Experimental Medicine* **173**, 647–658 (1991).

158. Bijen, H. M. *et al.* Preclinical Strategies to Identify Off-Target Toxicity of High-Affinity TCRs. *Molecular Therapy* **26**, 1206–1214 (2018).

159. Kunert, A., Obenaus, M., Lamers, C. H. J., Blankenstein, T. & Debets, R. T-cell receptors for clinical therapy: In vitro assessment of toxicity risk. *Clinical Cancer Research* **23**, 6012–6020 (2017).

160. Calis, J. J. A. *et al.* Role of peptide processing predictions in T cell epitope identification: contribution of different prediction programs. *Immunogenetics* **67**, 85–93 (2015).

161. di Carluccio, A. R., Triffon, C. F. & Chen, W. Perpetual complexity: predicting human CD8 + T-cell responses to pathogenic peptides. *Immunology & Cell Biology* **96**, 358–369 (2018).

162. Singh, S. P. & Mishra, B. N. Major histocompatibility complex linked databases and prediction tools for designing vaccines. *Human Immunology* **77**, 295–306 (2016).

163. Kessler, J. H. *et al.* Efficient Identification of Novel HLA-A * 0201-presented Cytotoxic T Lymphocyte Epitopes in the Widely Expressed Tumor Antigen PRAME by Proteasome-mediated Digestion Analysis. *The Journal of Experimental Medicine* **193**, 73–88 (2001).

164. Kessler, J. H. & Melief, C. Identification of T-cell epitopes for cancer immunotherapy. *Leukemia* **21**, 1859–1874 (2007).

165. Sijts, E. J. A. M. & Kloetzel, P. M. The role of the proteasome in the generation of MHC class I ligands and immune responses. *Cellular and Molecular Life Sciences* **68**, 1491–1502 (2011).

166. Liepe, J. *et al.* A large fraction of HLA class I ligands are proteasome-generated spliced peptides. *Science* **354**, 354–358 (2016).

167. Rolfs, Z., Müller, M., Shortreed, M. R., Smith, L. M. & Bassani-Sternberg, M. Comment on "A subset of HLA-I peptides are not genomically templated: Evidence for cis-and trans-spliced peptide ligands." *Science Immunology* **4**, 1622 (2019).

168. Mylonas, R. *et al.* Estimating the contribution of proteasomal spliced peptides to the HLA-I ligandome. *Molecular and Cellular Proteomics* **17**, 2347–2357 (2018).

169. Mishto, M. *et al.* An in silico-in vitro Pipeline Identifying an HLA-A*02:01+ KRAS G12V+ Spliced Epitope Candidate for a Broad Tumor-Immune Response in Cancer Patients. *Frontiers in Immunology* **10**, 1–17 (2019).

170. Paes, W. *et al.* Contribution of proteasome-catalyzed peptide cis-splicing to viral targeting by CD8+ T cells in HIV-1 infection. *Proceedings of the National Academy of Sciences of the USA* **116**, 24748–24759 (2019).

171. Eyquem, J. *et al.* Targeting a CAR to the TRAC locus with CRISPR/Cas9 enhances tumour rejection. *Nature* **543**, 113–117 (2017).

172. Schober, K. *et al.* Orthotopic replacement of T-cell receptor α- and β-chains with preservation of near-physiological T-cell function. *Nature Biomedical Engineering* **3**, 974–984 (2019).

173. Oda, S. K. *et al.* A Fas-4-1BB fusion protein converts a death to a pro-survival signal and enhances T cell therapy. *The Journal of Experimental Medicine* **217**, (2020).

174. Rüder, C. *et al.* The tumor-associated antigen EBAG9 negatively regulates the cytolytic capacity of mouse CD8+ T cells. *Journal of Clinical Investigation* **119**, 2184–2203 (2009).

175. Cohen, C. J., Zhao, Y., Zheng, Z., Rosenberg, S. A. & Morgan, R. A. Enhanced Antitumor Activity of Murine-Human Hybrid T-Cell Receptor (TCR) in Human Lymphocytes Is Associated with Improved Pairing and TCR/CD3 Stability. *Cancer Research* **66**, 8878–86 (2006).

176. Okamoto, S. *et al.* A promising vector for TCR gene therapy: Differential effect of siRNA, 2A peptide, and disulfide bond on the introduced TCR expression. *Molecular Therapy - Nucleic Acids* **1**, 63–71 (2012).

177. Okamoto, S. *et al.* Immunology Improved Expression and Reactivity of Transduced Tumor-Specific TCRs in Human Lymphocytes by Specific Silencing of Endogenous TCR. *Cancer Research* **69**, 9003–9011 (2009).

178. Chong, C., Coukos, G. & Bassani-Sternberg, M. Identification of tumor antigens with immunopeptidomics. *Nature Biotechnology* **40**, 175–188 (2021).

179. Rijensky, N. M. *et al.* Identification of tumor antigens in the HLA peptidome of patient-derived xenograft tumors in mouse. *Molecular and Cellular Proteomics* **19**, 1360–1374 (2020).

180. Pertmer, T. M. *et al.* Gene gun-based nucleic acid immunization: elicitation of humoral and cytotoxic T lymphocyte responses following epidermal delivery of nanogram quantities of DNA. *Vaccine* **13**, 1427–1430 (1995).

181. Kotturi, M. F. *et al.* Of mice and humans: how good are HLA transgenic mice as a model of human immune responses? *Immunome Research* **17**, 1–7 (2009).

182. Kula, T. *et al.* T-Scan: A Genome-wide Method for the Systematic Discovery of T Cell Epitopes Human genome-wide screening Kula. *Cell* **178**, 1015–1042 (2019).

183. Birnbaum, M. E. *et al.* Deconstructing the peptide-MHC specificity of t cell recognition. *Cell* **157**, 1073–1087 (2014).

7. Abbreviations

A	adenine
ABC	ATP binding cassette
APC	antigen presenting cell
ATT	adoptive T cell therapy
bp	base pair
BV	brilliant violet
C	cysteine
CAR	chimeric antigen receptor
CD	cluster of differentiation
CDK4	cyclin dependent kinase 4
cDNA	complementary DNA
CDR3	complementarity determining region 3
CEA	carcinoembryonic antigen
CMV	cytomegalievirus
CRISPR	clustered regularly interspersed short palindromic repeat
CTL	cytotoxic T cell
CTLA-4	cytotoxic T-lymphocyte antigen 4
d	day(s)
D	diversity region
DC	dendritic cell
DIPG	diffuse intrinsic pontine glioma
DMG	diffuse midline glioma
DMSO	dimethyl sulfoxide
DNA	deoxyribonucleid acid
DN	double negative
CNS	central nervous system
DP	double positive
EBV	epstein-Barr virus
EGFRvIII	epidermal growth factor receptor variant III
ELISA	enzyme-linked-immunosorbent assay
ER	endoplasmic reticulum
ERAP	endoplasmic reticulum aminopeptidase

ERK	extracellular signal-regulated kinases
EZH2	enhancer of zeste homolog 2
FACS	fluorescence-activated cell sorting
FDA	U.S. food and drug administration
FGF-5	fibroblast growth factor-5
FITC	fluorescein isothiocyanate
G	glycine
G	guanine
GD2	disialoganglioside
gDNA	genomic DNA
GEF	guanine nucleotide exchange factor
GFP	green fluorescent protein
GM-CSF	granulocyte-macrophage colony stimulating factor
gp33	glycoprotein 33
gRNA	guide RNA
GTP	guanosine triphosphate
h	hour
H3.3	histone 3 gene
HBV	hepatitis B virus
HEK 293T	human embryonic kidney 293T
HER2	human epidermal growth factor receptor 2
HLA	human leukocyte antigen
HPV	human papillomavirus
IC50	half maximal inhibitory concentration
IFN	interferon
I/Iono	Ionomycine
IL	interleukin
IRES	internal ribosomal entry site
J	joining region
K	lysine
kb	kilobase
Kras	kirsten rat sarcoma virus
L	leucine
LCL	lymphoblastoid cell line

LDH	lactate dehydrogenase
LTR	long terminal repeats
M	methionine
max	maximum stimulation
MAGE	melanoma antigen gene
MART	melanoma-associated antigen recognised by T cells
MCA	methylcholanthrene
me	methylation
Mel	melanoma
MFI	mean fluorescence intensity
MHC	major histocompatibility complex
min	minute
MP71	MPSV-derived promoter variant
mRNA	messenger RNA
mut	mutant
NSG	NOD-SCID-IL2rγnull mouse
NY-ESO1	New York esophageal squamous cell carcinoma-1
OS12	overall survival at 12 months
P	proline
p2a	picorna virus-derived peptide element
PA	prostate antigen
pA2 tetramer	peptide HLA-A*02:01 tetramer
PAM	protospacer adjacent motif
PBL	peripheral blood lymphocyte
PBMC	peripheral blood mononuclear cell
PBS	phosphate-buffered saline
PCR	polymerase chain reaction
PD-1	programmed death protein 1
PD-L1	programmed death ligand 1
PE	phycoerythrine
P/PMA	phorbol 12-myristate 13-acetate
pMHC	peptide-MHC complex
Plate-E	cell line platinum E
PRC2	polycomb repressive complex 2

PRE	post-transcriptional regulatory element
PCPS	proteasome-catalysed peptide splicing
PDX	patient-derived xenograft
PTM	post-translational modifications
R	arginine
Rac	ras-related C3 botulinum toxin substrate
RACE	rapid amplification of cDNA ends
Rag	recombination-activating gene
Ras	rat sarcoma virus
RNA	ribonucleic acid
RT	reverse transcriptase
S	serine
SCID	severe combined immunodeficiency mouse
scFv	single chain variable fragment
SD	standard deviation
SNV	single-nucleotide variant
SV40	simian virus 40
TAA	tumour-associated antigen
TAP	transporter associated with antigen processing
TCR	T cell receptor
T	thymine
Tet	tetramer
TIL	tumour infiltrating lymphocyte
TNF	tumour necrosis factor
TRA	TCR alpha
TRAC	TCR alpha constant
TRB	TCR beta
TRBC	TCR beta constant
TSA	tumour-specific antigen
UV	ultraviolet
vb	variable region of beta chain
V	valine
V	variable region
V	volt

wt	wild type
YAC	yeast artificial chromosome

Acknowledgement

Most of all, I would like to thank Gerald Willimsky for giving me the opportunity to do my PhD in his lab and for his valuable supervision and support along the way. He always took the time to answer all questions on my "to ask Gerald" list and guided me through my PhD. I would also like to thank Thomas Blankenstein for all the critical discussions and his expert opinion on crucial topics. Thanks to Thomas Sommer for supervising me at the HU.

Special thanks to George Papafotiou for mentoring and helping me along the way. I very much enjoyed working with him as a team on common projects. He was a great help during my PhD and I am very happy for all the scientific and non-scientific (often endless) discussions we have had. Thank you so much for making my time in the lab significantly more fun!

Thanks also to the rest of the Willimsky lab, especially to Sabrina Horn for her technical support and company in the lab and to Kathrin Borgwald and Mathias Pippow for their help with mouse work.

I also thank the Blankenstein and Leisegang teams, especially Josi, Vicky, Mete and Leonie for great office talks and fun times together. It was a pleasure to share my PhD time with you!

Finally, huge thanks to my family and friends, especially Elias and Stephan for sharing all the drama and gossip during lunches. Big uitzonderlijk thanks to my favourite person for all the laughs and support.

Selbständigkeitserklärung

Hiermit erkläre ich, die Dissertation selbstständig und nur unter Verwendung der angegebenen Hilfen und Hilfsmittel angefertigt zu haben. Ich habe mich anderwärts nicht um einen Doktorgrad beworben und besitze keinen entsprechenden Doktorgrad. Ich erkläre, dass ich die Dissertation oder Teile davon nicht bereits bei einer anderen wissenschaftlichen Einrichtung eingereicht habe und dass sie dort weder angenommen noch abgelehnt wurde. Ich erkläre die Kenntnisnahme der dem Verfahren zugrunde liegenden Promotionsordnung der Lebenswissenschaftlichen Fakultät der Humboldt-Universität zu Berlin vom 5. März 2015. Weiterhin erkläre ich, dass keine Zusammenarbeit mit gewerblichen Promotionsbearbeiterinnen/Promotionsberatern stattgefunden hat und dass die Grundsätze der Humboldt-Universität zu Berlin zur Sicherung guter wissenschaftlicher Praxis eingehalten wurden.

I hereby declare that I completed the doctoral thesis independently based on the stated resources and aids. I have not applied for a doctoral degree elsewhere and do not have a corresponding doctoral degree. I have not submitted the doctoral thesis, or parts of it, to another academic institution and the thesis has not been accepted or rejected. I declare that I have acknowledged the Doctoral Degree Regulations which underlie the procedure of the Faculty of Life Sciences of Humboldt-Universität zu Berlin, as amended on 5th March 2015. Furthermore, I declare that no collaboration with commercial doctoral degree supervisors took place, and that the principles of Humboldt-Universität zu Berlin for ensuring good academic practice were abided by.

Berlin, den 24.06.22 _____

Lena Immisch